KfK 2863
Februar 1981

# Thermophysical Properties of Sodium in the Liquid and Gaseous States

K. Thurnay
Institut für Neutronenphysik und Reaktortechnik
Projekt Schneller Brüter

Kernforschungszentrum Karlsruhe

KERNFORSCHUNGSZENTRUM KARLSRUHE

Institut für Neutronenphysik und Reaktortechnik

Projekt Schneller Brüter

KfK 2863

# Thermophysical Properties of Sodium in the Liquid and Gaseous States

K. Thurnay



Kernforschungszentrum Karlsruhe GmbH, Karlsruhe

Kernforschungszentrum Karlsruhe GmbH
ISSN 0303-4003

Abstract

A system of temperature and density dependent thermal-property-functions has been developed and checked for the sodium, using all of the accessible experimental data and the mutual relationships of the properties. In extending these properties beyond the range of the measurements substance independent physical relations have been used.

The property-descriptions are valid for all temperatures above the melting point of the sodium and for all densities below the melting density of the liquid.

The system consists of the following thermal properties: pressure, heat capacity at constant volume, thermal conductivity.

## Die thermophysikalischen Eigenschaften des flüssigen und gasförmigen Natriums

Zusammenfassung

Die thermophysikalischen Eigenschaften des Natriums werden mit Hilfe eines temperatur- und dichteabhängigen Funktionssystems beschrieben. Dieses Funktionssystem wurde aus den zur Verfügung stehenden Natriumdaten entwickelt durch Extrapolation der Eigenschaften mit stoffunabhängigen thermischen Relationen.

Die Zustandsdarstellungen sind gültig für alle Temperaturen oberhalb des Schmelzpunktes und für alle Dichtewerte unterhalb der Flüssigkeitsdichte am Schmelzpunkt.

Die dargestellten Eigenschaften sind der Druck, die spezifische Wärme bei konstantem Volumen und die Wärmeleitfähigkeit.

Contents

List of Figures

Glossary

| | |
|---|---|
| $T$ | temperature |
| $\rho$ | density |
| $V = 1/\rho$ | specific volume |
| $S$ | entropy |
| $U$ | internal energy |
| $H$ | enthalpy |
| $P$, $P^x$ | pressure, vapor pressure |
| $P_T = \partial P/\partial T$ | temperature - resp. density |
| $P_\rho = \partial P/\partial \rho$ | derivatives of the pressure |
| $P_S = \partial P/\partial \rho \mid_S$ | |
| $C_V$, $C_P$ | heat capacities at const. volume, resp. pressure |
| $r = \frac{T}{\rho} \cdot \frac{\partial \rho}{\partial T} \mid_P$ | |
| $Q_T$ | thermal conductivity |
| $Z = P/R \cdot \rho \cdot T$ | factor of reality |
| $\tilde{P}_T = P_T/R \cdot \rho$ | pressure derivatives |
| $\tilde{P}_\rho = P_\rho/R \cdot T$ | in reduced form |
| $\tilde{P}_S = P_S/R \cdot T$ | |
| $\rho_L(T)$, $\rho_V(T)$ | densities of the saturation line |
| $F(L,T) = F(\rho_L[T],T)$ | property in the state of the saturated liquid |
| $r_L = \frac{T}{\rho_L} \cdot \frac{d\rho_L}{dT}$ | |
| $C_s(L)$ | sonic velocity in the liquid |
| $\tilde{C}_V(L,T) = C_V(\rho_L - o,T)$ | marginal heat capacities |
| $\tilde{C}_V(V,T) = C_V(\rho_V + o,T)$ | of the two-phase area |
| $T^x = T_L^x(\rho)$, $T^x = T_V^x(\rho)$ | the inverted saturation line |

| | |
|---|---|
| $T_c = 2508$ K | the critical temperature |
| $\rho_c = 0{,}23$ g/cm$^3$ | the critical density |
| $P_c = 256{,}46$ bar | the critical pressure |
| $\alpha$, $\beta$, $\gamma$ | the critical exponents |
| $x = 1 - T/T_c$ | distance to the critical temperature |
| $w = \rho/\rho_c$ | reduced density |
| $y = T_c/T$ | reduced temperature |
| R | the gas law constant |

## 1. Introduction

The development of the sodium-cooled fast breeder reactors increased naturally the interest for the thermophysical properties of this metal. It is especially the safety analysis of the breeders, which requires a solid knowledge of a variety of the thermal properties of the sodium in a broad range of temperatures and densities - mainly for modelling the Fuel-Coolant-Interaction (FCI).

This phenomenon is a process of violent to explosive vaporisation, resulting from inadvertent mixing of hot, molten fuel into the liquid sodium. To describe the behaviour of this exotic mixture the pressure, the heat capacity and the thermal conductivity must be available at temperatures as high as 3100 K and at densities near to the melting density of the sodium.

Moreover, the space-dependent hydrodynamical FCI-codes - recently in use in the safety analysis - assume these properties to be a thermodynamically consistent set of smooth functions of both variables temperature and density.

None of the thermal properties of the sodium had been measured at such high temperatures so far, most of the experiments reached only just the vicinity of 1650 K, so the construction of the required Sodium-Thermal-Property-System (STPS) means a considerable extension of the measured data known at present.

Many attempts have been made in the past to obtain a complete description for the thermal properties of sodium. Stone et al. at the NRL developed a STPS for the region $T < 1650$ K, which also includes a pressure-description for the overheated vapor /8, 24/. Miller et al. /25/ estimated the critical properties of the sodium and extrapolated the saturation line and some other properties of the saturated liquid. A. Padilla developed a STPS for the subcritical states using the Rowlinson-Approximation (eq. (72)) beyond the two-phase region. In the earlier version /26/ of his STPS he used the critical data of D. Miller, later on /27/ he incorporated the data of Bhise and Bonilla /4/.

All these STPS bear common insufficiencies in calculating the FCI: the thermal properties given do not include the conductivity, a description of the heat capacity in the two-phase area is also lacking and none of these STPS cover either the supercritical or the high-temperature overheated vapor area.

The following pages describe the STPS developed and in use in Karlsruhe. The thermal properties included here are

the pressure P with both its derivatives $P_T$ and $P_\rho$
the heat capacity at constant volume $C_v$ and
the thermal conductivity $Q_T$.

The STPS (Karlsruhe) describe these properties for all temperatures, exceeding the melting point of the sodium ($T_M$ = 371 K) and for all densities, remaining below the density of the molten sodium at $T_M$ (see Fig. 1).

The presented STPS is actually the second edition of the original one from 1975. It differs from its predecessor mainly by taking into account the vapor pressure measurements of Bhise and Bonilla /4/ and by using more recent thermal conductivity dates for the sodium vapor /13/.

## 2. The Vapor Pressure of the Saturated Sodium

The saturation vapor pressure $P^x(T)$ is something like the backbone for the whole STPS. On the saturation line (SL) and in the two-phase area it is the sodium pressure

$$P(\varrho,T) = P^x(T) \tag{1}$$

for

$$T_M \leq T \leq T_c \quad , \quad \varrho_L(T) \geq \varrho \geq \varrho_V(T) \quad .$$

In addition it allows to extend the heat capacity $C_v$ along an isotherm in the two-phase region via the equation (see e.g. /20/):

$$\frac{\partial C_V}{\partial \varrho} = -\frac{T}{\varrho^2} \cdot \frac{d^2P^x}{dT^2} \quad . \tag{2}$$

It can be also used to substitute the saturated vapor density $\varrho_v(T)$ with the numerically more convenient "factor of reality"

$$Z_V(T) = \frac{P^x(T)}{R \cdot \varrho_V(T) \cdot T} \tag{3}$$

It is also needed to calculate one of the pressure derivatives $P_T$ or $P_\varrho$ on the saturation line using the mathematical relation

$$\frac{dP^x}{dT} = P_T(K) + P_\varrho(K) \cdot \frac{d\varrho_K}{dT} \quad , \quad K = L, V \tag{4}$$

Finally, the shape of the pressure-surface $P(\varrho,T)$ beyond the saturated area depends directly on the values of P and $P_T$ on the SL.

The vapor pressure description of the STPS (Karlsruhe) is based on the

vapor pressure data of Stone et al. /3/ (recommended in /12/) and on the $P^x$-measurements of Bhise and Bonilla /4/. The temperature ranges are 1141 - 1666 K resp. 1255 - 2500 K. From /4/ the results of the Run 2 were not used. To these data a Kirchhoff-type equation was fitted:

$$\ln P^x = 11{,}919 - \frac{12153{,}}{T} - 0{,}195 \cdot \ln T \quad , \qquad (5)$$

P in bars, T in K.

Fig. 2 displays the deviations of the measured pressures from this eq.

In /12/ a second Kirchhoff-equation /1/ is recommended for temperatures below the boiling point

$$T_B = 1154 \text{ K}$$

Using two $P^x$-equations would mean either to use more complicated formulas than eq. (5) (adding a $T^n$-term to eq. (5), for example), or a jump in $d^2p^x/dT^2$ and consequently in $C_v(V)$ too at the switching point (see eq. (2)). To avoid both of these alternatives and since the deviations are not large - the maximal departure of eq. (5) from the low-temperature Makanski-equation /2/ is only 2.75 % (at 700 K) - the vapor pressure is described in the whole temperature range from the melting to the critical point with the eq. (5).

## 3. The Saturation Line and the Critical Point of the Sodium

The shape of the saturation line in the "cold"-region

$$T < 1700\ K$$

of the STPS (Karlsruhe) is also based on the measurements of the NRL-Group already quoted /5,6/.

The density of the saturated liquid $\varrho_L(T)$ is described with the formula given in /5/.

The density of the saturated vapor $\varrho_V(T)$ has been calculated via $Z_V(T)$ (eq. (3)). To do this the derivative of Z was set to

$$\frac{1}{Z_V} \cdot \frac{dZ_V}{dT} = \sum_{n=0}^{3} a_n \cdot T^n \qquad (6)$$

with $$Z_V(334,5\ K) = 1 \quad .$$

Fig. 5 shows the shape of this derivative ( —— line) and the corresponding $Z_V$-function (-·—·—). The polynomial in the eq. (6) was determined by fitting $Z_V$ to the corresponding values, developed from the NRL-measurements (Δ-signs in Fig. 5). The pressures, measured by this group for various isochores in the overheated vapor displays Fig. 3 (signs □ - Z). The dashed curve represents the $P^X(T)$-equation (5). The remaining dashed lines are linear approximations for the pressure

$$P(T) = P^x(T^x) + (T - T^x) \cdot P_T(T^x) \quad , \qquad (7)$$

using best fit $P_T$-values for each isochor (as the reduced pressure-presentation - Fig. 4 - shows this equation is in fact not a good approximation in this area, $P_T$ is in reality decreasing for increasing

pressures). From the eq. (7) and (5) the saturation temperature of the isochor, $T^x$ can be calculated. The saturation volume of the isochor

$$V(T^x) = 1 / \varrho_V(T^x)$$

was corrected to $T = T^x$ by assuming that the measured volumina in each experiment increase slightly but linearly with T. From $P^x$, $T^x$ and $V(T^x)$ eq. (3) gives $Z_V(T^x)$. The correspondence between these "measured" $Z_V$-values and the calculation via eq. (6) is better than 0.2 %.

N.B. Calculating $Z_V$ from the virial-equation given in /8/ results in a non-monotonous $dZ_V/dT$ with a local minimum at ≈ 1000 K, leading to a $C_V(V)$-maximum of ≈5 R at this point.

The high temperature part of the SL was constructed using the Hypothesis of the Universality of the Critical Exponents (HUCE). This theory states (see e.g. /15/), that the behaviour of a material with phase-transition is - in the vicinity of the corresponding critical point - determined by a set of universal numbers, the critical exponents. The values of these exponents are

$$\alpha = 0,11 \quad , \quad \beta = 0,325 \quad , \quad \gamma = 1,24 \qquad (8)$$

according to calculations using the 3D-Ising-model /16/ or to recent measurements /15/. For the near-critical ($T \approx T_c$) saturation line of the liquids HUCE gives the following shape:

$$\begin{aligned} \varrho_L(T) &= \varrho_c \cdot ( 1 + b \cdot x^\beta ) \\ \varrho_V(T) &= \varrho_c \cdot ( 1 - b \cdot x^\beta ) \end{aligned} \qquad (9)$$

with

$$x = 1 - T / T_c \quad . \qquad (10)$$

A comparison of the near-critical densities of the saturated cesium /7/ with these equations gives b = 2. Taking this b-value for the sodium too results in the following high temperature SL:

$$\varrho_L(T) = \varrho_c \cdot [\, 1 + 2 \cdot x^{\beta} + x \cdot (a_L + x \cdot g_L + x^3 \cdot h_L) \,] \tag{11}$$

$$\varrho_V(T) = \varrho_c \cdot [\, 1 - 2 \cdot x^{\beta} + x \cdot (a_V + x \cdot g_V + x^3 \cdot h_V) \,]$$

for $T \geq 1700\ K$ .

The x-polynomials, added in this equation serve for a smooth connection with smooth first T-derivatives at the switching point.

As a sodium critical temperature

$$T_c = 2508\ K \tag{12}$$

is used. This value corresponds via eq. (5) to the critical pressure, measured in /4/:

$$P_c = 256{,}46\ bar \tag{13}$$

To achieve a smooth and monotonous density-connection at 1700 K a critical density value of

$$\varrho_c = 0{,}23\ g/cm^3 \tag{14}$$

was needed in the eq. (11).

The complete saturation line is presented in Fig. 6.

## 4. Heat Capacities of the Sodium in the Saturated Area. Enthalpy, Internal Energy, Entropy

The caloric properties of the STPS (Karlsruhe) are based - in the sub-critical region - on the heat capacity of the liquid with vanishing vapor content:

$$\tilde{C}_V(L, T) = C_V(\varrho_L - o, T)$$

$$\varrho_L - o = \varrho_L - \varepsilon, \quad \varepsilon \longrightarrow 0 \quad .$$

For other densities the $C_v$-s can be calculated either with eq. (2) or with

$$\frac{\partial C_V}{\partial \varrho} = - \frac{T}{\varrho^2} \cdot \frac{\partial^2 P}{\partial T^2} \tag{2A}$$

or, at the crossing of the saturation line, from the $C_v$-jump at this place.

The fact, that $C_v$ jumps crossing the SL (see Figs. 30, 31, 33, 34) is not broadly circulated in the thermal physics. The authors in /19/ - the single quotation I found - declare the eq. (19) to be "a well-known relation" without giving any further references.

The origin of this jump lies in the jump of the pressure derivative at this same place:

$$P_T(\varrho_L, T) \neq P_T(\varrho_L - o, T) = \frac{dP^x}{dT} \quad .$$

In the immediate neighborhood of $\varrho_L$ it is

$$C_V = T \cdot \frac{\partial S}{\partial T} = T \cdot \frac{dS}{dT} - T \cdot \frac{\partial S}{\partial \varrho} \cdot \frac{d\varrho_L}{dT} \tag{15}$$

Setting $$C(L,T) = T \cdot \frac{dS}{dT}(\varrho_L(T),T) \tag{16}$$

and using the thermostatic relation

$$S_\varrho = -P_T / \varrho^2$$

(see e.g. /20/) one has

$$C_V(\varrho_L - o) = C + \frac{T}{\varrho_L^2} \cdot \frac{d\varrho_L}{dT} \cdot \frac{dP^\times}{dT} \quad , \tag{17}$$

resp. $$C_V(\varrho_L) = C + \frac{T}{\varrho_L^2} \cdot \frac{d\varrho_L}{dT} \cdot P_T(\varrho_L) \quad . \tag{18}$$

These equations give a $C_v$-rise of

$$\tilde{C}_V(L) - C_V(L) = \frac{T}{\varrho_L^2} \cdot \frac{d\varrho_L}{dT} \cdot \left[ \frac{dP^\times}{dT} - P_T(L) \right] \tag{19}$$

at the crossing from the liquid into the saturated area.

Using the eq. (4) and with the reduced derivative

$$r_L = \frac{T}{\varrho_L} \cdot \frac{d\varrho_L}{dT} \tag{20}$$

eq. (19) can be transformed to

$$\tilde{C}_V(L) - C_V(L) = r_L^2 \cdot P_\varrho(L) / T \quad . \tag{21}$$

The constant pressure head capacity $C_p$, can be expressed in a similar way /20/:

$$C_p(L) - C_V(L) = r^2 \cdot P_\varrho(L) / T \qquad (22)$$

with

$$r = \frac{T}{\varrho} \cdot \left.\frac{\partial \varrho}{\partial T}\right|_P \quad . \qquad (23)$$

From the eq. (21) and (22) one has

$$C_p(L) = \tilde{C}_V(L) + (r^2 - r_L^2) \cdot P_\varrho(L) / T \quad . \qquad (24)$$

Since for the "cold" liquid the SL is practically "vertical", i.e.

$$\frac{d\varrho_L}{dT} \approx \frac{\partial \varrho_L}{\partial T}$$

(see Fig. 7), so it is

$$\tilde{C}_V(L,T) \approx C_p(L,T) \qquad \text{for} \qquad T << T_C \quad . \qquad (25)$$

On the other hand at near-critical temperatures the HUCE describes $C_v$ as

$$C_V(\varrho_C, T) = c(0) \cdot |x|^{-\alpha} \qquad \text{for} \qquad x << 1 \quad . \qquad (26)$$

The $C_v(L,T)$-shape, adopted in Karlsruhe (Fig. 8) was suggested by these two equations as follows:

$$\tilde{C}_V(L,T) = C_p(L,T) + c(-) \cdot [\, x^{-\alpha} - \delta(T) \,] \quad . \qquad (27)$$

For $C_p(L)$ the formula of Ginnings et al. /11/ was taken ($\Delta$-signs in Fig. 8). $\delta(T)$ is a polynomial subtracted in eq. (27) to equalize the term $x^{-\alpha}$ at low temperatures:

$$\delta(T) \approx x^{-\alpha} \qquad \text{for} \qquad T < 1700\ K \quad .$$

The factor $$c(-) = 5,53 \cdot R$$

was chosen to achieve a smooth and monotonous $C_v(L)$-shape at near-critical temperatures.

On the other side of the two-phase area the heat capacity of the vapor with vanishing humidity

$$\tilde{C}_V(V, T) = C_V(\varrho_V + o, T)$$

(--- line in Fig. 8) can be calculated from $C_v(L)$ with the eq. (2) to

$$\tilde{C}_V(V) = \tilde{C}_V(L) + \Delta V \cdot T \cdot \frac{d^2 p^x}{dT^2} \quad . \qquad (28)$$

Here is

$$\Delta V = 1/\varrho_V - 1/\varrho_L \qquad (29)$$

the volume-difference of the saturated states.

Actually, according to the eq. (2), for any volume

$$V = 1/\varrho$$

inside the two-phase region the heat capacity is

$$C_V(\varrho, T) = \tilde{C}_V(L, T) + \left(\frac{1}{\varrho} - \frac{1}{\varrho_L}\right) \cdot T \cdot \frac{d^2 p^x}{dT^2} \qquad (30)$$

$$\varrho_V < \varrho < \varrho_L \quad .$$

The heat capacity of the saturated vapor $C_v(V)$ is calculated from the $C_v$-step at this place:

$$\tilde{C}_V(V) - C_V(V) = C_V(\varrho_V + o) - C_V(\varrho_V) =$$

$$= \frac{T}{\varrho_V^2} \cdot \frac{d\varrho_V}{dT} \cdot \left[ \frac{dP^x}{dT} - P_T(V) \right] . \qquad (19A)$$

$C_p(V)$ can be determined as on the liquid side. Fig. 9 displays the saturated heat capacities $C_v(L)$ and $C_v(V)$, Fig. 10 gives the $C_p/C_v$-relations.

The enthalpy of the saturated liquid can be integrated using the SL-derivative

$$\frac{dH(L)}{dT} = T \cdot \frac{dS}{dT} + \frac{1}{\varrho} \cdot \frac{dP}{dT} =$$

$$= \tilde{C}_V(L) + \frac{1 - r_L}{\varrho_L} \cdot \frac{dP^x}{dT} \qquad (31)$$

(see /20/ and eq. (16), (17)). For the internal energy, U, one has a corresponding derivative

$$\frac{dU(L)}{dT} = \tilde{C}_V(L) + \frac{r_L}{\varrho_L} \cdot \left( \frac{P^x}{T} - \frac{dP^x}{dT} \right) . \qquad (32)$$

For the derivative of the entropy S a slightly transformed eq. (31) can serve. At low temperatures ($T < 1600$ K) as H(L,T) and S(L,T) the respective functions of the NRL-Group - cited in /12/ - can be used.

The properties H, U, and S in the saturated vapor are easier to determine from the liquid properties than by using the derivatives. The equation of Clausius-Clapeyron gives here

$$\Delta S = S(V) - S(L) = \Delta V \cdot \frac{dP^x}{dT} = \Delta H / T , \qquad (33)$$

resp. $$\Delta U = T \cdot \Delta V \cdot \left( \frac{dP^{\times}}{dT} - \frac{P^{\times}}{T} \right) \quad . \tag{34}$$

Fig. 11 shows the enthalpy of the saturated liquid and vapor.

## 5. The Pressure Derivatives of the Sodium on the Saturation Line

In the following for the pressure derivatives reduced forms will be used:

$$\tilde{P}_T = P_T / R \cdot \varrho \quad , \tag{35}$$

$$t = \frac{dP^x}{dT} / R \cdot \varrho \quad , \tag{36}$$

$$\tilde{P}_\varrho = P_\varrho / R \cdot T \quad , \tag{37}$$

$$\tilde{P}_S = \left.\frac{\partial P}{\partial \varrho}\right|_S / R \cdot T \quad . \tag{38}$$

These are more convenient in having no dimensions, giving a simpler form to the physical relations and varying in a more restricted version - mostly near to the unity - as the not reduced properties (compare the Figs. 12 and 16 with Fig. 17). Moreover, by using the properties (34) - (37) all the heat capacities are given in R-units.

In the STPS (Karlsruhe) the pressure derivatives of the saturated liquid are calculated - at low temperatures

$$T < 1700\ K$$

- from the measured values of the velocity of sound, $C_s$ /9, 10/. This can be done by using the relations /20/

$$\left.\frac{\partial P}{\partial \varrho}\right|_S = C_s^2 \tag{39}$$

and

$$\tilde{P}_S = \frac{C_P}{C_V} \cdot \tilde{P}_\varrho \quad . \tag{40}$$

With the equations (21)

$$C_V = \tilde{C}_V - r_L^2 \cdot \tilde{P}_S \tag{21A}$$

and (24)

$$C_P = \tilde{C}_V + (r^2 - r_L^2) \cdot \tilde{P}_S \tag{24A}$$

One can eliminate $C_p$ and $C_v$ from the eq. (40):

$$\frac{C_P - C_V}{C_V} = \frac{r^2 \cdot \tilde{P}_S}{\tilde{C}_V - r_L^2 \cdot \tilde{P}_S} \quad . \tag{41}$$

With the relation /20/

$$\tilde{P}_T / \tilde{P}_S = -r \tag{42}$$

and with the reduced form of the eq. (4)

$$t = \tilde{P}_T + r_L \cdot \tilde{P}_S \tag{4A}$$

eq. (41) can be transformed to

$$\frac{C_P - C_V}{C_V} = \frac{(t - r_L \cdot \tilde{P}_S)^2}{\tilde{P}_S \cdot (\tilde{C}_V - r_L^2 \cdot \tilde{P}_S)} \quad . \tag{43}$$

This equation and eq. (40) gives

$$\tilde{P}_S = \tilde{P}_S + \frac{(t - r_L \cdot \tilde{P}_S)^2}{\tilde{C}_V - r_L^2 \cdot \tilde{P}_S} \quad . \tag{44}$$

The inverted form of this relation

$$\tilde{P}_S = \tilde{P}_S - \frac{(t - r_L \cdot \tilde{P}_S)^2}{\tilde{C}_V - 2 \cdot t \cdot r_L + r_L^2 \cdot \tilde{P}_S} \tag{45}$$

together with the eq. (39), (4A) and (21A) allows to calculate the thermal properties $\tilde{P}_\varrho$, $\tilde{P}_T$, $C_v$, $C_p$ of the liquid from the sonic velocity, $\tilde{C}_v(L)$, $\varrho_L$ and $P^x(T)$.

In the "cold"-statre of the saturated vapor

$$T \leqslant 2320 \text{ K}$$

the basic property is $\tilde{P}_T$; $\tilde{P}_\varrho$ and $C_v$ are determined by the eq. (4A) resp. (21A).

$\tilde{P}_T$ in this region is described with T-polynomials (--- line in Fig. 13) fitted to satisfy the following conditions:

1. for low temperatures $\tilde{P}_T$ must converge to the ideal gas value

$$\tilde{P}_T(V,T) \longrightarrow 1 \qquad \text{for} \qquad T \longrightarrow T_M \ ,$$

2. $\tilde{P}_T$ must suffice the values gained from the PVT-measurements /6/ (0-signs in Fig. 13),

3. both $\tilde{P}_T$ and the $C_v(V)$ calcualted from it (0-0 line in Fig. 9) must have the simplest possible form compatible with 1. and 2.

In the fitting of the polynomials to the $\tilde{P}_T$-values only the first 8 best-fit $P_T(T^x)$-values (eq. (7)) were used. The latest one, corresponding to the exp. 7 (Z-signs in Figs. 3 and 4) has been omitted for having a value much too high:

$$\tilde{P}_T(T^x = 1674 \text{ K}) = 1{,}86 \ .$$

At near-critical temperatures, i.e. at

$$T \geqslant 1700 \text{ K}$$

for the liquid and at

$$T > 2320 \text{ K}$$

for the vapor $P_\varsigma$ was chosen as basic property, since the HUCE prescribes for this function a shape:

$$P_\varsigma(K,T) = p_o \cdot x^\beta \cdot \varsigma_K(T) / \varsigma_C \quad , \quad K = L, V \tag{46}$$

for $$x \longrightarrow 0 \quad .$$

To have smooth connections with the respective low-temperature $P_\varsigma$-s form-polynomials $\varphi(K,x)$ had to be included in the eq. (46). So the high-temperature functions are:

$$P_\varsigma(L,T) = \varphi(L,x) \cdot p_o \cdot x^\beta \cdot \varsigma_L(T) / \varsigma_C \tag{47}$$

and

$$P_\varsigma(V,T) = \varphi(V,x) \cdot p_o \cdot x^\beta \cdot \varsigma_V(T) / \varsigma_C \quad , \tag{48}$$

with

$$\varphi(K,x) = 1 + \sum_{n=1}^{4} f_n(K) \cdot x^n \quad , \quad K = L, V \quad . \tag{49}$$

As $p_o$ the fitting at the switching points gave

$$p_o = 7150{,}89 \text{ J/g} \quad .$$

## 6. The Thermal Conductivity of the Sodium on the Saturation Line

Thermal conductivity measurements of the sodium are scarce and the temperature range of the data is very limited, T ≈ 1100 K being the highest temperature as well for the liquid as for the vapor. Correspondingly the switching point between measured $Q_T$-functions and extrapolated ones lies also low at

$$T = 1280 \text{ K}$$

for both saturated states.

For the thermal conductivity of the cold liquid the T-polynomial - recommended by Golden and Tokar /12/ - is used in Karlsruhe.

The most recent data concerning the sodium vapor thermal conductivity has been published by Timrot et al. /13/. This group measured the $Q_T$ of the sodium in the overheated vapor along five different isotherms as functions of the pressure (see ⊡ - x signs on the Figs. 20 and 21). They calculated the thermal conductivity for the saturated vapor, $Q_T^*(V,T)$ (— line on Fig. 23) by extending the isothermal data up to the saturation points ( ¦ -lines on the Figs. 20, 21) via the equation

$$P \longrightarrow P^{\times}(T)$$

$$Q_T(P,T) = \hat{Q}_T(T)\cdot[\,1 + b(T)\cdot P + e(T)\cdot P^2\,] \,. \qquad (50)$$

$\hat{Q}_T$ is here the conductivity of the monatomic vapor. The factors b and e had been determined for each isotherm individually.

Since $Q_T^*(V,T)$ has a vanishing derivative at T ≈ 1200 K, it is not practical to use it as saturated conductivity, giving no help in the $Q_T$-extrapolation to higher temperatures. To avoid this hindrance, a temperature-independent description was developed, instead of the eq. (50) for the thermal conductivity ( —— lines on Figs. 20, 21):

$$Q_T(P,T) = \hat{Q}_T(T)\cdot[\,1 + \hat{b}\cdot\pi + \hat{e}\cdot\pi^2\,] \qquad (51)$$

using the reduced pressures

$$\pi = P(T) / P^{\times}(T) \tag{52}$$

and the isotherm-independent factors

$$\hat{b} = 0,8957 \quad , \quad \hat{e} = -0,3353 \quad . \tag{53}$$

Fig. 22 displays the deviations of the measurements /13/ from the eq. (51) as a function of the reduced pressure . Since Timrot et al. estimate their maximum error as about 5 % /13/, the T-independent description (50) is well within the margins of the experimental uncertainties. From the equations (51) - (53) one has the following saturation-conductivity:

$$Q_T(V,T) = \hat{Q}_T(T) \cdot 1,5604 \tag{54}$$

(see -o-o- line on Fig. 23).

There is a certain lack of ideas about the shape of the near-critical thermal conductivity beside the obvious notion

$$Q_T(L,T) \longrightarrow Q_T(c) \longleftarrow Q_T(V,T)$$

for $$T \longrightarrow T_c \quad .$$

One of the few non-trivial relations for the near-critical conductivities has been proposed by P. E. Liley /17/. He found that for many substances the difference between the liquid and vapor conductivities vanishes as the enthalpy difference:

$$Q_T(L) - Q_T(V) = q_o \cdot \Delta H \quad \text{if} \quad 0 < x < x_G \, . \tag{55}$$

The $T_c$-distance limit $X_G$ is only 0.05 for the substances N and O but 0.14 for A and even 0.27 for water /17/.

The eq. (55) suggest a density-like shape for the near-critical thermal conductivity, for it is

$$\Delta H = F \cdot ( \varrho_L - \varrho_V )$$

(see eq. (33)).

Hence the extrapolated thermal conductivities were designed as

$$\lambda_T(L,T) = \lambda_T(c) \cdot [ 1 + 2 \cdot x^{\beta} + x \cdot ( \bar{a}_L + x \cdot \bar{g}_L + x^3 \cdot \bar{h}_L ) ] \quad (56)$$

resp.

$$\lambda_T(V,T) = \lambda_T(c) \cdot [ 1 - 2 \cdot x^{\beta} + x \cdot ( \bar{a}_V + x \cdot \bar{g}_V + x^3 \cdot \bar{h}_V ) ] . \quad (57)$$

The conditions

1. the linearity-limit, $X_G$ had to be as large as possible (see Fig. 25) and
2. the connections at 1280 K had to be smooth and monotonous

determined the parameters $\bar{a}_L$, $\bar{a}_V$,... as well as the critical conductivity:

$$\lambda_T(c) = 0,05 \quad W/cm/K \quad . \quad (58)$$

Fig. 24 shows the reduced conductivities $\lambda_T(T)/\lambda_T(C)$ in the 1/T-dependence. The dashed lines indicate the extrapolated properties. The saturated vapor function, given in /12/ resp. /14/ and used in the first version of the STPS in Karlsruhe is also indicated here (x-signs).

## 7. The Static Thermal Conductivity in the Two-Phase Region

In the two-phase area the substance consists of a mass of saturated liquid ($M_L$) dispersed in a mass of saturated vapor ($M_V$), both having beside the common temperature, T, a common pressure, $P^x(T)$. The quality of this mixture depends at a given T on the mass relation of the vapor:

$$\xi = M_V / ( M_V + M_L ) \quad . \tag{59}$$

Since the specific volume of the mixture is

$$V = \xi \cdot V_V + ( 1 - \xi ) \cdot V_L \tag{60}$$

with

$$V_K = 1 / \varrho_K \tag{61}$$

the mixture quality can be calculated directly from the densities:

$$\xi ( \varrho , T ) = \frac{V - V_L(T)}{\Delta V} = \frac{\varrho_V(T)}{\varrho} \cdot \frac{\varrho_L(T) - \varrho}{\varrho_L(T) - \varrho_V(T)} \tag{62}$$

The transfer of heat can proceed in this mixture in four different ways: beside the radiation, convection and conduction heat can be also moved here in latent form, i.e. by transporting and subsequently condensating saturated vapor. As the static thermal conductivity only the conductive heat transfer is considered.

For the calculation of the conductivity in the two-phase region the following, very simple liquid-vapor-mixture concept was devised (see sketch):

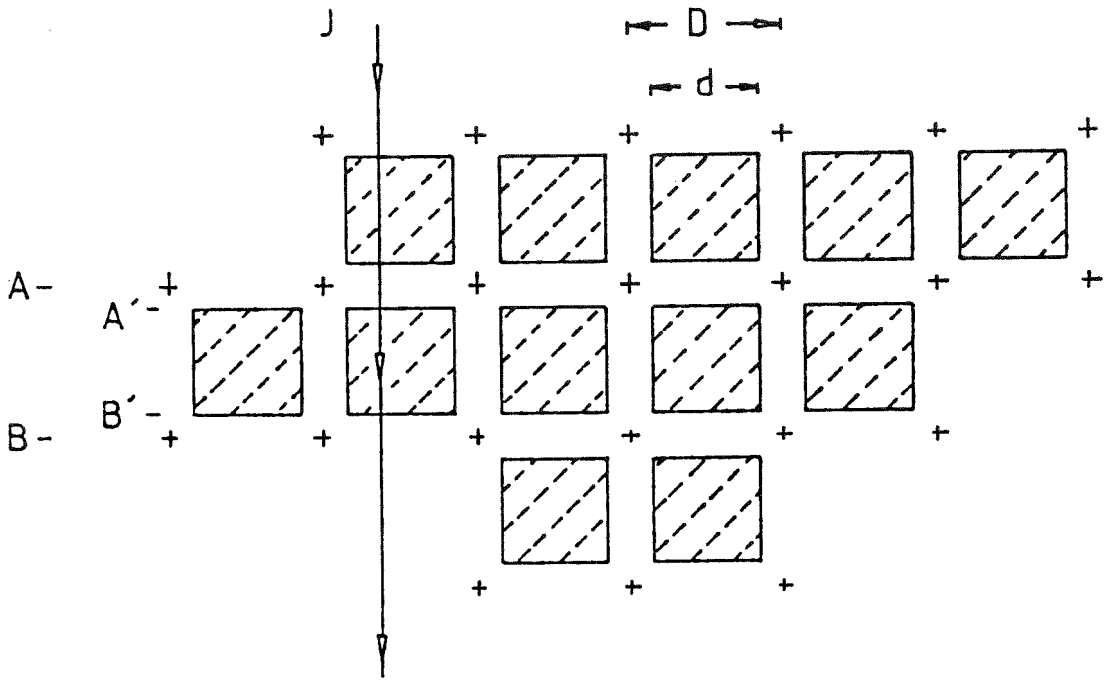


The liquid is uniformly distributed in the vapor, as a number of little cubes, each mixture volume $D^3$ containing a liquid volume $d^3$. In a $D^3$-volume there is $\varrho$ two-phase substance and $\varrho_V \cdot (1 - \eta^3)$ saturated vapor, $\eta$ being

$$\eta = d / D \tag{63}$$

the length-ratio of the liquid. The mixture-quality is therefore

$$\xi = \varrho_V \cdot ( 1 - \eta^3 ) / \varrho \quad ,$$

giving with eq. (62) the following relation between length ratio and mixture density:

$$\eta ( \varrho , T ) = \sqrt[3]{\frac{\varrho - \varrho_V(T)}{\varrho_L(T) - \varrho_V(T)}} \quad . \tag{64}$$

To facilitate the calculation of $Q_T(\varrho)$ it is assumed, that the heat current J crosses perpendicularly one D-layer of the mixture-lattice, on a surface F. D is supposedly small enough to render $Q_T(L)$ and $Q_T(V)$ space-independent inside of this layer. Further, since evaporation and condensation had been excluded, the heat currents in all three sub-layers must be the same and equal to J:

$$J_{BB'} = J_{B'A'} = J_{A'A} = J \quad . \tag{65}$$

Denoting the temperatures on the surfaces A, A',... as $T_A$, $T_{A'}$,... the currents in the first and in the third layer are:

$$J_{A'A} = 2 \cdot \frac{T_A - T_{A'}}{D \cdot (1 - \eta)} \cdot F \cdot Q_T(V) \quad , \tag{66}$$

resp. $$J_{B'B} = 2 \cdot \frac{T_B - T_{B'}}{D \cdot (1 - \eta)} \cdot F \cdot Q_T(V) \quad . \tag{67}$$

In the second layer there are two different heat currents, one in the liquid part of the layer

$$J_L = \frac{T_{A'} - T_{B'}}{D \cdot \eta} \cdot F \cdot \eta^2 \cdot Q_T(L)$$

and one in the vapor part:

$$J_V = \frac{T_{A'} - T_{B'}}{D \cdot \eta} \cdot F \cdot (1 - \eta^2) \cdot Q_T(V)$$

rendering the total layer-current to

$$J_{B'A'} = J_L + J_V =$$

$$= \frac{T_{A'} - T_{B'}}{D \cdot \eta} \cdot F \cdot (Q_T(V) + \eta^2 \cdot \Delta Q_T) \quad . \tag{68}$$

Here is $$\Delta Q_T = Q_T(L) - Q_T(V) \quad . \tag{69}$$

The equivalent heat current for the total layer AB is

$$J = \frac{T_A - T_B}{D} \cdot F \cdot Q_T(\varsigma) \quad . \tag{70}$$

The identity

$$T_A - T_B = T_A - T_{A'} + T_{A'} - T_{B'} + T_{B'} - T_B$$

and the equation (65) in connection with the eq. (66) - (68) and (70) gives

$$1 / Q_T(\varsigma) = (1 - \eta) / Q_T(V) + \eta / (Q_T(V) + \eta^2 \cdot \Delta Q_T)$$

or

$$Q_T(\varsigma) = Q_T(V) \cdot \frac{Q_T(V) + \eta^2 \cdot \Delta Q_T}{Q_T(V) + (1-\eta) \cdot \eta^2 \cdot \Delta Q_T} \quad . \tag{71}$$

Mixture conductivities, calculated with this equation for various isotherms are displayed on Fig. 26 (—— lines).

## 8. The Thermal Properties of the Sodium as a Compressed Liquid

In the state of the compressed liquid

$$T < T_C \quad , \quad \varrho > \varrho_L(T)$$

the sodium pressure is derived using a $P_T$-approximation recommended by Rowlinson /18/. It is assumed that in the compressed sodium - as in many other compressed liquids - $P_T$ depends practically only on the density:

$$P_T(\varrho, T) \approx P_T(\varrho) = P_T(L, T^x) \quad . \tag{72}$$

$T^x$ is here a "density-temperature", the inverted form of the saturated liquid density, i.e.

$$T^x = T^x_L(\varrho) \qquad \text{resp.} \qquad \varrho = \varrho_L(T^x) \quad . \tag{73}$$

With this assumption the pressure of the liquid is

$$P(\varrho, T) = P^x(T^x) + \int_{T^x}^{T} dt \cdot P_T(\varrho, t) =$$

$$= P^x(T^x) + (T - T^x) \cdot P_T(L, T^x) \quad . \tag{74}$$

As a density derivative eq. (74) gives:

$$P_\varrho(\varrho, T) = \left[ \frac{dP^x}{dT}(T^x) - P_T(L, T^x) + \right.$$

$$\left. + (T - T^x) \cdot \frac{dP_T}{dT}(L, T^x) \right] / \frac{d\varrho_L}{dT}(T^x) \quad . \tag{75}$$

Since, due to the assumption (72) the second thermal derivative of P vanishes in this state, the $C_v$-derivative (eq. (2A)) vanishes too and the heat capacity remains $C_v(L,T)$ on the whole isotherm T in the compressed liquid.

In describing the thermal conductivity in this state - for the sake of simplicity - also a temperature-independence-assumption was used:

$$Q_T(\varsigma, T) \approx Q_T(\varsigma) = Q_T(L, T^{\times}) \quad . \tag{76}$$

## 9. The Thermal Properties of the Sodium as an Overheated Vapor

It is natural to try in this state

$$T < T_C \quad , \quad \varrho < \varrho_V(T)$$

too a pressure-description with T-independent $P_T$:

$$P_T(\varrho,T) \approx P_T(\varrho) = P_T(V,T^x) \tag{77}$$

with $T^x = T^x_V(\varrho)$ resp. $\varrho = \varrho_V(T^x)$ . (78)

The assumption (77) would give here - as in the compressed liquid -

$$P(\varrho,T) = P^x(T^x) + (T - T^x)\cdot P_T(V,T^x) , \tag{79}$$

with

$$P_\varrho(\varrho,T) = \left[\frac{dP^x}{dT}(T^x) - P_T(V,T^x) + (T - T^x)\cdot\frac{dP_T}{dT}(V,T^x)\right] / \frac{d\varrho_V}{dT}(T^x) \tag{80}$$

and

$$C_V(\varrho,T) = C_V(V,T) \quad . \tag{81}$$

The approximation (77) is unfortunately not fully adequate in the whole superheated vapor area; at low densities (rarified sub-region on Fig. 1) the equations (77), (79) calculate too high values for $P_T$ and P. At densities as low as

$$\varrho = 10^{-4} \ g/cm^3$$

(corresponding to $T^x \approx 1050$ K) the sodium could be expected to behave as an ideal gas, especially far from the saturation line, on the critical isotherm. So

$$Z(\varrho,T) \approx 1 \quad , \quad \tilde{P}_T(\varrho,T) \approx 1$$

were reasonable values here. As the Figs. 13 and 14 prove, the respective calculated properties (---- line on Fig. 13, -·- line on Fig. 14) are too high for these low density states.

There is also an experimental evidence for the insufficiency of the eq. (77) as $P_T$-description in this sub-range. As the reduced representation of the PVT-data of the NRL /6/ indicates, $P_T$ on an isochor is not constant but decreases markedly with increasing T from a maximum at $T = T^x$ (Fig. 4).

To achieve a better pressure-description in the rarified region, a $(\varrho,T)$-dependent correction-term was added here to the $P_T$-equation:

$$\tilde{P}_T(\varrho,T) = \tilde{P}_T(V,T^x) + G(s)\cdot H(u) \quad . \tag{82}$$

The T-dependence is included in the variable

$$u(\varrho,T) = 0,2\cdot\frac{T_c - T^x}{T - T^x} \quad , \tag{83}$$

s is only a function of the density:

$$s(\varrho) = \ln \varrho_c / \ln \varrho \tag{84}$$

($s(\varrho)$ has a similar shape to $T^x(\varrho)$, but it is easier to calculate).

The selection of the functions

$$\mu(u) = u / (e^u - 1) \tag{85}$$

and

$$H(u) = \mu(u)\cdot[u + \mu(u)] \tag{86}$$

was dictated by the fact, that the necessary $P_T$- and P-corrections on the critical isotherm are of the same size, i.e.

$$\Delta P_T(T^x,T_c) \approx \Delta P(T^x,T_c) / (T_c - T^x) \quad . \tag{87}$$

A polynomial term for the correction:

$$\Delta P_T(\varrho, T) = f(\varrho)\cdot(T - T^x)^m$$

would give

$$\frac{\Delta P}{T - T^x} = f\cdot\frac{(T - T^x)^m}{1 + m} \quad .$$

Using here a small m-value ($m < 1$) to suffice to the equation (87) would render

$$\partial \Delta P_T / \partial T = f\cdot m\cdot(T - T^x)^{m-1}$$

infinite at $T^x = T$, giving an unphysical jump in the heat capacity (eq. (2A)) at this point, instead of a $C_v$-shape, gradually decreasing with $T^x \to 0$.

Integrating eq. (82) - the necessary derivatives are

$$\frac{\partial u}{\partial T} = -\frac{u}{T - T^x} \tag{88}$$

and

$$\frac{d\mu}{du} = \frac{\mu}{u}\cdot(1 - u - \mu) \quad - \tag{89}$$

the term G·H gives the following additional pressure:

$$\Delta P(\varrho, T) = \int_{T^x}^{T} dt\cdot R\cdot\varrho\cdot G(s)\cdot H(u) =$$

$$= R\cdot\varrho\cdot(T - T^x)\cdot G(s)\cdot\mu(u) \quad . \tag{90}$$

A comparison of H(u) with $\mu(u)$ for $T = T_c$ results in a (87)-relation: $1 \approx 0.9$.

The pressure correction (90) gives, using

$$\frac{\partial u}{\partial T^{\times}} = \frac{u}{T - T^{\times}} \cdot \left( 1 - \frac{0,2}{u} \right) \tag{91}$$

the following $P_\varrho$-correction:

$$\frac{\partial \Delta P}{\partial \varrho} = R \cdot \left[ (T - T^{\times}) \cdot \left( G + \varrho \cdot \frac{dG}{d\varrho} \right) \cdot \mu + \right.$$

$$\left. - \frac{T^{\times}}{r_V(T^{\times})} \cdot \left( H - 0,2 \cdot \frac{H - \mu}{u} \right) \cdot G \right] . \tag{92}$$

To the heat capacity the $P_T$-correction supplies (eq. (2A)):

$$\Delta C_V(\varrho, T) = C_V(\varrho, T) - C_V(V, T) =$$

$$= - R \cdot T \cdot \int_{\varrho_V}^{\varrho} d\varrho \cdot \frac{G(s)}{\varrho} \cdot \frac{\partial H}{\partial T} . \tag{93}$$

With $$\frac{dH}{du} = - \frac{H}{u} \cdot [ 2 \cdot (\mu - 1) + u ]$$

this can be converted to $$\Delta C_V(\varrho, T) =$$

$$= R \cdot \int_{T^{\times}}^{T} \frac{dt}{t} \cdot \frac{T}{T - t} \cdot G \cdot H \cdot [ 2 \cdot (\mu - 1) + u ] \cdot r_V(t) . \tag{94}$$

The heat capacity, calculated by this equation for extremely low densities, $C_v(0,T)$ is shown on Fig. 9 as a dashed line.

The boundary of the rarified sub-region of the overheated vapor in the STPS (Karlsruhe) lies at

$$\varrho_G = 0{,}01 \ \mathrm{g/cm^3} \tag{95}$$

(see ⋮ -line on Fig. 18). This value corresponds to a density-temperature of

$$T_G^{\times} = 1850 \ \mathrm{K}$$

(on Figs. 13 and 14) or to

$$s_G = 0{,}32$$

In the dense-area ($\varrho > \varrho_G$) P and $C_v$ are described with the equations (77), (79), (80) and (81).

For the density-fitting of the correction-term in the rarified vapor a

$$G(s) = s^2 \cdot (0{,}32 - s)^2 \cdot \eta(s) \tag{96}$$

form was used. The function $\eta(s)$ in this equation was shaped to give the "right" P and $P_T$-functions on the critical isotherm and physically meaningful $C_v$-values in the "vacuum". As a requirement for correcting $P(\varrho, T_c)$ and $P_T(\varrho, T_c)$ a smooth crossing of the critical isotherm on the pressure-surface is demanded:

$$P(\varrho, T_c - o) \stackrel{!}{=} P(\varrho, T_c + o) \tag{97}$$

$$P_T(\varrho, T_c - o) \stackrel{!}{=} P_T(\varrho, T_c + o) \tag{98}$$

for $\varrho \leq \varrho_G$

(for the supercritical functions see the following chapter).

As for the $C_V(0,T)$ one expects this property not to descend below the $C_V$-value for the monatomic vapor, and yet to lie - at low temperatures - not much higher than this value, i.e.

$$C_V(0,T) \geq 3/2 \cdot R \quad ,$$

$$C_V(0,T) \longrightarrow 3/2 \cdot R \quad \text{f.} \quad T \longrightarrow 0 \quad . \tag{99}$$

Fig. 19 shows the compromise-$\eta(s)$ chosen for the rarified vapor (— line). The dashed lines on this Fig. correspond to $\eta$-s demanded by the eq. (97) and (98). The maximal deviations in these equations - resulting from the use of the actual $\eta(s)$ instead of the needed functions - are 0.65 % for the pressure and 3.5 % for $P_T$. The $\eta$-departure from the common prescribed shape for low s-values ($s < 0.12$) is due to the heat capacity values in the vacuum. Without this departure $C_V(0,T)$ would be less than 3/2 R at $T \approx 900$ K (see Fig. 9) and even higher at $T < 600$ K than with the corrected $\eta$. Actually, it is not $C_V(0,T)$, which is too large at low temperatures, but $C_V(V,T)$ - since the density of the saturated state at low temperatures is very low - and therefore

$$C_V(0,T) \approx C_V(V,T) \quad \text{at} \quad T \approx 400 \text{ K}$$

is not unreasonable. This overestimated $C_V(V,T)$ results probably from the incorrect description of the vapor pressure with the eq. (5) in the low temperature area (see eq. (28) and (19A)). The dent in $C_V(0,T)$ at $T \approx 1750$ K (Fig. 9) has no physical foundations and could have been eliminated with a more complicated description of $\tilde{P}_T(V,T)$.

The corrected functions $P(\varrho,T_c)$ and $P_T(\varrho,T_c)$ are shown on the Figs. 13 and 14 as solid lines.

The thermal conductivity of the overheated vapor has been set - as those of the compressed liquid - temperature-independent:

$$Q_T(\varrho,T) \approx Q_T(\varrho) = Q_T(V,T^{\times}) \quad . \tag{100}$$

## 10. The Thermal Properties of the Gaseous (Supercritical) Sodium

In the supercritical or gaseous area

$$T \geq T_c$$

of a non-ideal substance the easiest way to describe the pressure is to use the equation of van der Waals /20/:

$$(P + q / V^2) \cdot (V - V_o) = R \cdot T \quad . \tag{101}$$

q and $V_o$ are the van der Waals constants representing the attractive forces between the gas-particles resp. the self-volume of these. Unfortunately the sodium is in the high-density critical states

$$T = T_c \quad , \quad \varrho > \varrho_c$$

much softer than the "van der Waals"-gas. At the critical point, for example the sodium has a reality of

$$Z_{Na}(\varrho_c, T_c) = 0{,}123$$

whereas the equation (101) gives here

$$Z_{vW}(\varrho_c, T_c) = 3 / 8 \quad ,$$

i.e. at the same pressure the sodium requires only a third of the volume of the van-der-Waals substance.

To derive from the eq. (101) a more compressible P(V)-relation the self-volume had been rendered density-dependent:

$$V_o \longrightarrow V_o / (1 + w^2 \cdot B)$$

with

$$w = \varrho / \varrho_c \quad . \tag{102}$$

As a density-exponent in the denominator the smallest possible value, 2 was

chosen, which is able to give a monotonous $P(\varrho,T_c)$-function in the whole range of the liquid densities

$$\varrho_c < \varrho < \varrho_L(T_M) \quad .$$

A further requirement for the pressure-shape in the gas state is, to become with increasing temperature and with decreasing density more and more ideal, i.e.

$$Z(w,y) \longrightarrow 1 \quad \text{f.} \quad w \cdot y \longrightarrow 0 \quad . \tag{103}$$

Here is

$$y = T_c / T \quad . \tag{104}$$

To comply with this behaviour the self-volume acquired a T-dependence:

$$V_o \longrightarrow V_o(w,y) = \frac{A}{\varrho_c} \cdot \frac{y}{1 + w^2 \cdot B} \quad . \tag{105}$$

As for the coefficient of internal attraction, this property turned also $(\varrho,T)$-dependent, to allow a smooth crossing of the critical isotherm on the P-surface in the region of moderate to high densities. The following form was selected:

$$q \longrightarrow q(w,y) = Q(w,y) \cdot R \cdot T_c / \varrho_c \quad , \tag{106}$$

with

$$Q(w,y) = \sum_{n=1}^{5} w^{n-1} \cdot F_n(y) \tag{107}$$

and

$$F_n(y) = G_n + (y-1) \cdot H_n \quad . \tag{108}$$

These modifications of the self-volume and of the internal attractions transforms eq. (101) into

$$Z(w,y) = 1 + w \cdot y \cdot [\, A / S(w,y) - Q(w,y) \,] \quad , \tag{109}$$

with $$S(w,y) = 1 - w\cdot y\cdot A + w^2\cdot B \quad . \tag{110}$$

The respective pressure derivatives are here

$$\tilde{P}_\varrho = Z + w\cdot Z_w \tag{111}$$

and

$$\tilde{P}_T = Z - y\cdot Z_y \quad , \tag{112}$$

with

$$w\cdot Z_w = w\cdot y\cdot A\cdot(1 - w^2\cdot B)/S^2 - y\cdot\sum_{n=1}^{5} w^n\cdot n\cdot F_n \tag{113}$$

and

$$y\cdot Z_y = w\cdot y\cdot A\cdot(1 + w^2\cdot B)/S^2 + - y\cdot\sum_{n=1}^{5} w^n\cdot(F_n + y\cdot H_n) \quad . \tag{114}$$

As a base-line for the $C_v$-calculation in the gas-area the critical isochor was chosen

$$C_V(\varrho_C, T) = c(+)\cdot|x|^{-\alpha} \tag{115}$$

(see eq. (26)). The constant C(+) was gained from $C_v(L,T)$:

$$c(+) = \lim_{x \to +0} x^{\alpha}\cdot C_V(L,T) \quad . \tag{116}$$

Using here $\tilde{C}_v(L,T)$ would result in much too large supercritical $C_v$-values (see Figs. 30 or 32).

The density-derivative in this region is (see eq. (2A)):

$$\frac{\partial C_V}{\partial \varrho} = -\frac{R}{\varrho}\cdot y^2\cdot\frac{\partial^2 Z}{\partial y^2} =$$

$$= -2\cdot\frac{R}{\varrho}\cdot y^2\cdot\left[\,(w\cdot A)^2\cdot\frac{1+w^2\cdot B}{S^3}-\sum_{n=1}^{5} w^n\cdot H_n\,\right] \quad (117)$$

Hence the heat capacity beyond the critical isochor can be given as

$$C_V(\varrho,T) = C_V(\varrho_C,T) + \Delta C_V(\varrho,T) \quad , \quad (118)$$

with

$$\Delta C_V(\varrho,T) = \int_{\varrho_C}^{\varrho} dC_V =$$

$$= R\cdot y^2\cdot\left[\,2\cdot\sum_{n=1}^{5}\frac{w^n-1}{n}\cdot H_n - A^2\cdot\Delta I(w,y)\,\right] \quad (119)$$

The integral

$$\Delta I(w,y) = 2\cdot\int_{1}^{w}\frac{dw\cdot w}{S^2}\cdot\left(1+A\cdot y\cdot\frac{w}{S}\right) \quad (120)$$

is evaluated in the Appendix I.

The coefficients of the gas-equation (109) A, B, $G_1,\ldots,H_5$ had been determined by adjusting the pressure to the subcritical values (see Fig. 18) and by demanding a "correct" pressure-shape at the critical point:

$$P = P_c \quad , \quad P_\varrho = 0 \quad , \quad \frac{\partial^2 P}{\partial \varrho^2} = 0 \quad , \quad \frac{\partial^3 P}{\partial \varrho^3} > 0 \qquad (121)$$

at $(\varrho_c, T_c)$.

These four equations determine A, B, $G_1$ and $G_2$. The rest of the set $G_3$ - $H_5$ were calculated to fulfill the requirements (97) resp. (98) in the domain

$$0{,}85 \cdot \varrho_c < \varrho < 1{,}1 \cdot \varrho_c$$

The remaining parts of the critical isotherm had been cut in four liquid and four dense-vapor areas, and in each area the $G_i$-s and $H_i$-s had been calculated (eq. (97), (98)) separately. The maximal deviations in P, and $P_T$ in these dense parts ($\varrho > 0.01$) have the magnitude 0.1 %.

For the description of the thermal conductivity of the gas the same approximations were set as in the compressed liquid resp. in the overheated vapor:

$$Q_T(\varrho, T) = Q_T(L, T^\times) \quad \text{f.} \quad \varrho \geq \varrho_c \qquad (122)$$

$$Q_T(\varrho, T) = Q_T(V, T^\times) \quad \text{f.} \quad \varrho < \varrho_c \; . \qquad (123)$$

## 11. Conclusions

The shape of the thermal and caloric properties of the sodium - evaluated in the foregoing chapters - are shown in the Figs. 27 - 41. The Figs. 27 - 37 are property-surfaces, giving a complete account of the temperature-specific volume dependence. On the Figs. 38 - 41 one of the relationships is given only in a parametric way.

The pressure surface of the STPS (Karlsruhe) is displayed on the Figs. 27, 28, 29, 38 and 39. Fig. 27 shows the pressure for temperatures above the boiling point in logarithmic scale. Fig. 28 is a small, near-critical part of the P-surface in linear scale. Fig. 29 presents the pressure in reduced form, i.e. the factor of reality, Z. Fig. 39 is, for the benefit of a customary $P^x(T)$-picture, in the log P(1/T)-dependence.

From all the sodium-properties given in this STPS it is the pressure, one can most safely depend upon. Not only is $P^x(T)$ based in the whole range on measurements, but so are also - in a smaller T-domain - the P-derivatives on the two-phase-border. Moreover the surface shows the correct, ideal-gas-behaviour for $V \cdot T \rightarrow \infty$ (see Fig. 29). Unappropriate P-values are expected only in two areas:

- in the compressed, nearly-critical liquid far from the saturated state and
- in the state of very hot gas.

The caloric equation of state is presented on the Figs. 30 - 36, 40 and 41. The Figs. 30 - 32 show three different views of the $C_V$-surface from the liquid, vapor and from the gas side in logarithmic scale. Figs. 40 and 41 are the corresponding $(V,C_V)$- resp. $(T,C_V)$-projections. Figs. 33 and 34 show a blown-up part of this surface near to the critical point in linear scale (the vertical walls on the Figs. 31 - 34 should indicate the infiniteness of the $C_V$ on the critical isotherm). The internal energy and the entropy - corresponding to this $C_V$ (eq. (22), (30)) are presented on the Figs. 35 and 36.

The $C_V$-surface of this STPS is secured by only one directly-measured data-

set /11/. It depends also heavily on the exact description of $d^2p^x/dT^2$, especially at low temperatures. So this surface is correct probably only in a qualitative way. In any case the currently available measured $C_v$-surfaces (/21/ describes the $C_v$ of the $CO_2$ in the two-phase and in the gaseous area, /22/ gives the two-phase $C_v$-surface of the n-Heptane) shows great similarities with the Figs. 30 - 34 (the $C_v$-ridge of the supercritical $CO_2$ lies much nearer to the critical isochore as it is on the Fig. 32).

As for the surface of the thermal conductivity (Fig. 37, for the $(V,Q_T)$-projection see Fig. 26), the greatest part of it is conjectural. Not only the measured data are scarce for this property but also there are not any cross-relations available with other thermal properties to check the calculated values. Still, the electrical conductivity measurements of the cesium /23/ disclose, that this property is also practically temperature-independent at densities in the liquid range.

So an assumption of a proportionality between the two conductivities at high temperatures too would give some support for the temperature-independent description of the $Q_T$ at high densities.

References

/1/ R. W. Ditchburn and J. C. Gilmour,
The Vapor Pressures of Monatomic Vapors, Revs. Mod. Phys. 13, 310 (1941).

/2/ M. M. Makansi, C. H. Muendel, and W. A. Selke,
Determination of the Vapor Pressure of Sodium, J. Phys. Chem. 59, 40 (1955).

/3/ J. P. Stone, C. T. Ewing, J. R. Spann, E. W. Steinkuller, D. D. Williams, R. R. Miller,
High-Temperature Vapor Pressures of Sodium, Potassium, and Cesium,
J. Chem. and Eng. Data, 11, 315 (1966).

/4/ V. S. Bhise and C. F. Bonilla,
The Experimental Vapor Pressure and Critical Point of Sodium,
Proc. Int. Conf. on Liquid Metal Technology in Energy Production,
CONF-760503-P2 Champion, PA, May 1976.

/5/ J. P. Stone et al.,
High Temperature Specific Volumes of Liquid Sodium, Potassium, and Cesium, J. Chem. and Eng. Data, 11, 321 (1966).

/6/ J. P. Stone et al.,
High Temperature PVT Properties of Sodium, Potassium, and Cesium,
Ibid., p. 309.

/7/ C. T. Ewing, J. P. Stone, J. R. Spann, R. R. Miller,
High-Temperature Properties of Cesium, J. Chem. and Eng. Data, 11, 474 (1966).

/8/ C. T. Ewing et al.,
High-Temperature Properties of Sodium, Ibid., p. 468.

/9/ L. Leibowitz, M. G. Chasanov, R. Blomquist,
Speed of Sound in Liquid Sodium to 1000°C, J. of Appl. Phys. 42, p. 2135 (1971).

/10/ M. G. Chasanov, L. Leibowitz, D. F. Fischer, R. Blømquist, Speed of Sound in Liquid Sodium from 1000 to 1500°C, J. of Appl. Phys. 43, p. 748 (1972).

/11/ D. C. Ginnings, T. B. Douglas, A. F. Ball, J. Res. Natl. Bur. Stds., 45, 23 (1950).

/12/ G. H. Golden, J. V. Tokar, Thermophysical Properties of Sodium, ANL-7323, Argonne (1967).

/13/ D. L. Timrot, V. V. Makhrov, V. I. Sviridenko, Method of the Heated Filament for Use in Corrosive Media..., High Temperature, 14, 58 (1976).

/14/ B. I. Stefanov, D. L. Timrot, E. E. Totskii, and Chu Wen-hao, Viscosity and Thermal Conductivity of the Vapors of Sodium and Potassium, High Temperature 4, 131 (1966).

/15/ A. L. Sengers, R. Hocken, J. V. Sengers, Critical-Point Universality and Fluids, Physics Today, December 1977, p. 42.

/16/ Yu. E. Sheludryak, V. A. Rabinovich, On the Values of the Critical Indices of the Three-Dimensional Ising Model, High Temperature, 17, 40 (1979).

/17/ P. E. Liley, Correlations for the Thermal Conductivity and Latent Heat of Saturated Fluids near the Critical Point, Proc. Fifth Symp. on Therm. Prop., Boston, 1970.

/18/ J. S. Rowlinson, Liquids and Liquid Mixtures, 2nd Edition Plenum Press, New York, 1969.

/19/ Kh. I. Amirkhanov, B. G. Alibekov, B. A. Mursalov, G. V. Stepanov, Calculation of the Derivatives of Thermal and Caloric Quantities on a Saturation Line, High Temperature, 10, 475 (1972).

/20/ O. A. Hougen, K. M. Watson and R. A. Ragatz, Chemical Process Principles - Vol. II, Thermodynamics, 2nd Ed., John Wiley (1959).

/21/ Kh. I. Amirkhanov, N. G. Polikhronidi, B. G. Alibekov, R. G. Batyrova, Isochoric Specific Heat-Capacity of Carbon Dioxide, Thermal Engineering, 18, 87 (1971).

/22/ Kh. I. Amirkhanov, B. G. Alibekov, D. I. Vikhrov, V. A. Mirskaya, L. N. Levina, V. A. Antonov, Investigation of the Heat Capacity $C_v$ of n-Heptane in the Two-Phase Region... High-Temperature, 11, 59 (1973).

/23/ H. Renkert, F. Hensel, E. U. Franck, Elektrische Leitfähigkeit flüssigen und gasförmigen Cäsiums bis 2000°C und 1000 bar, Ber. Bunsenges. physik. Chem. 75, 507 (1971).

/24/ J. P. Stone et al., High-Temperature Properties of Sodium, NRL-6241, Naval Research Laboratory (1965).

/25/ D. Miller, A. B. Cohen, C. E. Dickerman, Estimation of Vapor and Liquid Density and Heat of Vaporisation of the Alkali Metals to the Critical Point, Proc. Int. Conf. on the Safety of Fast Breeder Reactors, Aix-en-Provence (1967).

/26/ A. Padilla Jr., High-Temperature Thermodynamic Properties of Sodium, ANL-8095 (1974).

/27/ A. Padilla Jr., Extrapolation of Thermodynamic Properties of Sodium to the Critical Point, Proc. 7th Symp. on Thermophysical Properties, Gaithersburg (1977).

Appendix G

Fitting the gas-equation at the critical point.

For the reduced pressure the description of the critical point (eq. (121)) takes the following shape:

$$Z = Z_C \quad , \quad \frac{\partial Z}{\partial w} = -Z_C \quad , \quad \frac{\partial^2 Z}{\partial w^2} = 2 \cdot Z_C \quad , \quad \frac{\partial^3 Z}{\partial w^3} = 6 \cdot ( \lambda - Z_C )$$

with $$\lambda = \frac{Z_C}{6} \cdot \frac{\varrho_C^3}{P_C} \cdot \frac{\partial^3 P}{\partial \varrho^3} \quad .$$

Z and $\partial Z/\partial W$ are defined with the eq. (109) and (113), the two other derivatives are

$$\frac{\partial^2 Z}{\partial w^2} = \frac{2 \cdot y \cdot A}{S^3} \cdot [ \, y \cdot A - w \cdot B \cdot ( 3 - w^2 \cdot B ) \, ] +$$

$$- \; y \cdot \sum_{n=1}^{5} n \cdot ( n - 1 ) \cdot F_n \cdot w^{n-2}$$

and

$$\frac{\partial^3 Z}{\partial w^3} = \frac{6 \cdot y \cdot A}{S^4} \cdot [ \, ( y \cdot A - 2 \cdot w \cdot B )^2 - B \cdot ( 1 - w^2 \cdot B )^2 \, ] +$$

$$- \; y \cdot \sum_{n=1}^{5} n \cdot ( n - 1 ) \cdot ( n - 2 ) \cdot F_n \cdot w^{n-3} \quad .$$

To simplify the critical-description new variables are introduced for A, B, G1 and G2:

$$\sigma = 1 - B$$

$$x = 1 + B - A$$

$$t = \sum_{n=1}^{5} G_n + Z_c - 1$$

$$- t \cdot u = \sum_{n=2}^{5} (n-1) \cdot G_n - 2 \cdot Z_c + 1$$

along with the abbreviations

$$g = \sum_{n=3}^{5} (n-1) \cdot \frac{n-2}{2} \cdot G_n + 3 \cdot Z_c - 1$$

and

$$h = \sum_{n=4}^{5} (n-1) \cdot \frac{n-2}{2} \cdot \frac{n-3}{3} \cdot G_n - 4 \cdot Z_c + 1 + \lambda \quad .$$

These equations turn the critical point description into the following form:

$$A = x \cdot t$$

$$\sigma = x \cdot (1 - u)$$

$$\sigma^2 - x = x^2 \cdot (g / t - u)$$

$$\sigma^3 - 2 \cdot \sigma \cdot x + x^2 = x^3 \cdot (g + h) / t \quad .$$

The first two of these equations give

$$x = 2 / N \qquad \text{with} \qquad N = 2 + t - u$$

so A and B can be calculated from t and u:

$$A = 2 \cdot t / N$$

$$B = ( t + u ) / N$$

The second two equations - from which t and u can be calculated - transform by eliminating x and $\sigma$ to

$$t^2 - t \cdot u \cdot ( 2 \cdot u - 1 ) + 2 \cdot g = 0 \qquad \text{resp.}$$

$$t^2 \cdot ( 2 \cdot u - 1 ) - t \cdot u \cdot ( 2 \cdot u^2 - 4 \cdot u + 1 ) - 2 \cdot ( g + h ) = 0 \,,$$

or in a simplified form

$$t^2 + t \cdot \frac{u}{1 + 2 \cdot u} + \frac{2 \cdot g - 4 \cdot ( g \cdot u + h )}{1 + 2 \cdot u} = 0$$

and

$$u^2 + u \cdot ( t - 2 \cdot g / t ) - 2 \cdot h / t = 0 \,.$$

To fit the gas equation at the critical point this system of coupled quadratic equations was solved (by iterations) using the best fit coefficients $G_3$ - $G_5$ in g and h. As $\lambda$ 0.0001 was used.

The solutions t and u give then beside A and B the coefficients $G_2$ and $G_1$ via the equation for-t·u resp. for t.

Appendix I

The Integral $$\Delta I = 2 \cdot \int_1^w \frac{dw \cdot w}{S^2} \cdot \left( 1 + a \cdot \frac{w}{S} \right)$$

The abbreviations s and a are here

$$S = 1 - a \cdot w + B \cdot w^2$$

resp. $$a = y \cdot A$$

To evaluate $\Delta I$ the following primitive functions are needed:

$$J_1(w) = \int^w \frac{dw}{S} = \frac{2}{\sqrt{\sigma}} \cdot \text{arc tg} \left( \frac{S'}{\sqrt{\sigma}} \right)$$

$$J_2(w) = \int^w \frac{dw}{S^2} = \frac{1}{\sigma} \cdot \left( \frac{S'}{S} + 2 \cdot B \cdot J_1 \right)$$

$$J_3(w) = \int^w \frac{dw}{S^3} = \frac{1}{\sigma} \cdot \left( \frac{S'}{2 \cdot S^2} + 3 \cdot B \cdot J_2 \right)$$

with $$S' = 2 \cdot B \cdot w - a$$

and $$\sigma = 4 \cdot B - a^2$$

With these functions the first term in $\Delta I$ turns to

$$\int^{W} \frac{dw \cdot w}{S^2} = \frac{1}{\sigma} \cdot \left( \frac{a \cdot w - 2}{S} + a \cdot J_1 \right)$$

and for the second one get

$$\int^{W} \frac{dw \cdot w^2}{S^3} = \frac{1}{3 \cdot B} \cdot \left[ \frac{1}{2 \cdot \sigma} \cdot \left( 3 \cdot a^2 \cdot J_2 - \frac{(2 \cdot \sigma - a^2) \cdot w + 2 \cdot a}{S^2} \right) + \right.$$

$$\left. + J_3 \right] = \frac{1}{2 \cdot B} \cdot \left( f \cdot J_2 + \frac{S' - w \cdot \sigma}{\sigma \cdot S^2} \right) =$$

$$= \frac{1}{\sigma} \cdot \left[ f \cdot J_1 + \frac{1}{2 \cdot B \cdot S} \cdot \left( f \cdot S' + \frac{S' - w \cdot \sigma}{S} \right) \right]$$

with $$f = (a^2 + 2B) / \sigma \quad ,$$

so the complete primitive function to $\Delta I$ is

$$I(w) = 2 \cdot \int^{W} \frac{dw \cdot w}{S^2} \cdot \left( 1 + a \cdot \frac{w}{S} \right) = \frac{1}{\sigma} \cdot \left[ 2 \cdot \xi \cdot J_1(w) + \varphi(w) \right]$$

with $$\xi = 6 \cdot a \cdot B / \sqrt{\sigma}$$

and $$\varphi(w) = \frac{1}{B \cdot S} \cdot \left( \xi \cdot S' - \sigma + a \cdot \frac{S' - \sigma \cdot w}{S} \right)$$

The difference corresponding to a w-difference

$$\Delta w = w - 1$$

is in the first function

$$\Delta \operatorname{arc\,tg}(S' / \sqrt{\sigma}) = \operatorname{arc\,tg}(\Delta w \cdot \sqrt{\sigma} / u) \quad .$$

Here is

$$u(w) = 2 \cdot x + (2 \cdot B - a) \cdot \Delta w$$

with

$$x = 1 + B - a \quad .$$

The corresponding $\varphi$-difference is

$$\Delta \varphi = \frac{\Delta w}{S \cdot x} \cdot \left[ g + 2 \cdot (a + \sigma) - \xi \cdot u + \frac{a}{S} \cdot (\sigma \cdot w - u) \right]$$

with

$$g(w) = [a \cdot \sigma + B \cdot (4 - 2 \cdot a + \sigma) \cdot \Delta w] / x$$

so the integral $\Delta I$ turns out to be

$$\Delta I = \frac{1}{\sigma} \cdot \left[ \frac{4 \cdot \xi}{\sqrt{\sigma}} \cdot \operatorname{arc\,tg}\left( \frac{\Delta w \cdot \sqrt{\sigma}}{u} \right) + \Delta \varphi \right] \quad .$$

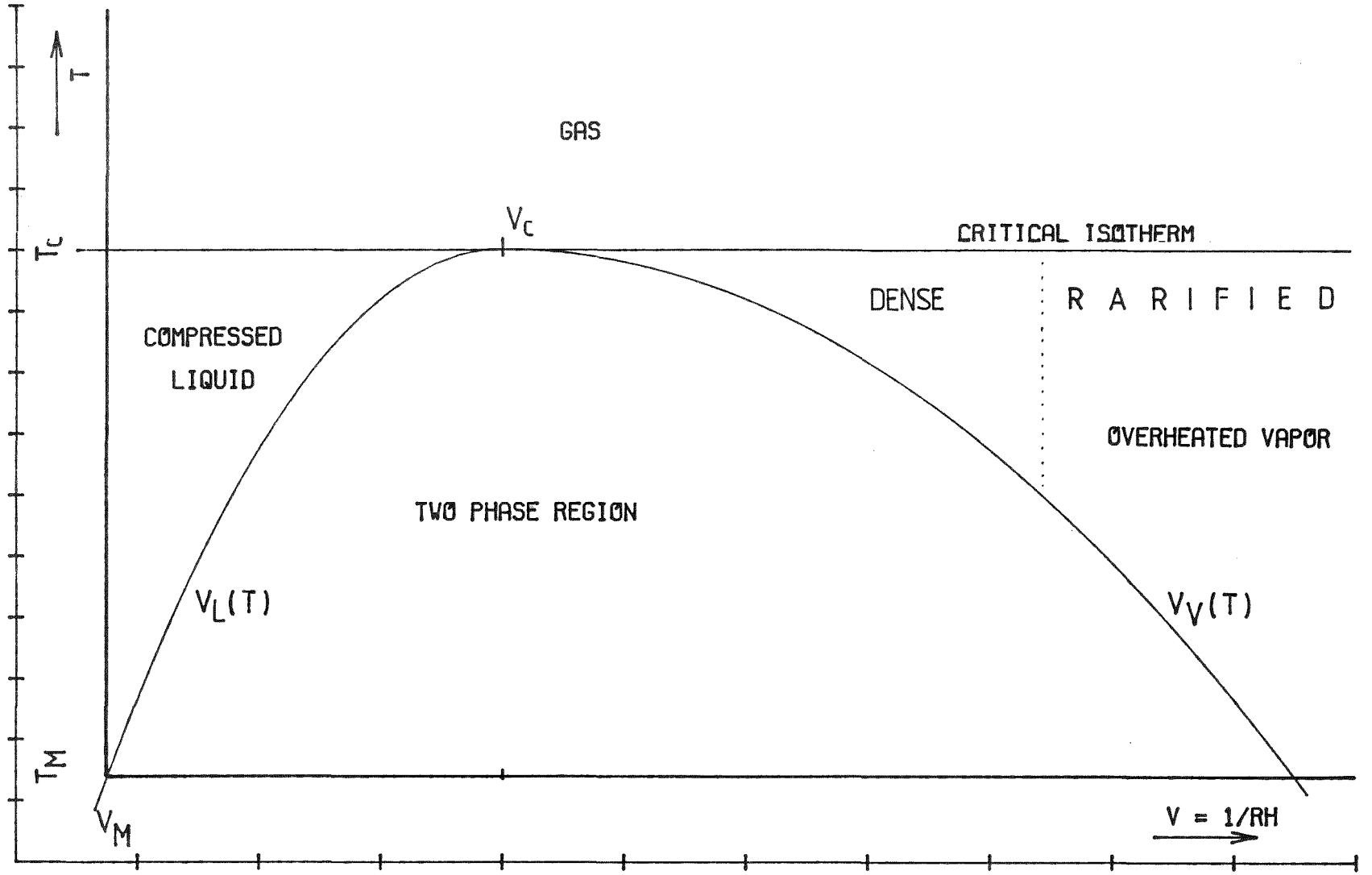


FIG. 1 SODIUM . RANGE OF VALIDITY OF THE THERMAL PROPERTIES

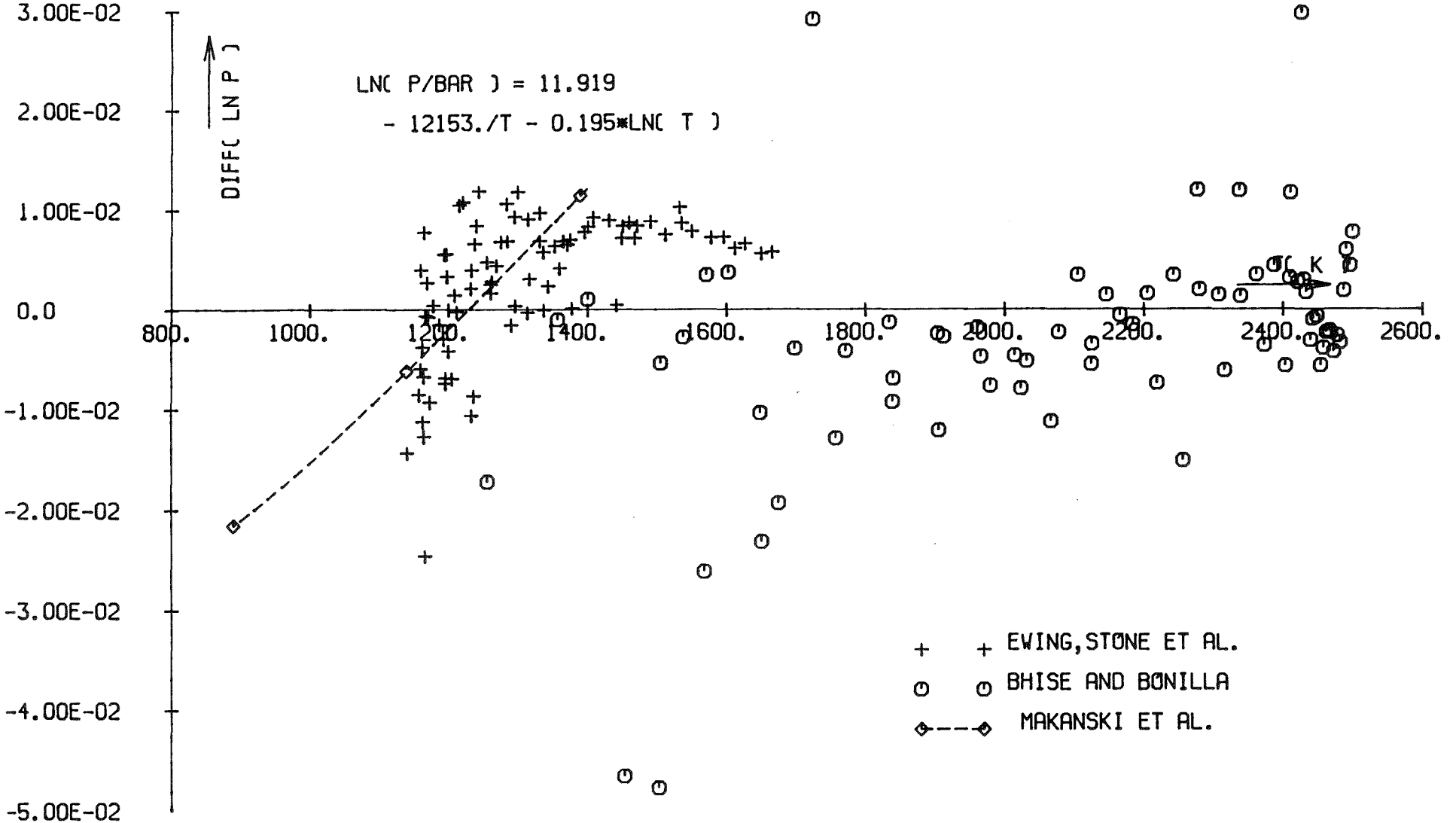


FIG. 2 SODIUM . DEVIATIONS FROM THE VAPOR PRESSURE EQUATION

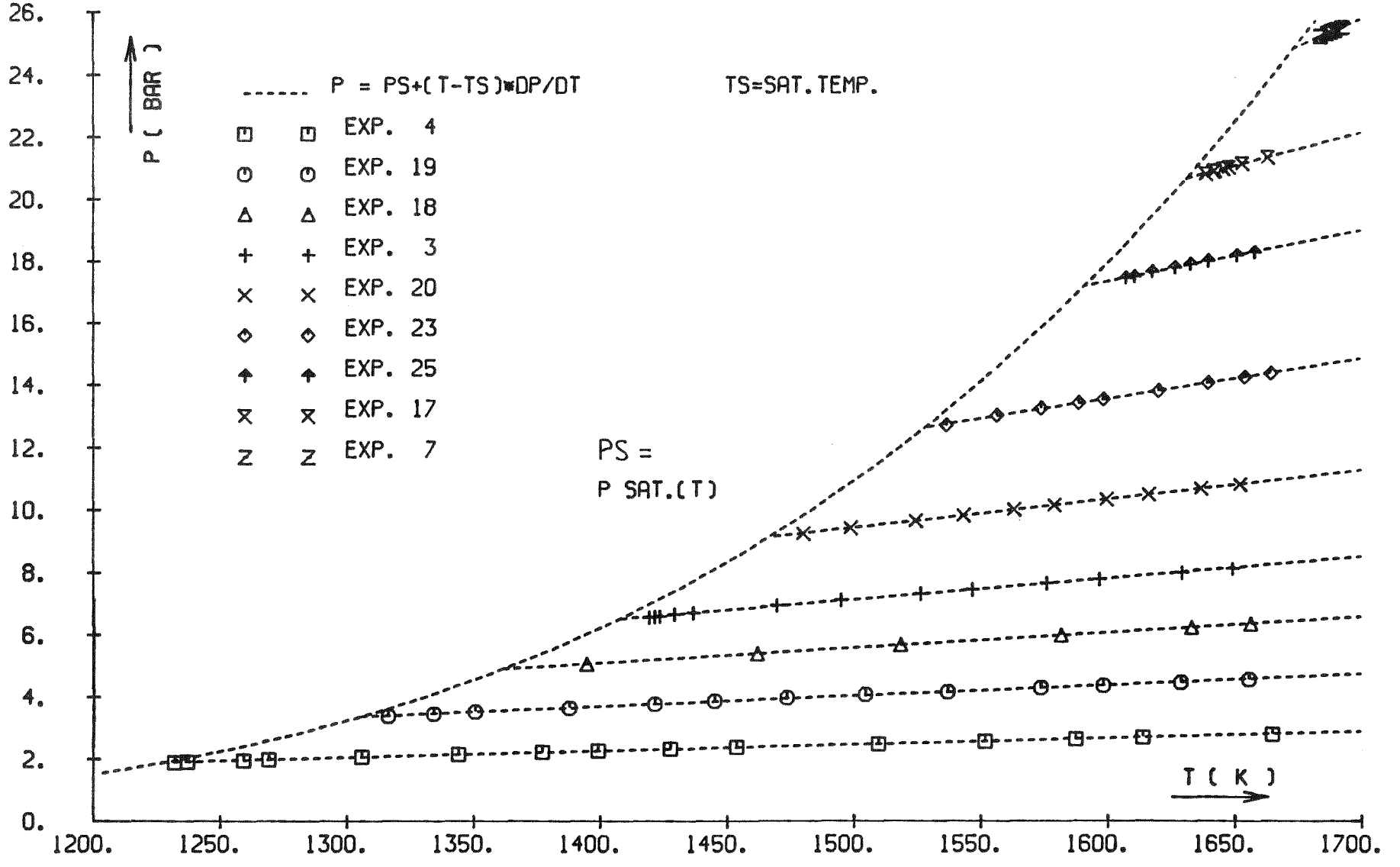


FIG. 3 P V T -PROPERTIES OF THE SODIUM VAPOR ( STONE & AL )

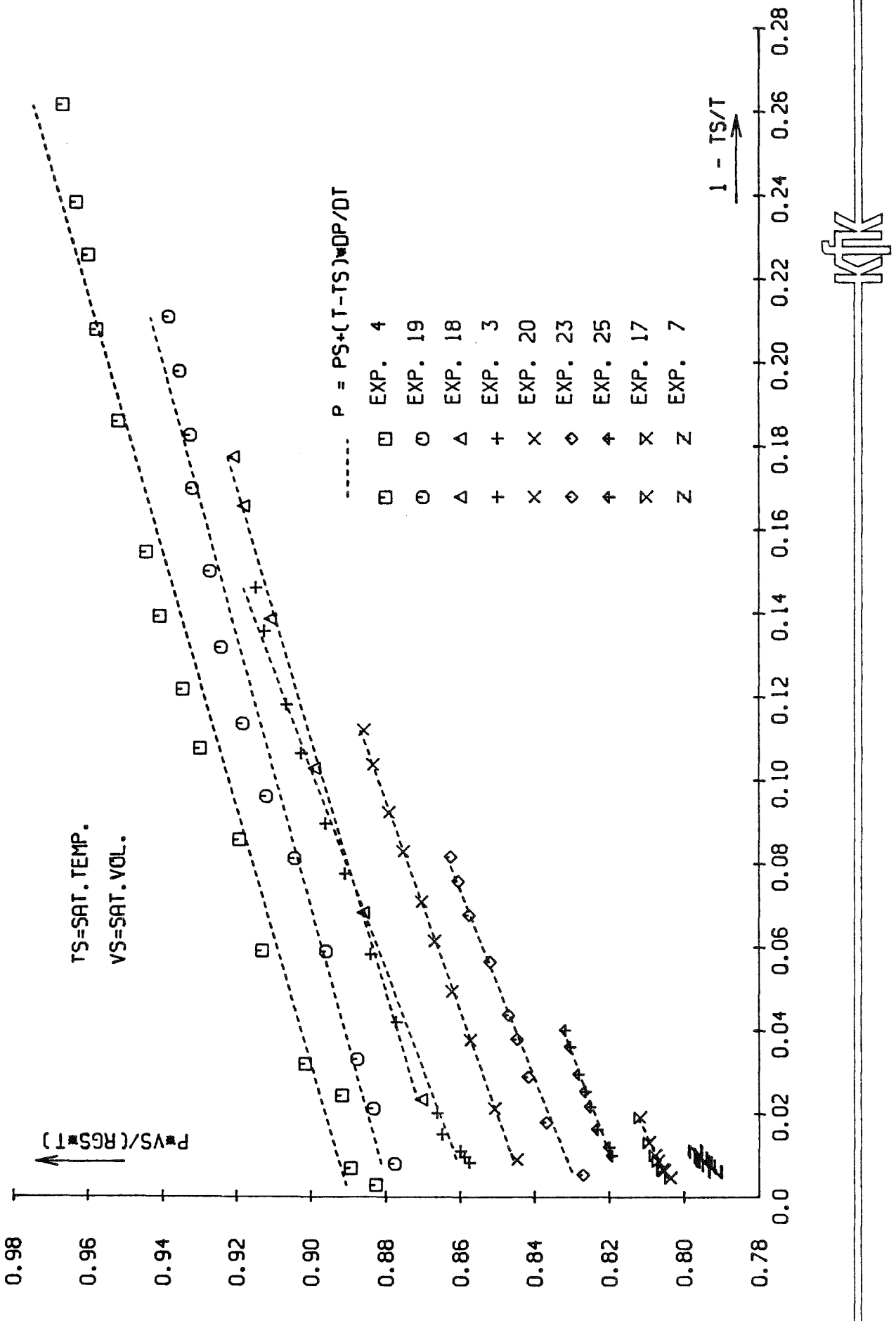


FIG. 4 REDUCED P V T -PROPERTIES OF THE SODIUM VAPOR

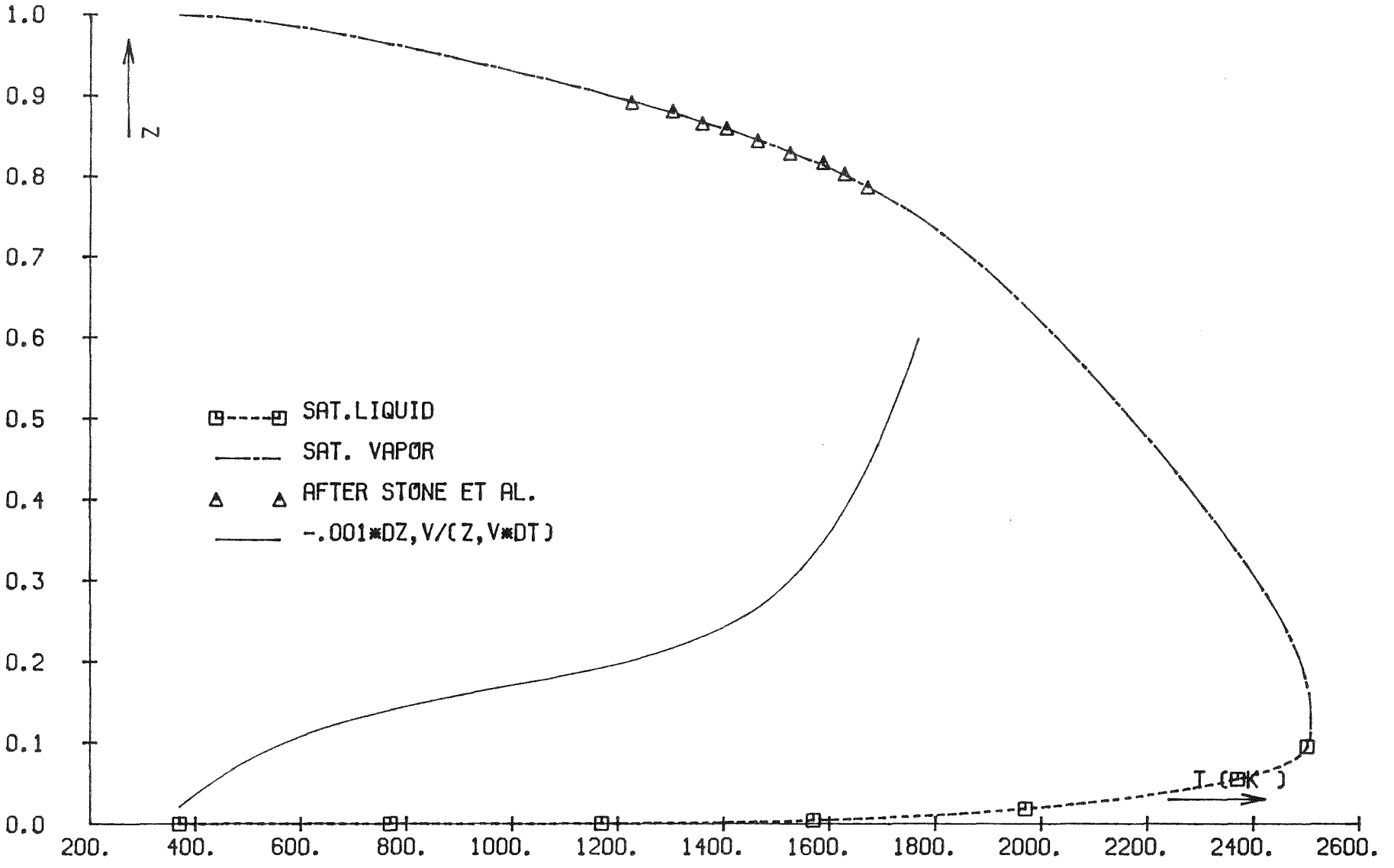


FIG. 5 FACTOR OF REALITY ( Z=P/(RGAS*RH*T) ) OF THE SODIUM

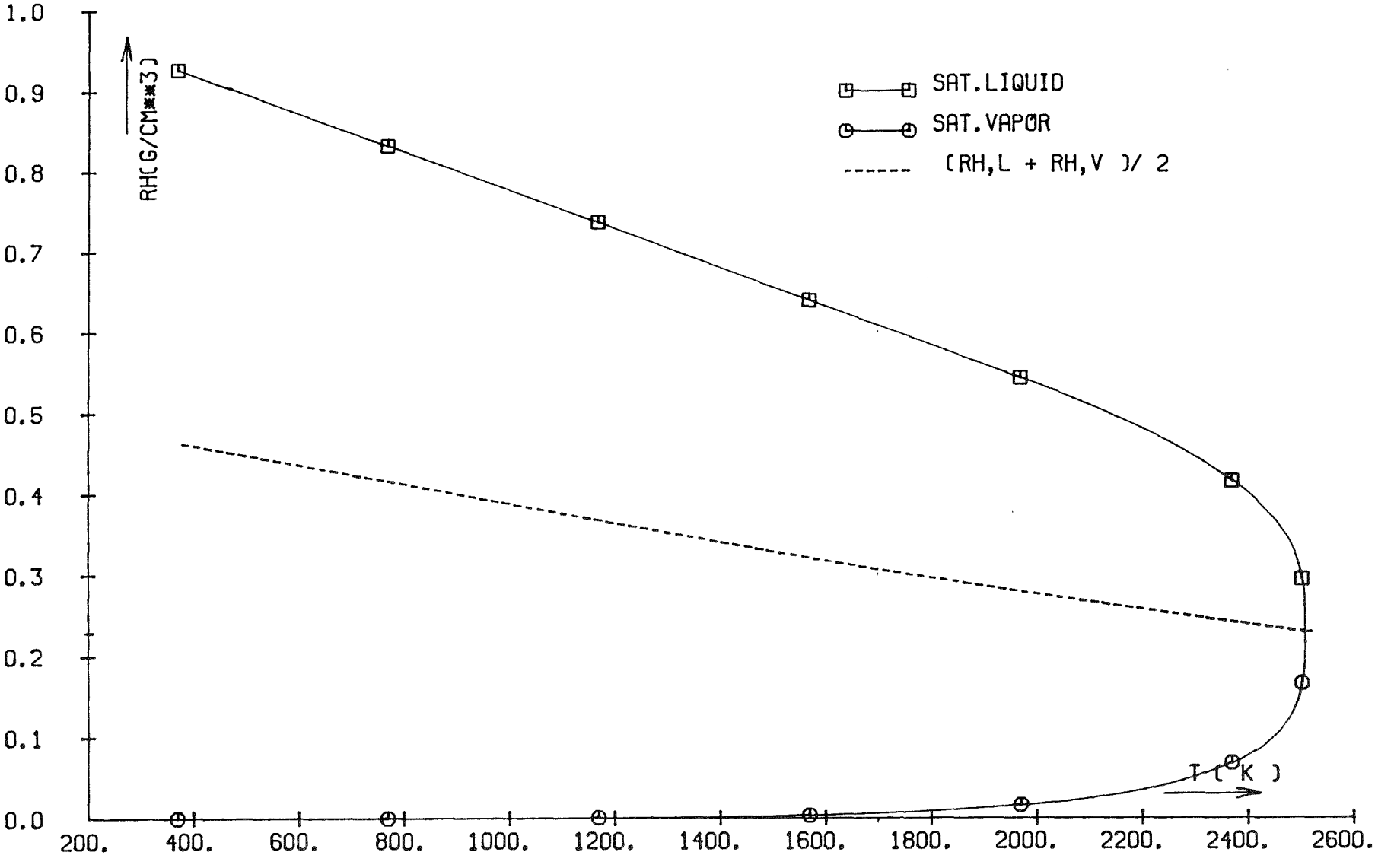


FIG. 6 THE SATURATION LINE OF THE SODIUM

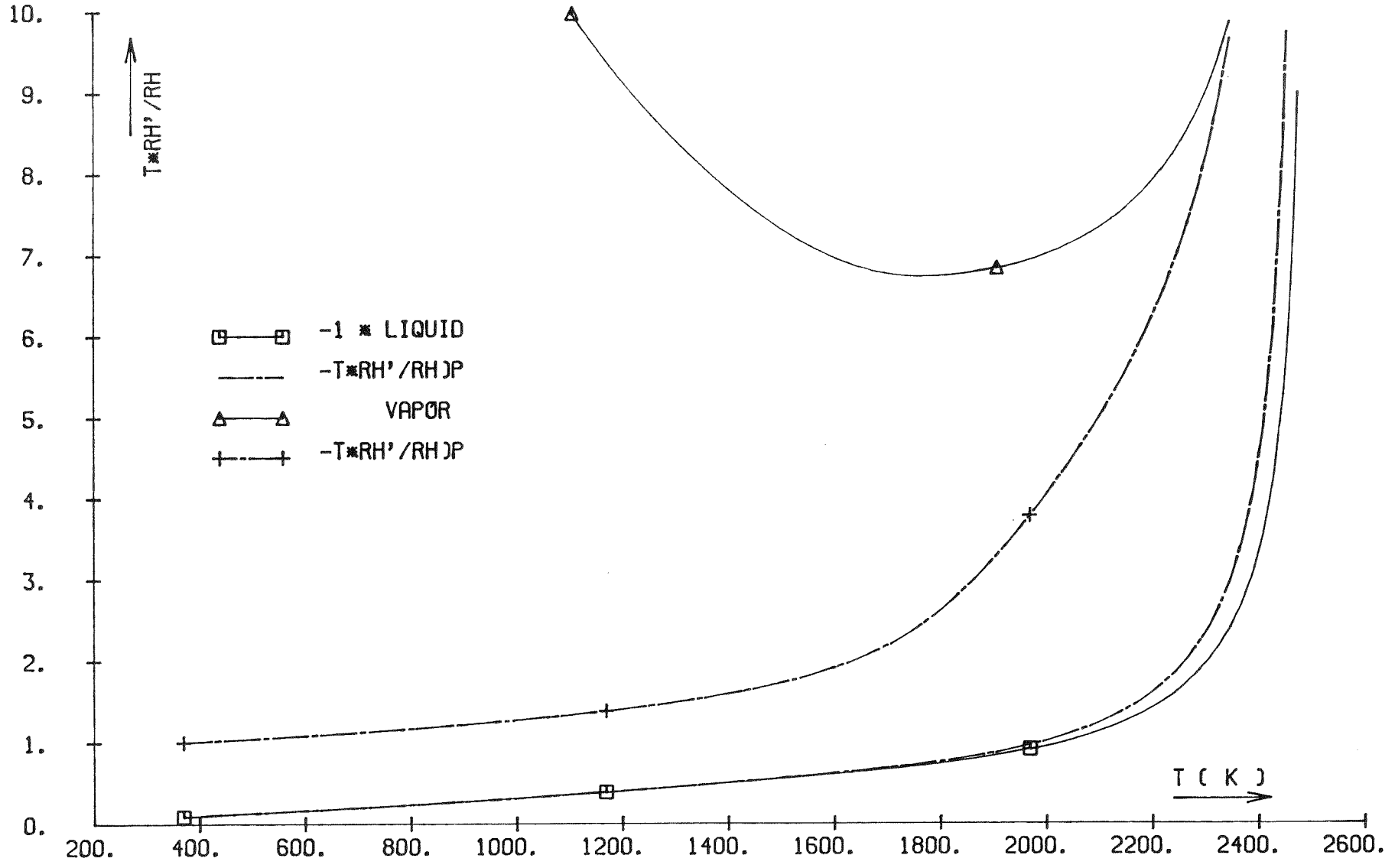


FIG. 7 SODIUM . T*D(RH)/(RH*DT) ON THE SAT.LINE

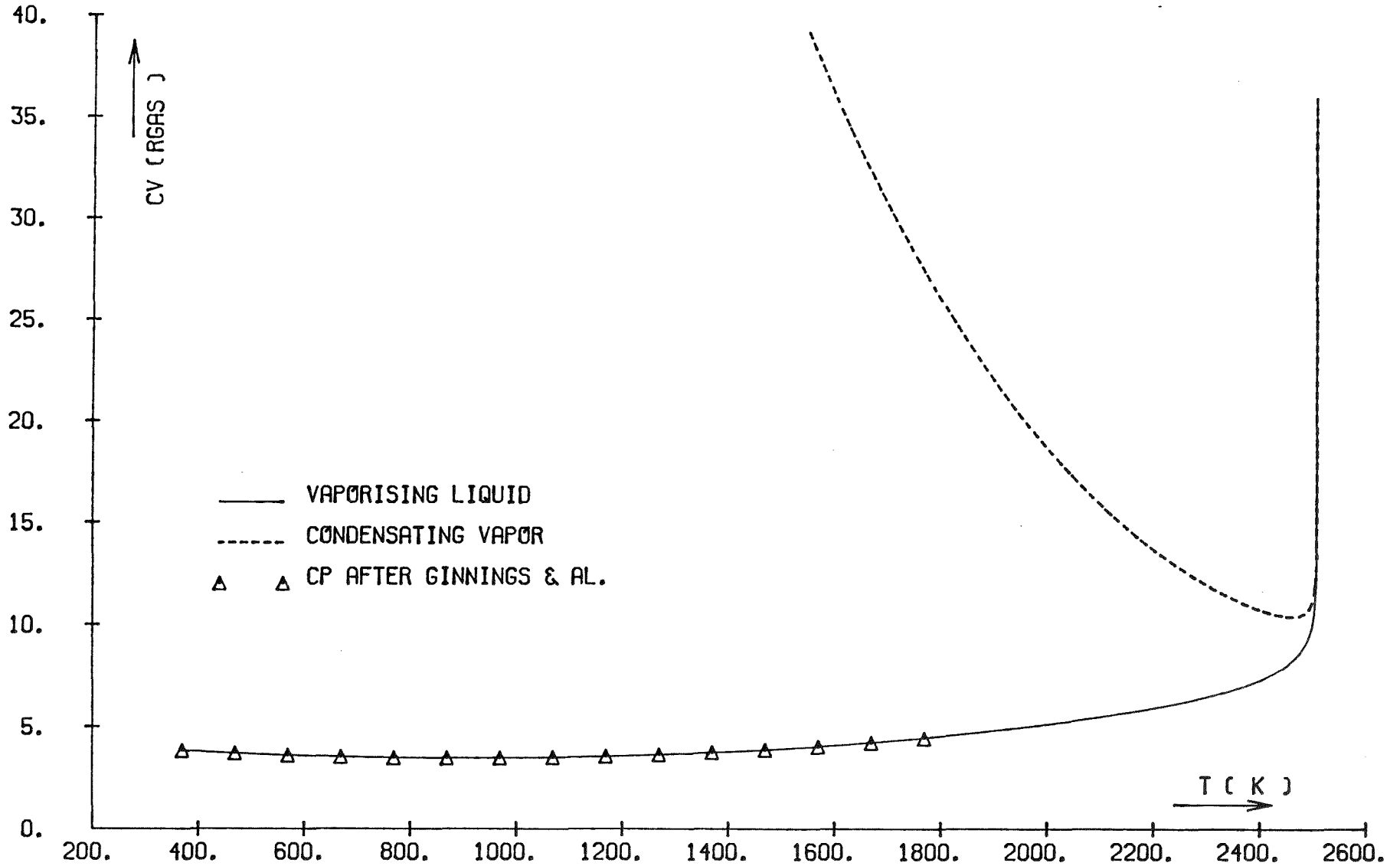


FIG. 8 CV(RH,L(T)-0,T) & CV(RH,V(T)+0,T) OF THE SODIUM

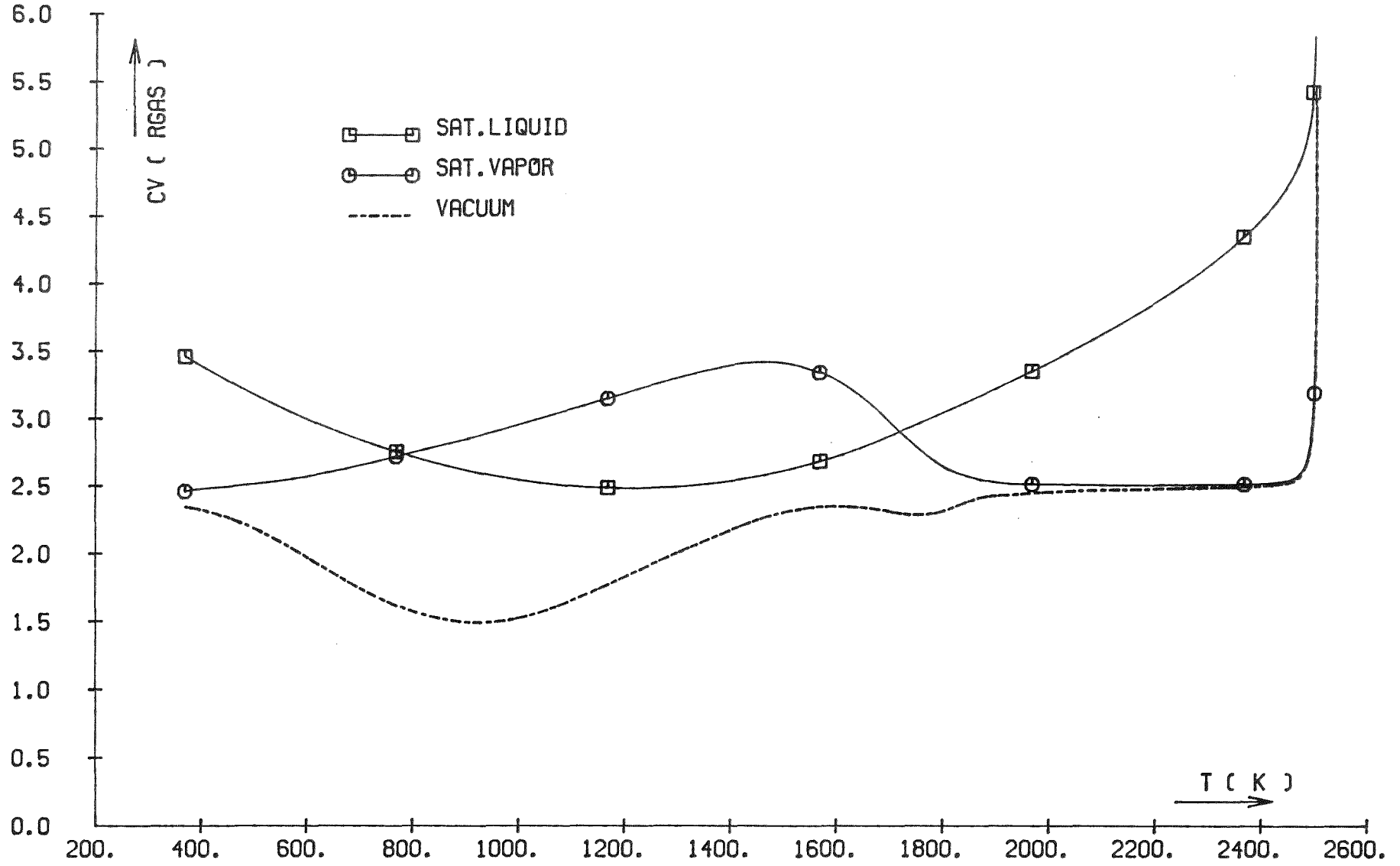


FIG. 9 SODIUM . HEAT CAPACITY AT CONST. VOLUME

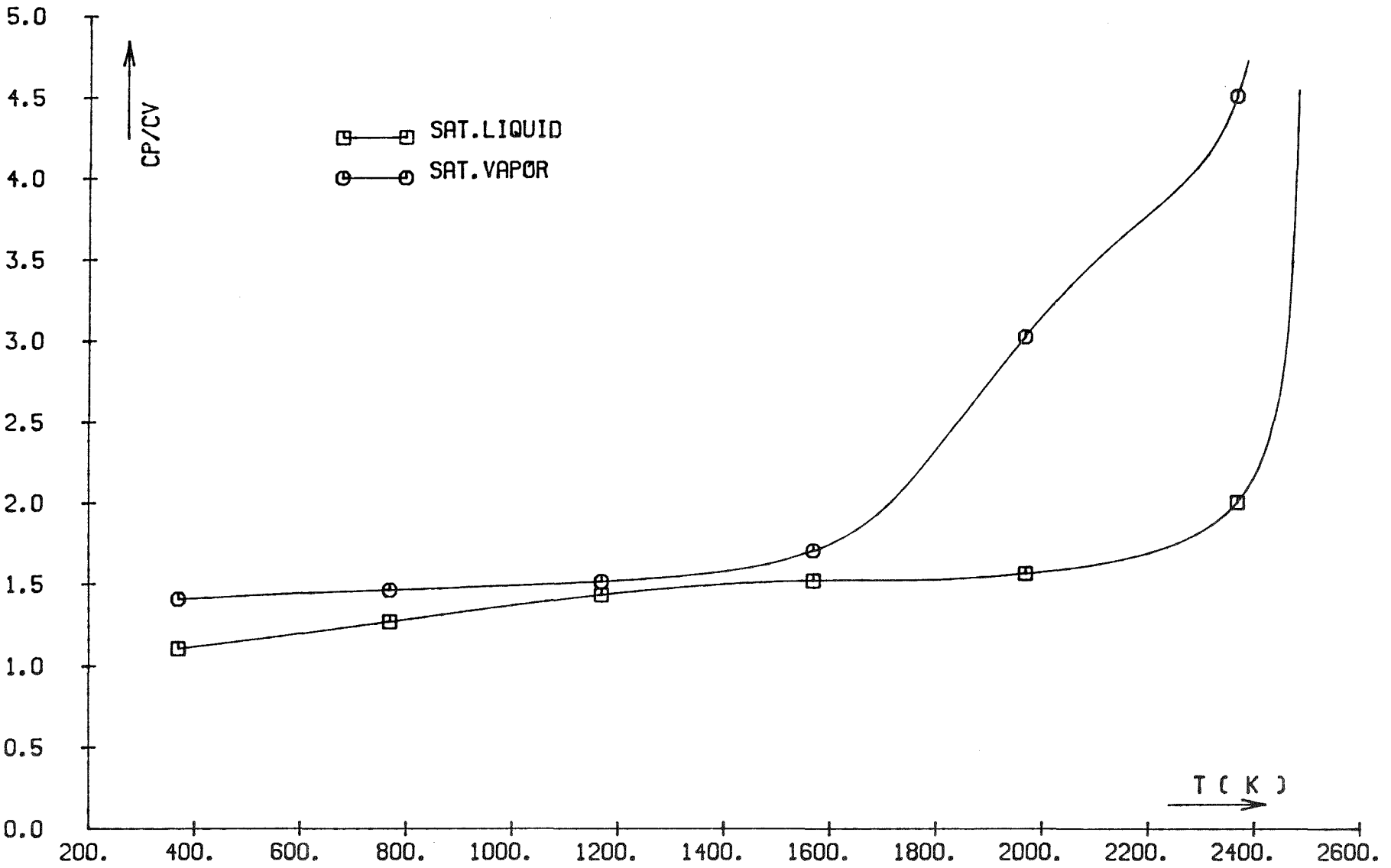


FIG. 10 SODIUM . CP/CV ON THE SATURATION LINE

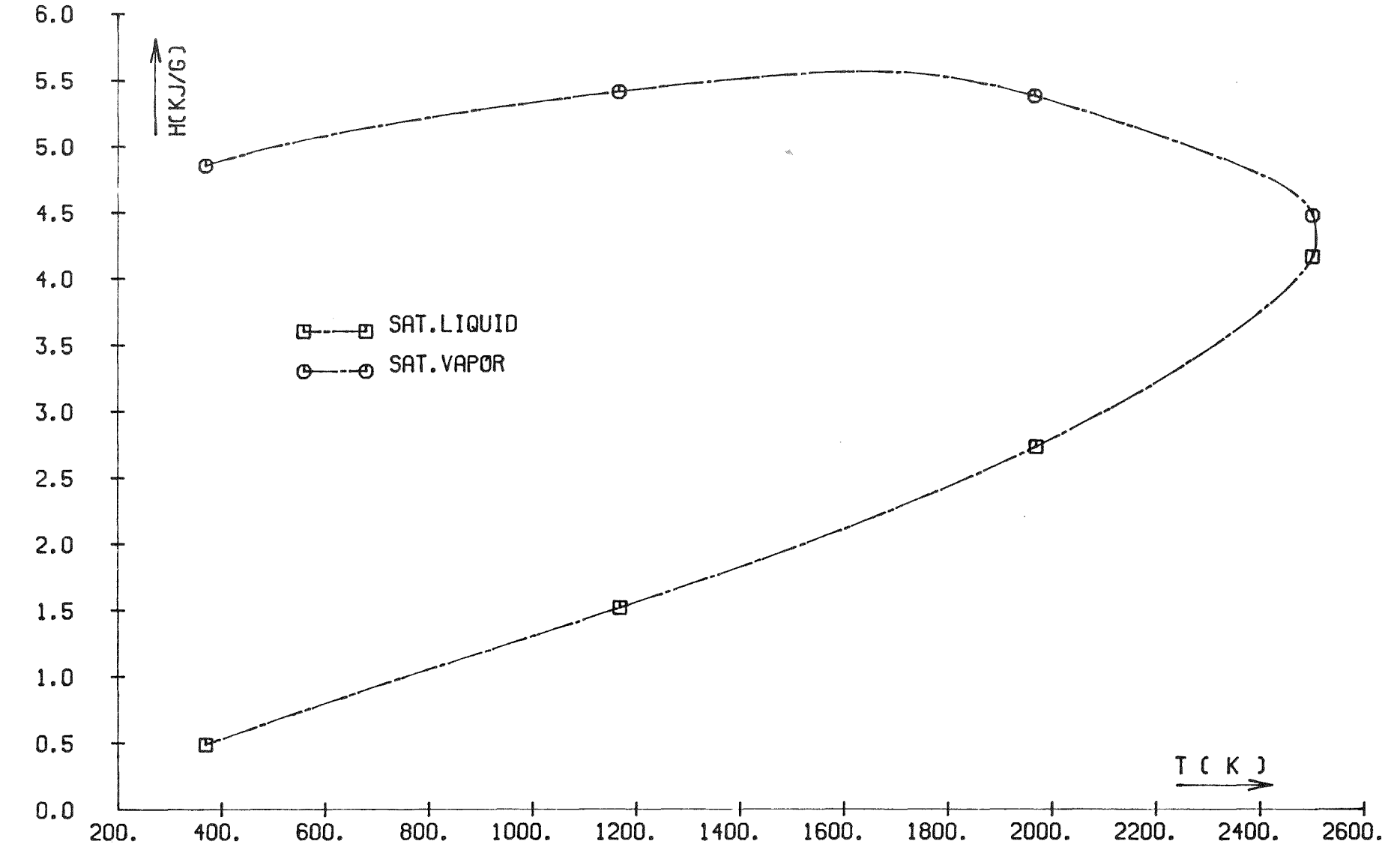


FIG. 11 SODIUM . THE ENTHALPY ON THE SAT. LINE

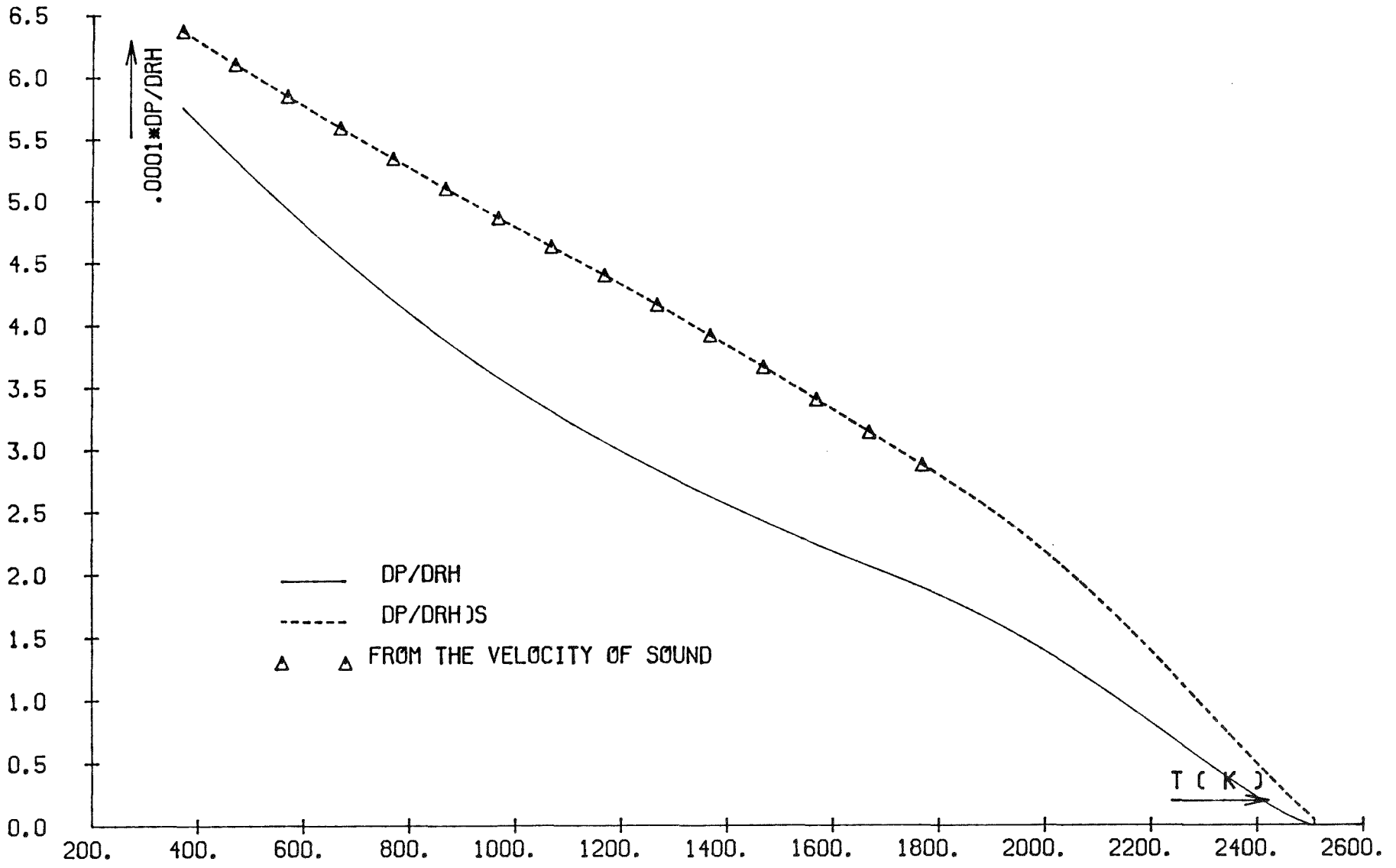


FIG. 12 DP/DRH & DP/DRHJS IN THE SATURATED LIQUID SODIUM

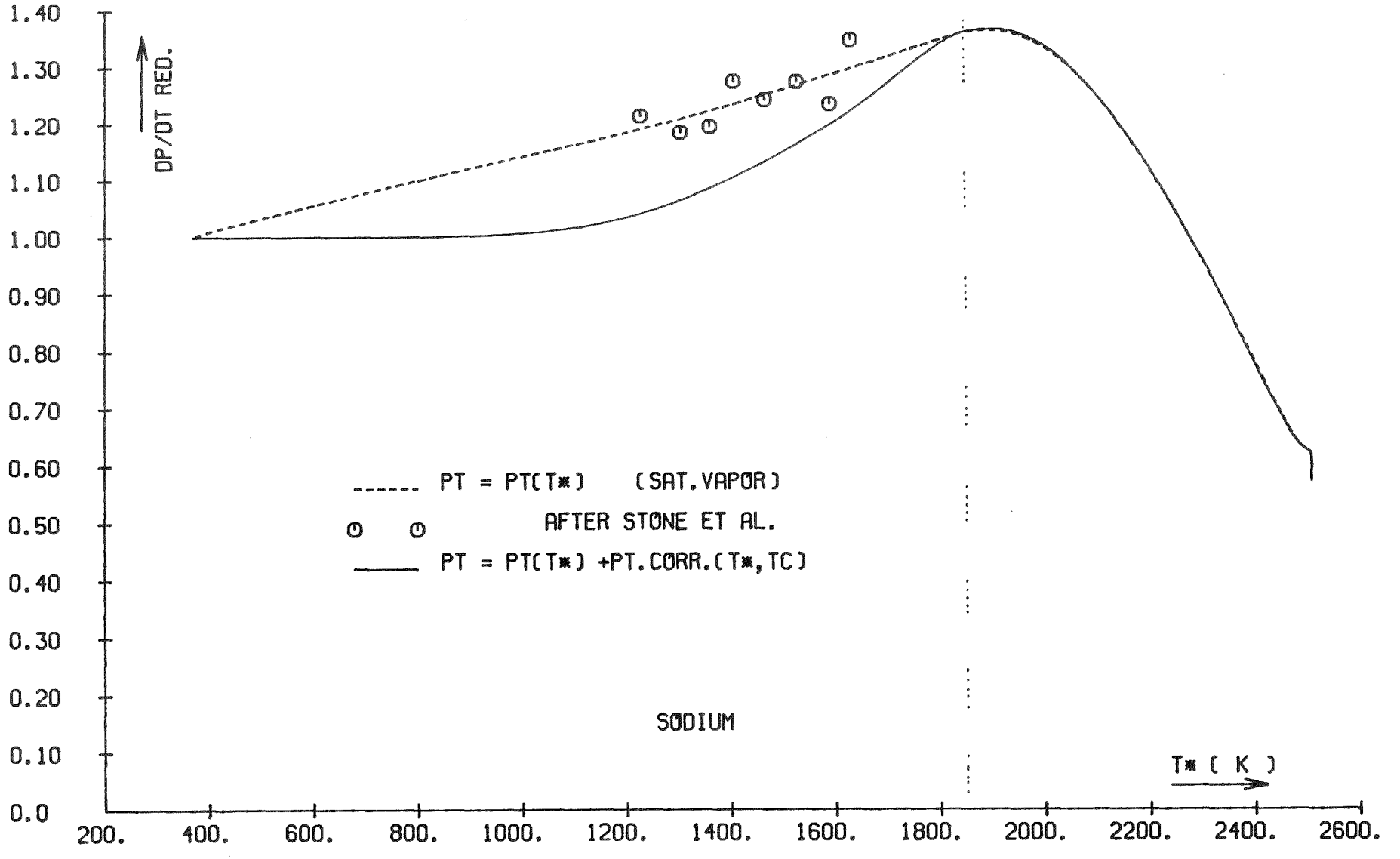


FIG. 13 PT(T*,T) ON THE VAPOR SIDE OF THE CRITICAL ISOTHERM

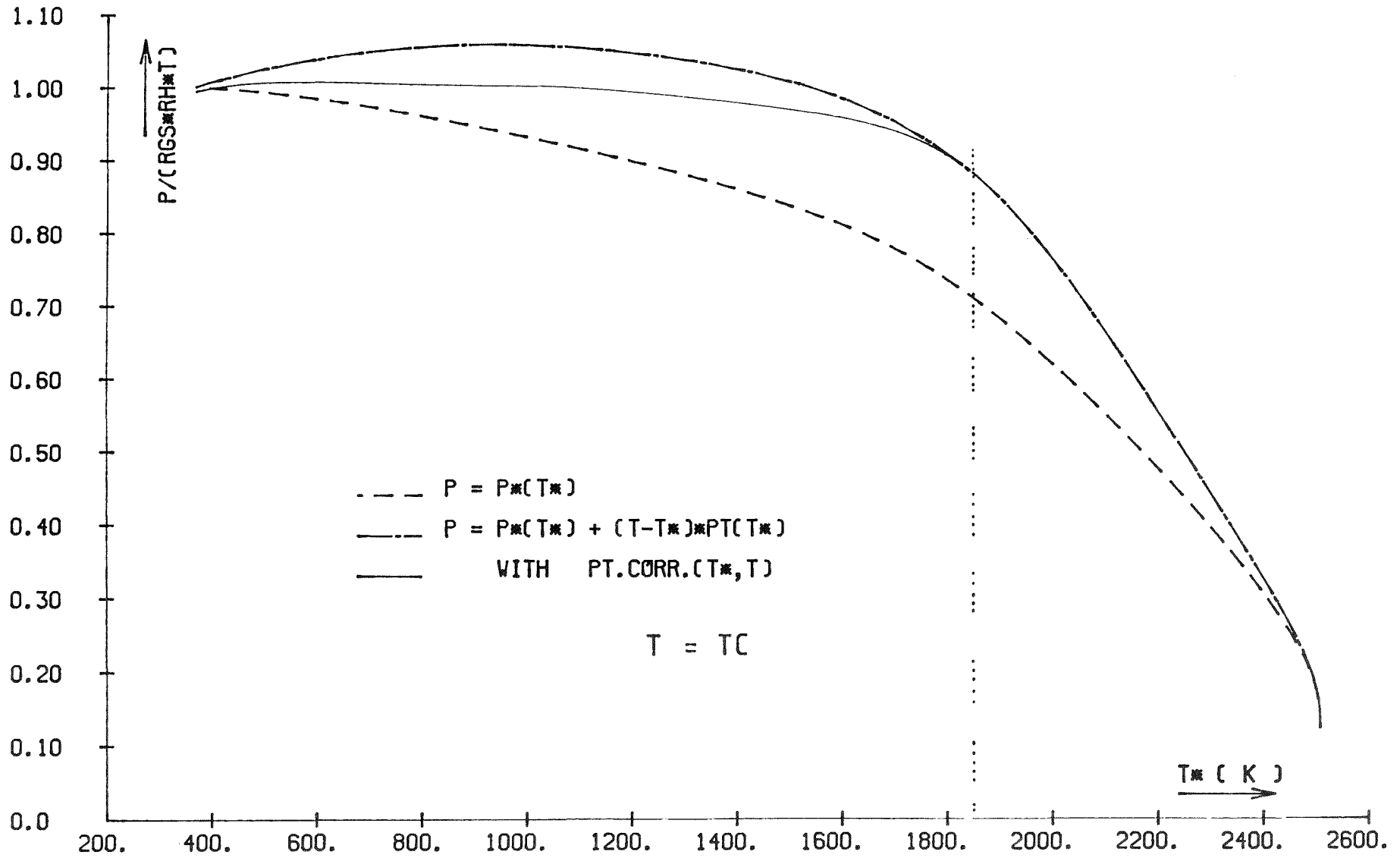


FIG. 14 SODIUM . P (T*) ON THE VAPOR SIDE OF THE CRITICAL ISOTHERM




FIG. 15 DP/(RGAS*RH*DT) IN THE SATURATED LIQUID SODIUM

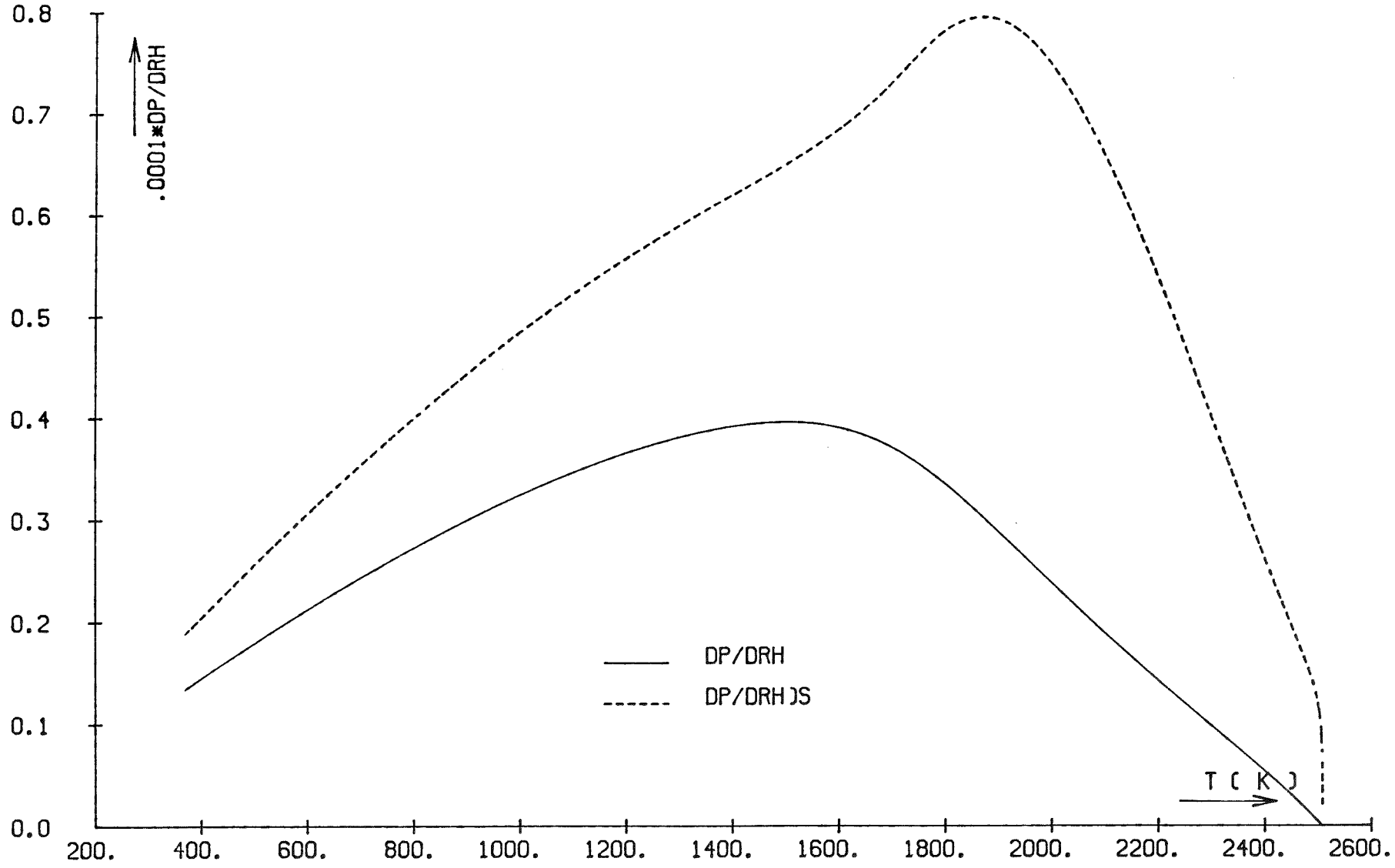




FIG. 16 DP/DRH & DP/DRH)S IN THE SAT.VAPOR OF THE SODIUM

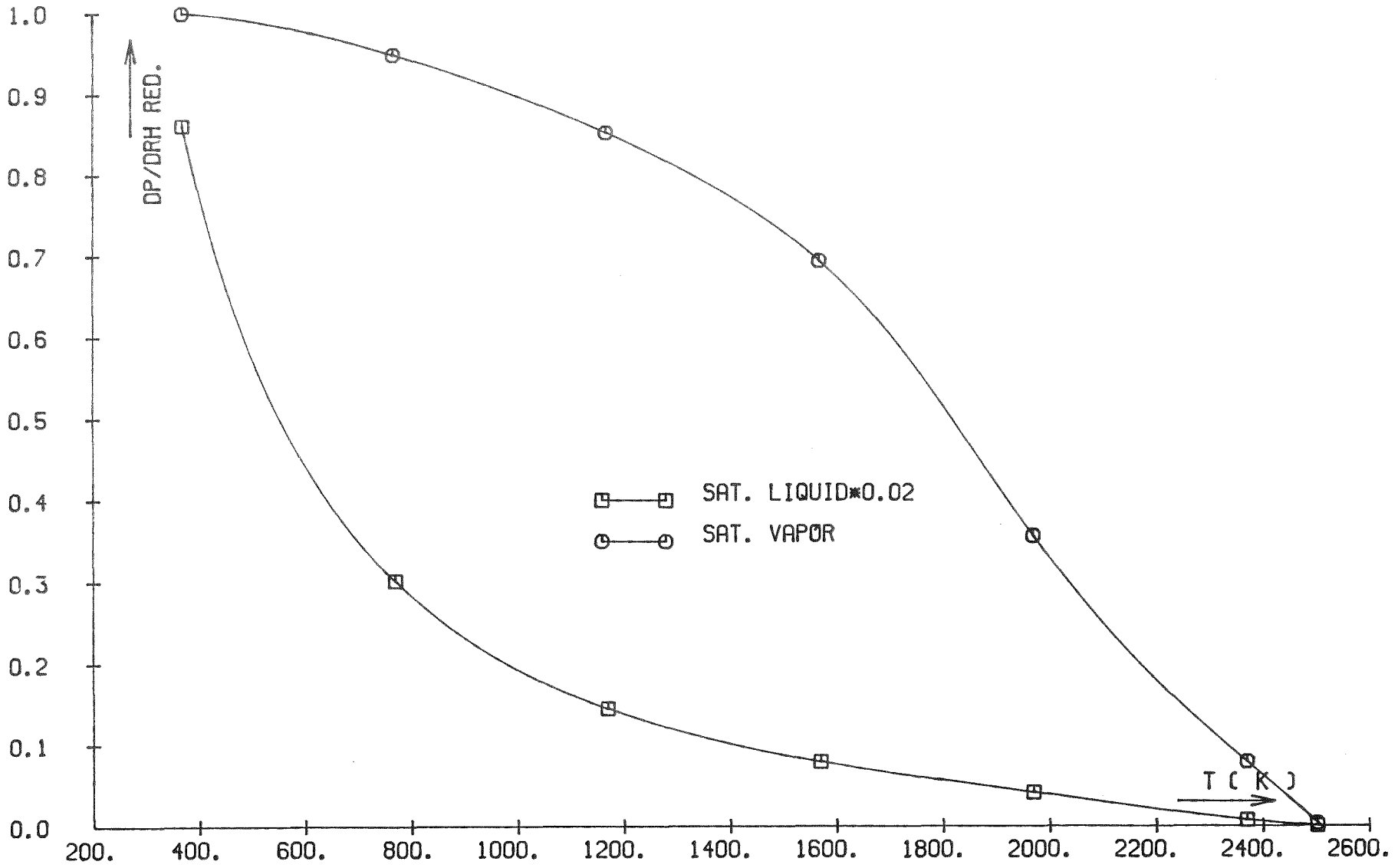


FIG. 17 DP/(RGAS*T*DRH) OF THE SATURATED SODIUM

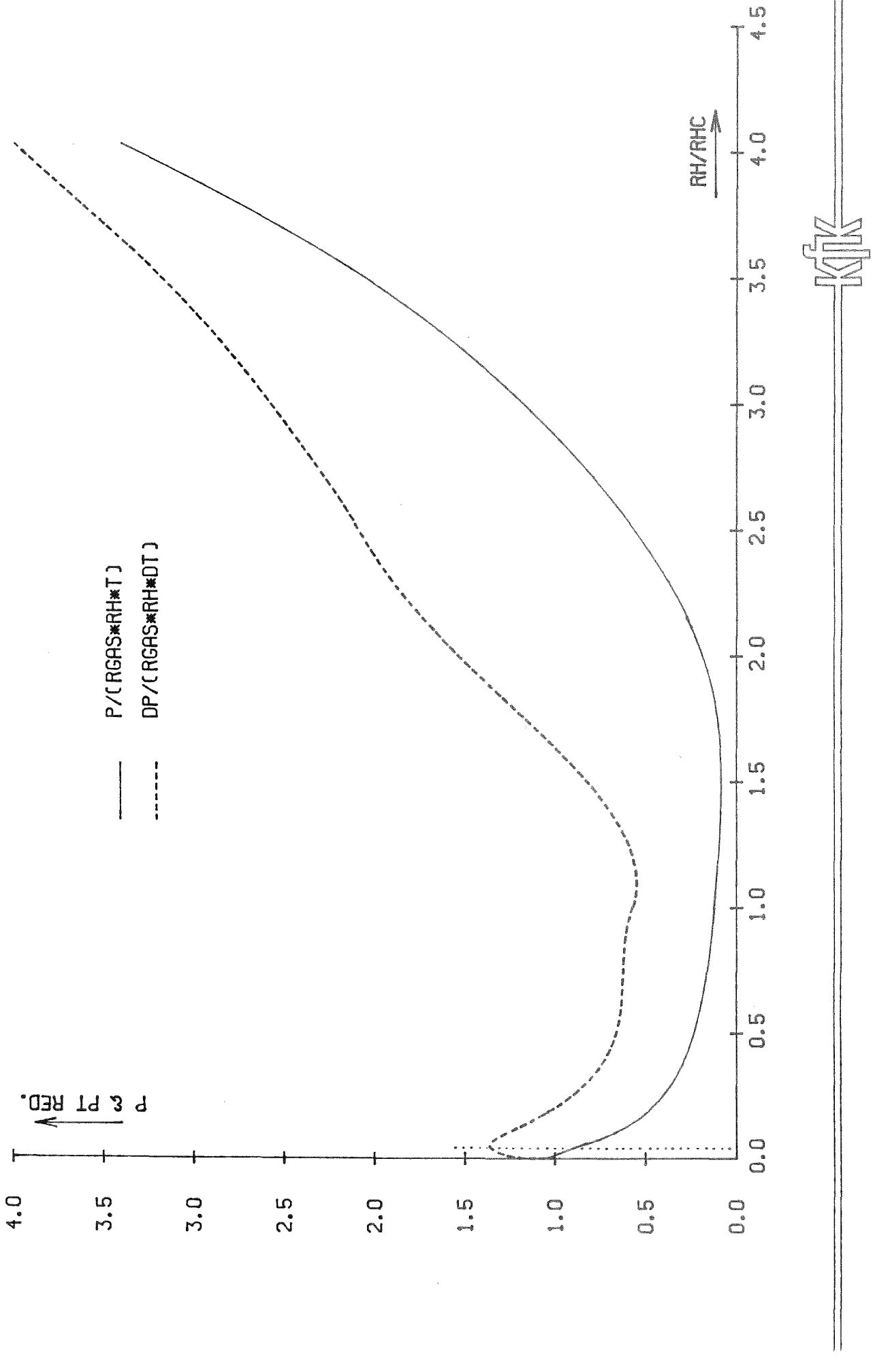


FIG. 18 SODIUM . P AND DP/DT ON THE CRITICAL ISOTHERM

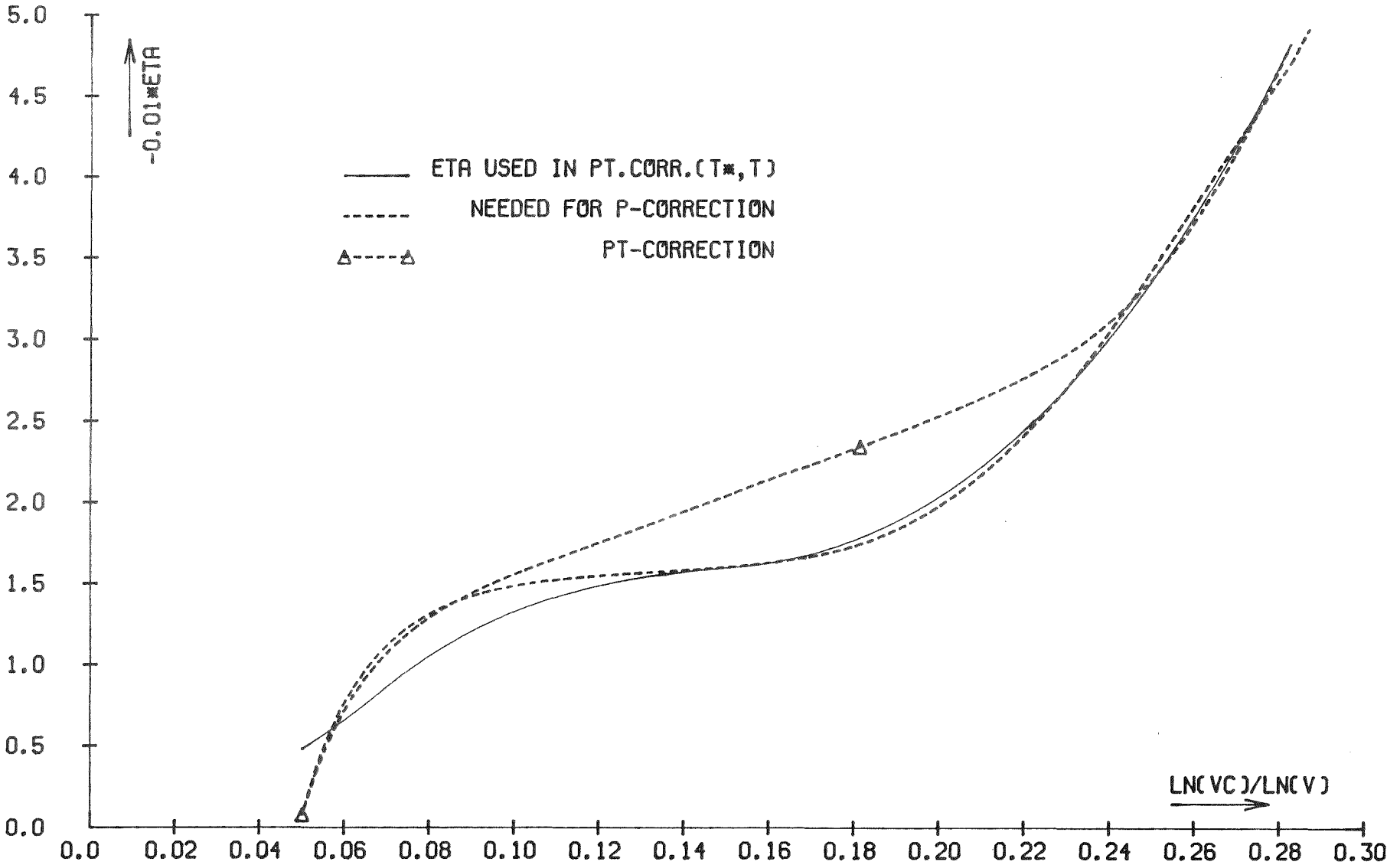




FIG. 19 SODIUM VAPOR . CORRECTING FACTOR ETA

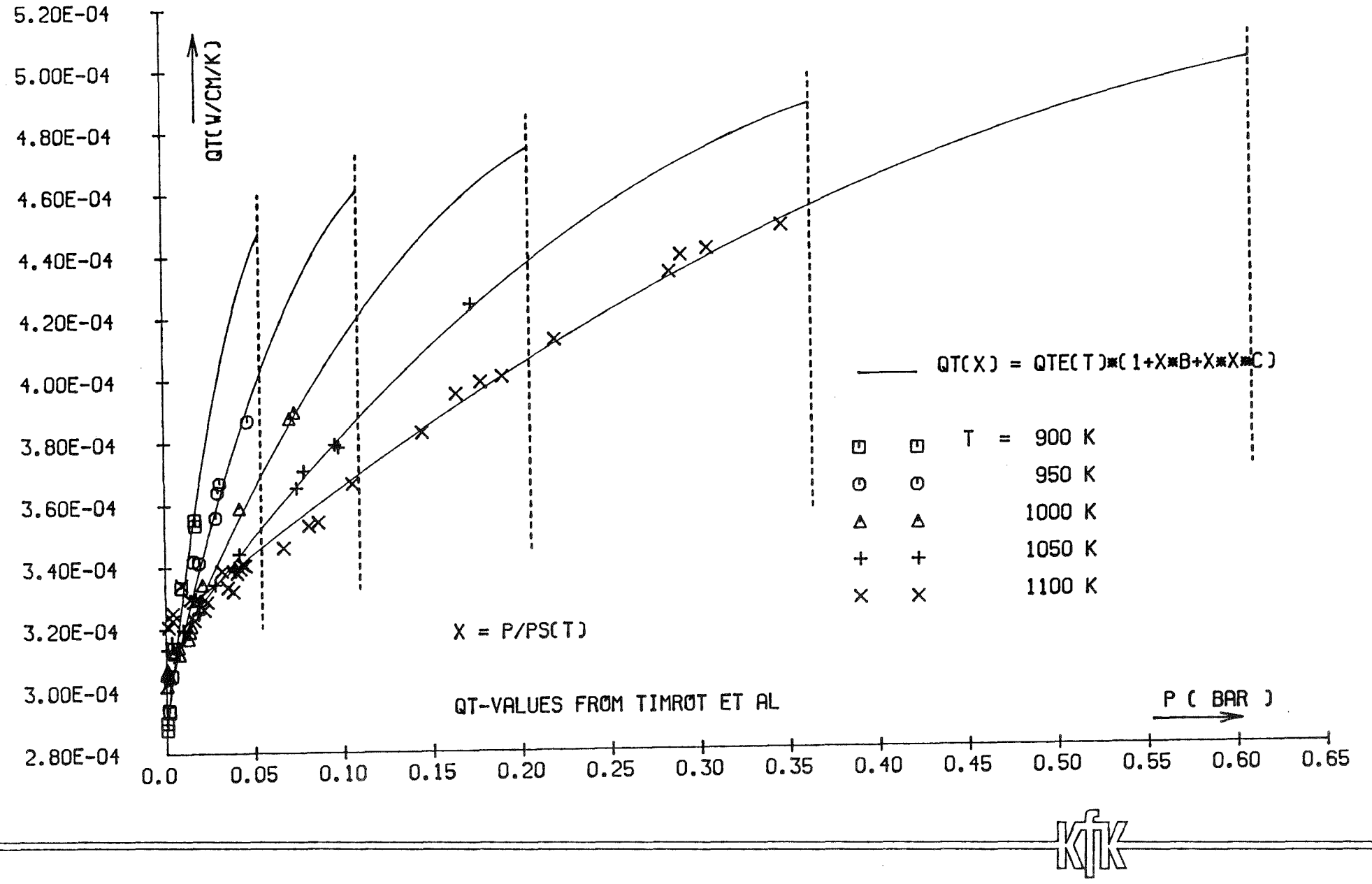


FIG. 20 THERMAL CONDUCTIVITY OF THE SODIUM VAPOR

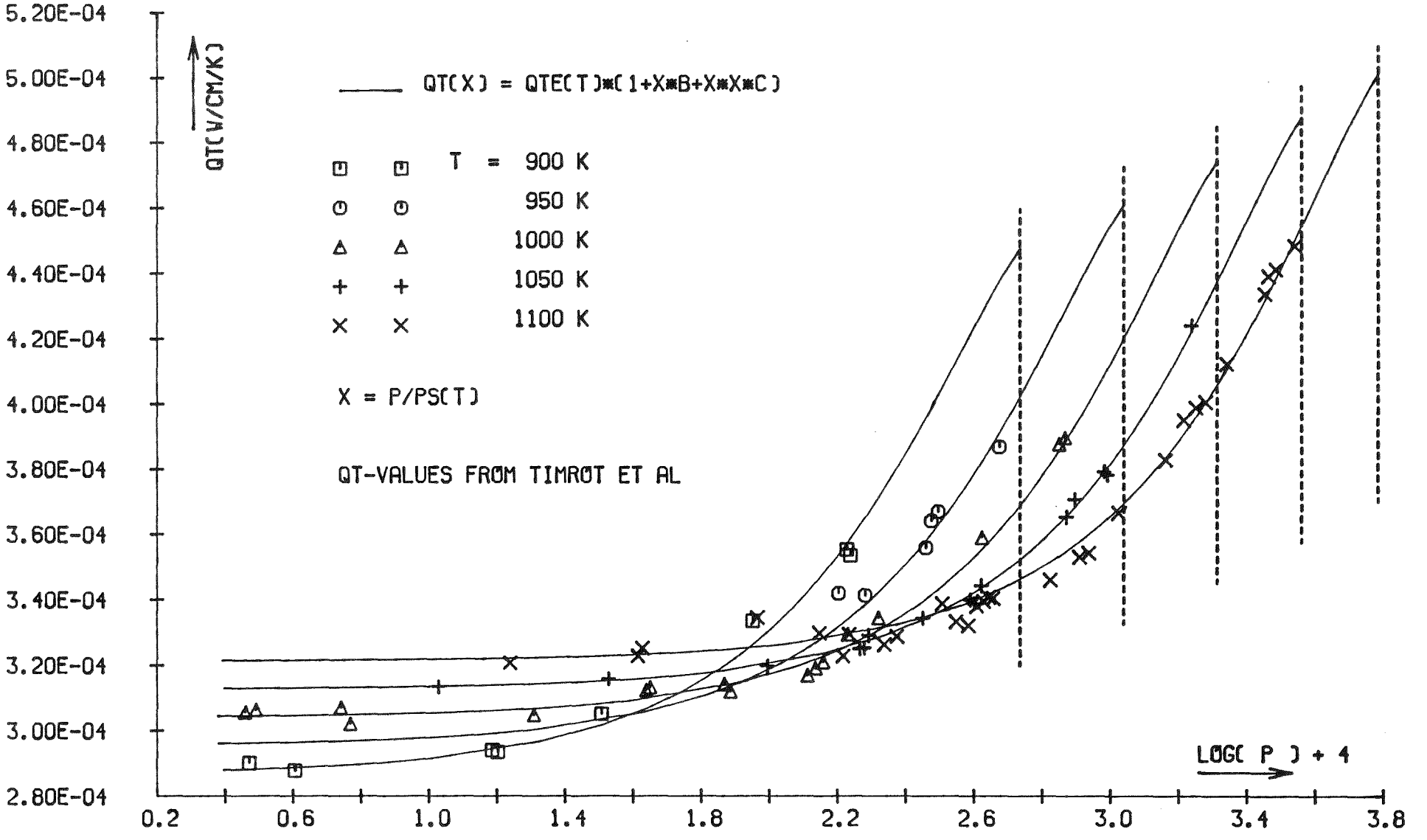


FIG. 21 THERMAL CONDUCTIVITY OF THE SODIUM VAPOR

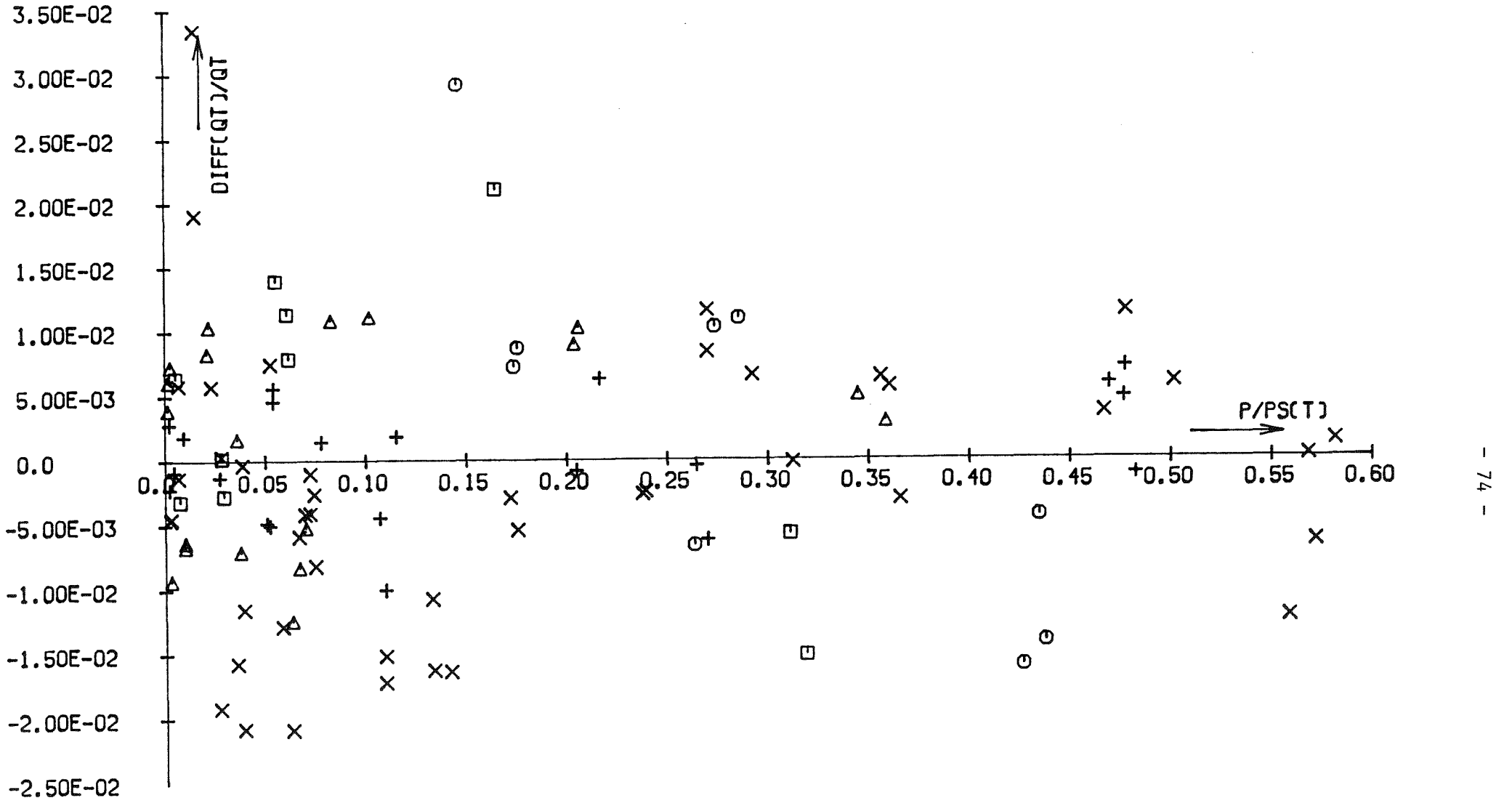


FIG. 22 DEVIATIONS OF THE DATA FROM THE REDUCED DESCRIPTION

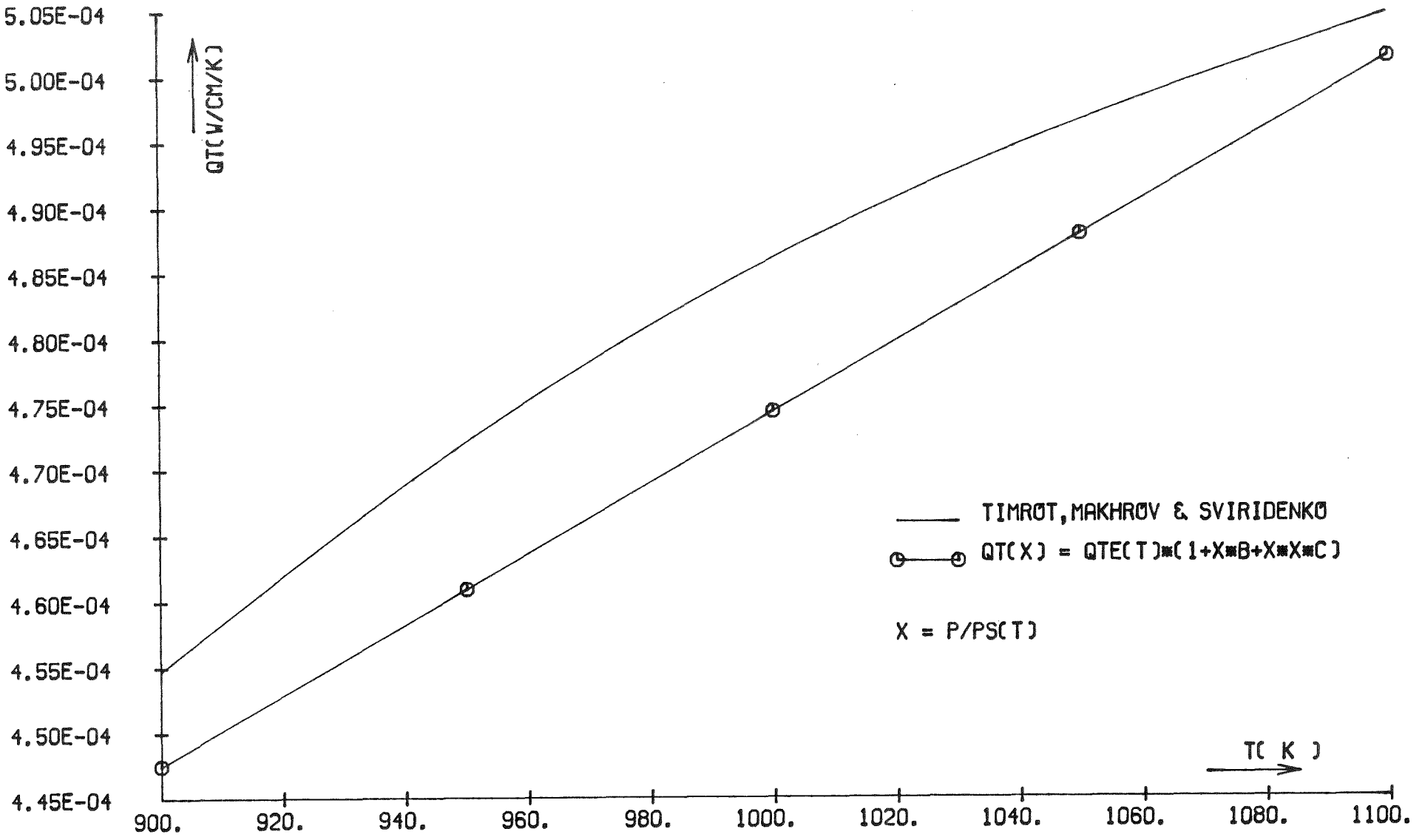


FIG. 23 THERMAL CONDUCTIVITY OF THE SATURATED SODIUM VAPOR

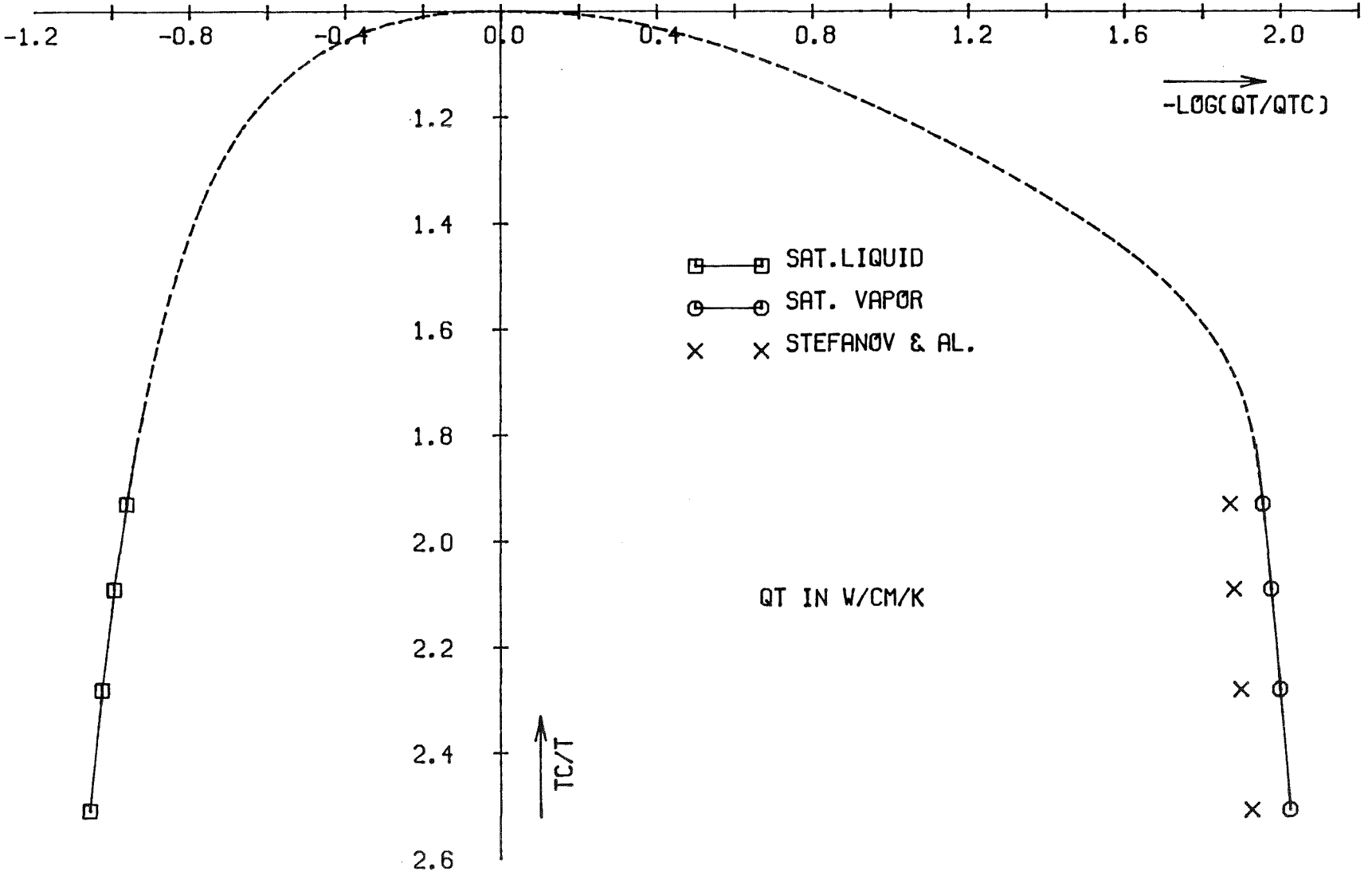


FIG. 24 SODIUM . QT ON THE SATURATION LINE (REDUCED PROPERTIES)

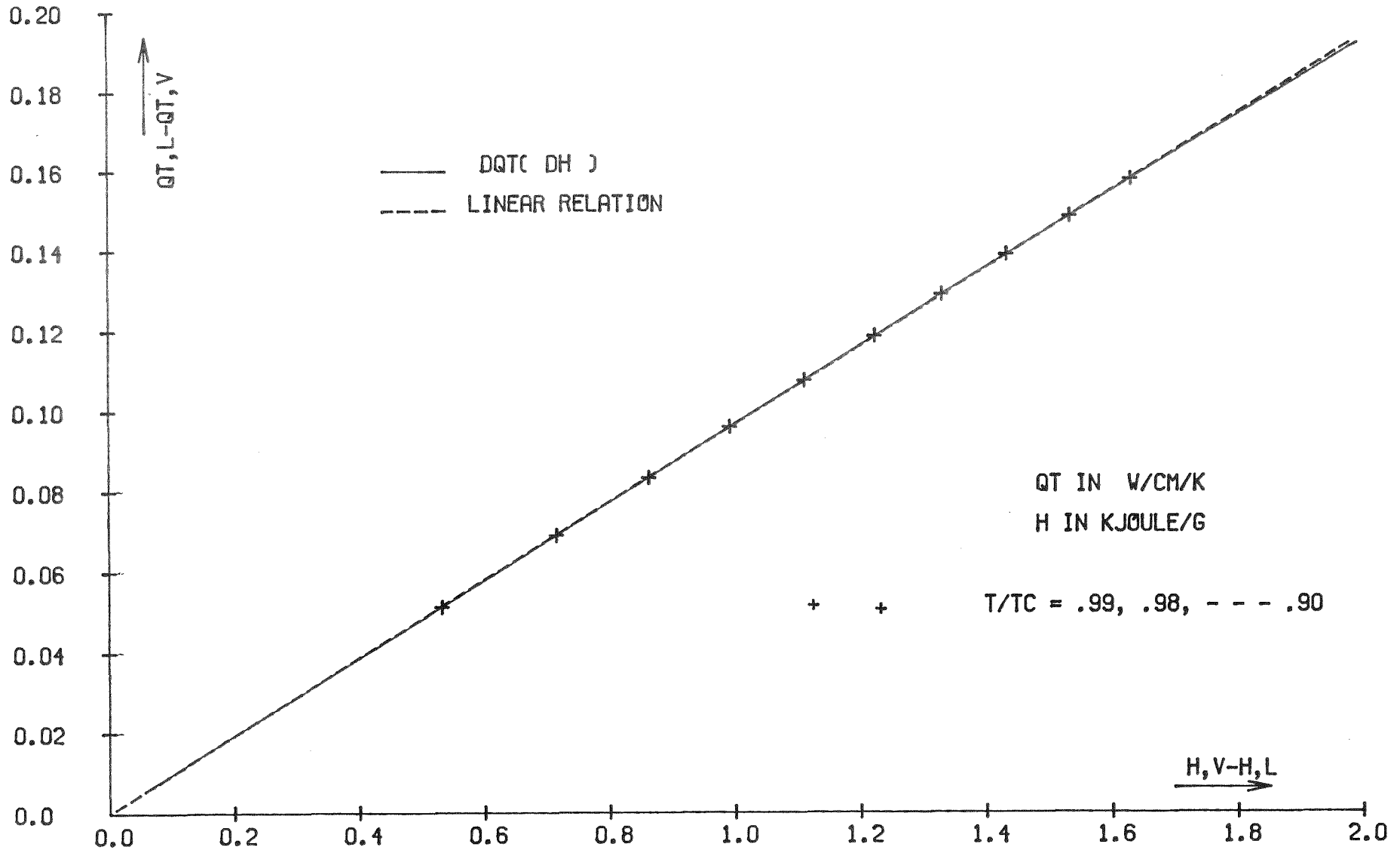


FIG. 25 SODIUM . DQ AS A LINEAR FUNCTION OF DH FOR T → TC

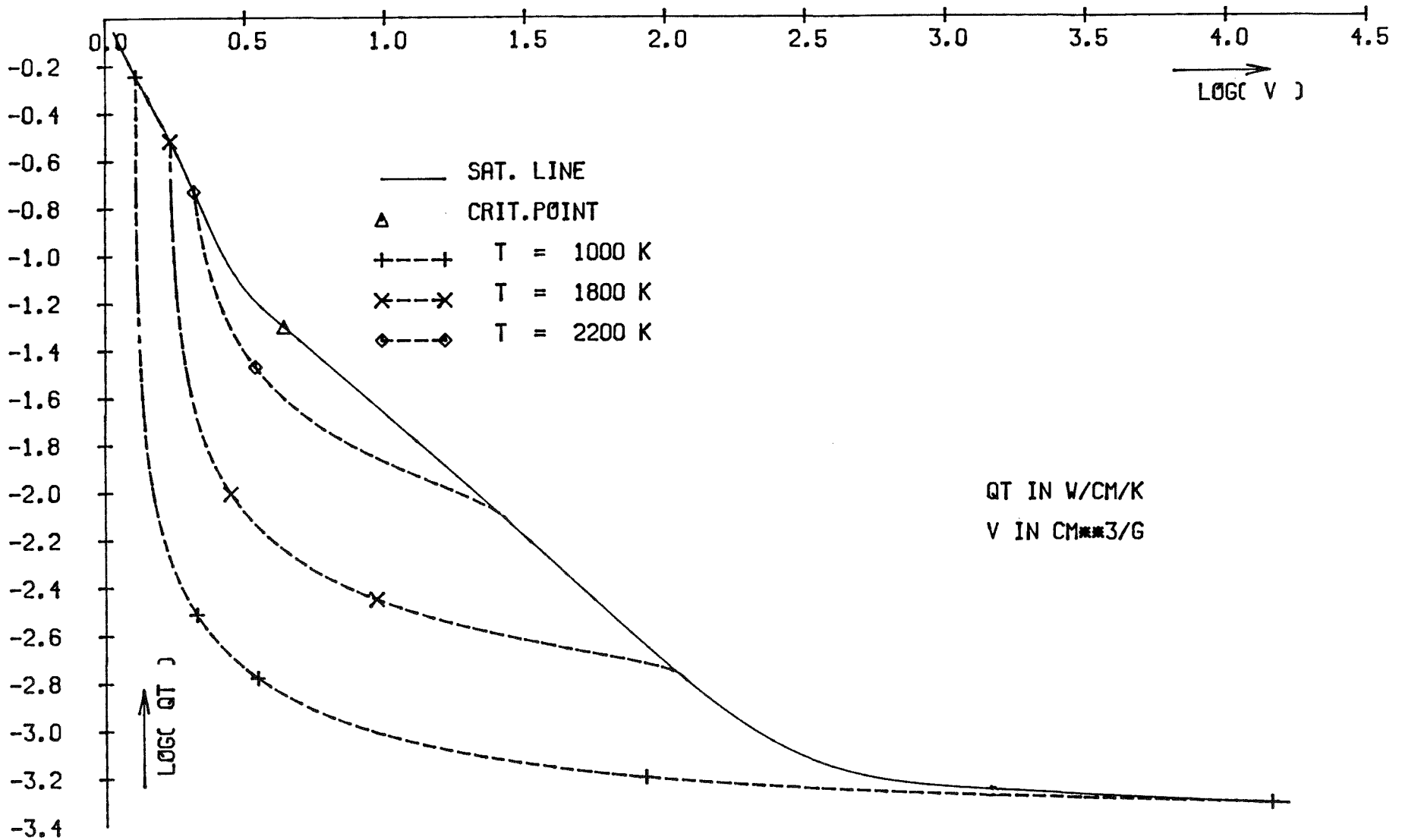




FIG. 26 STATIC THERMAL CONDUCTIVITY OF THE TWO-PHASE SODIUM

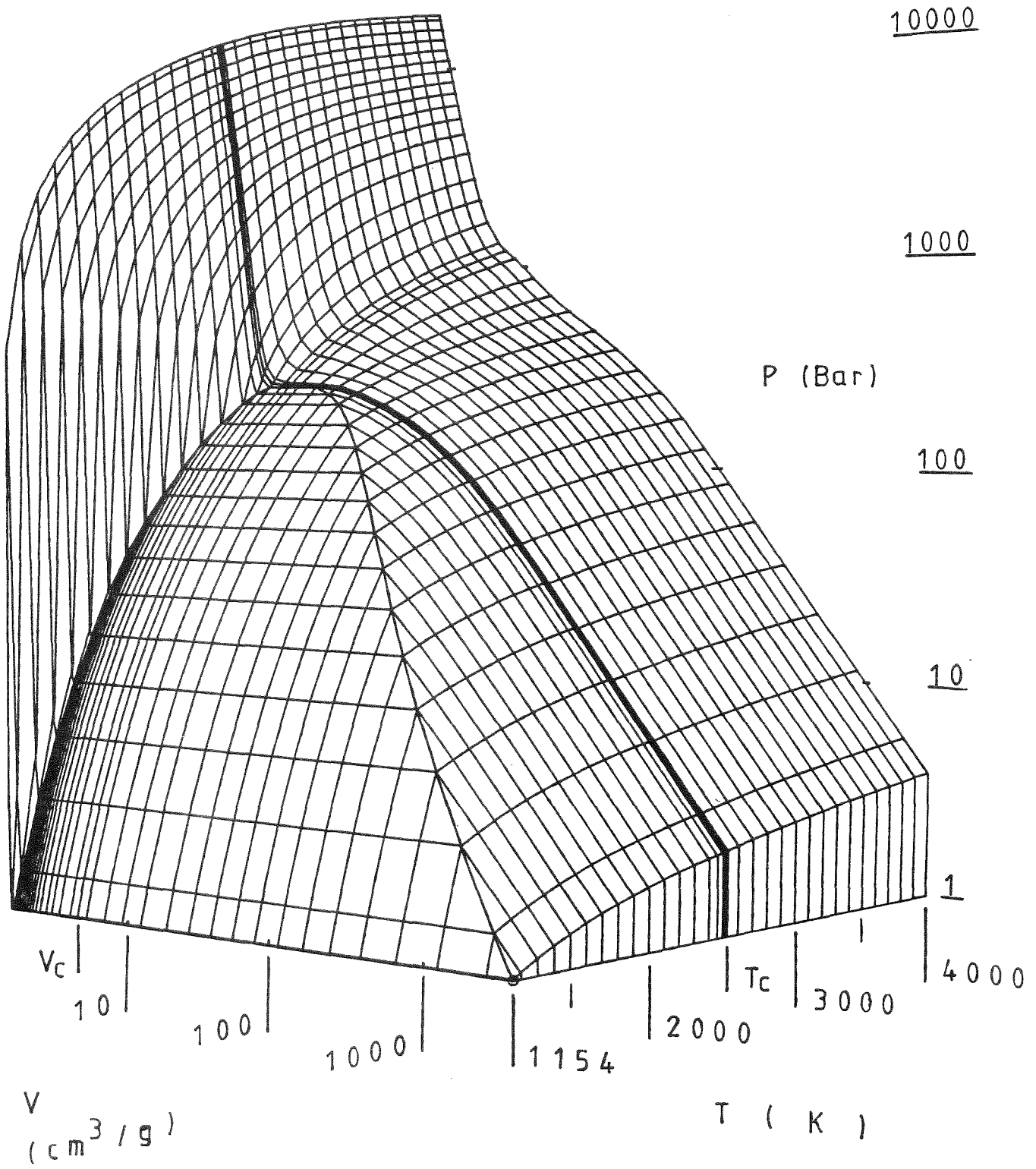


FIG. 27 SØDIUM . THE PRESSURE - VØLUME - TEMPERATURE SURFACE

P( V , T )

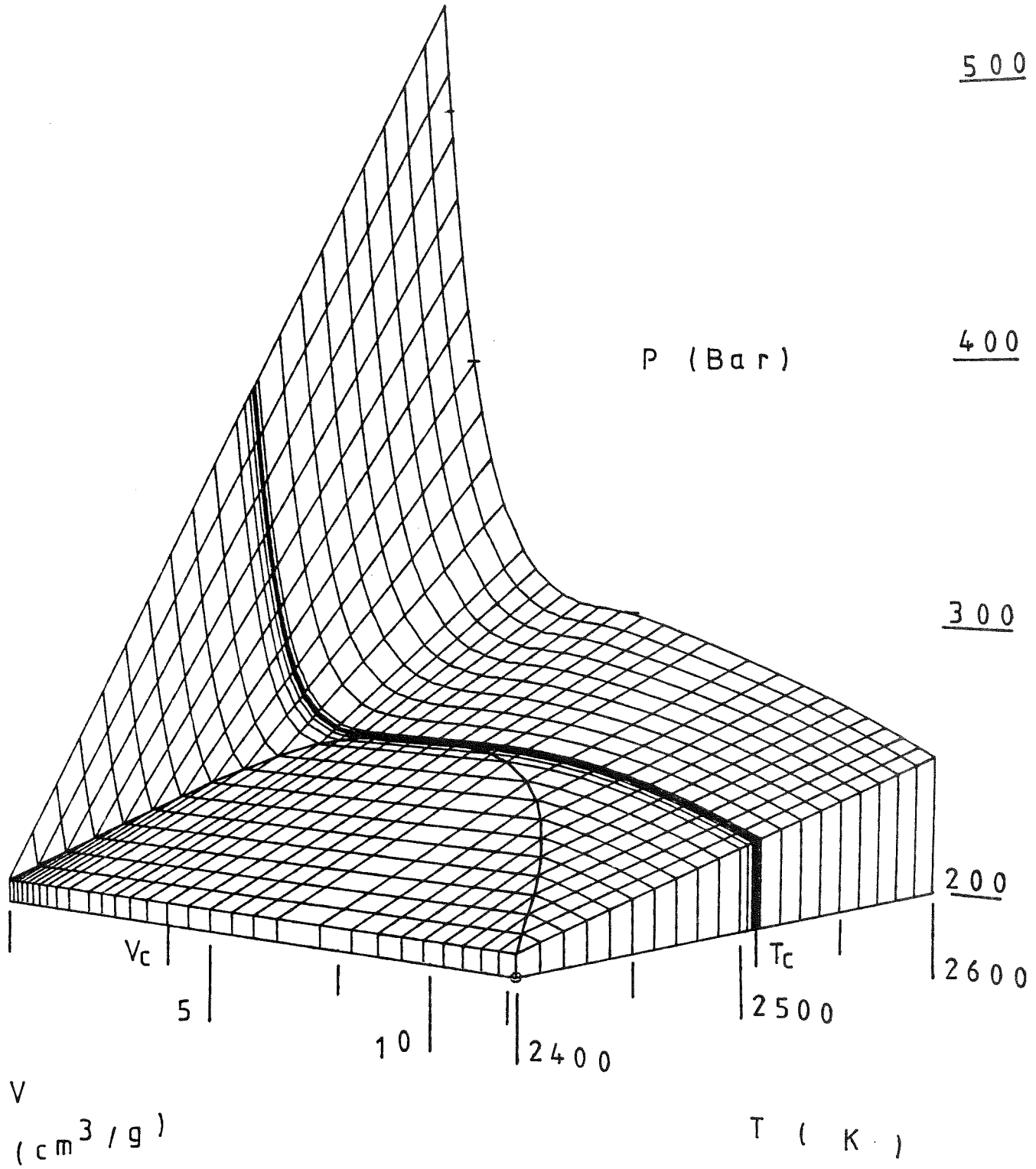


FIG. 28 SODIUM . THE NEAR-CRITICAL PART OF THE PRESSURE - SURFACE P( V , T )

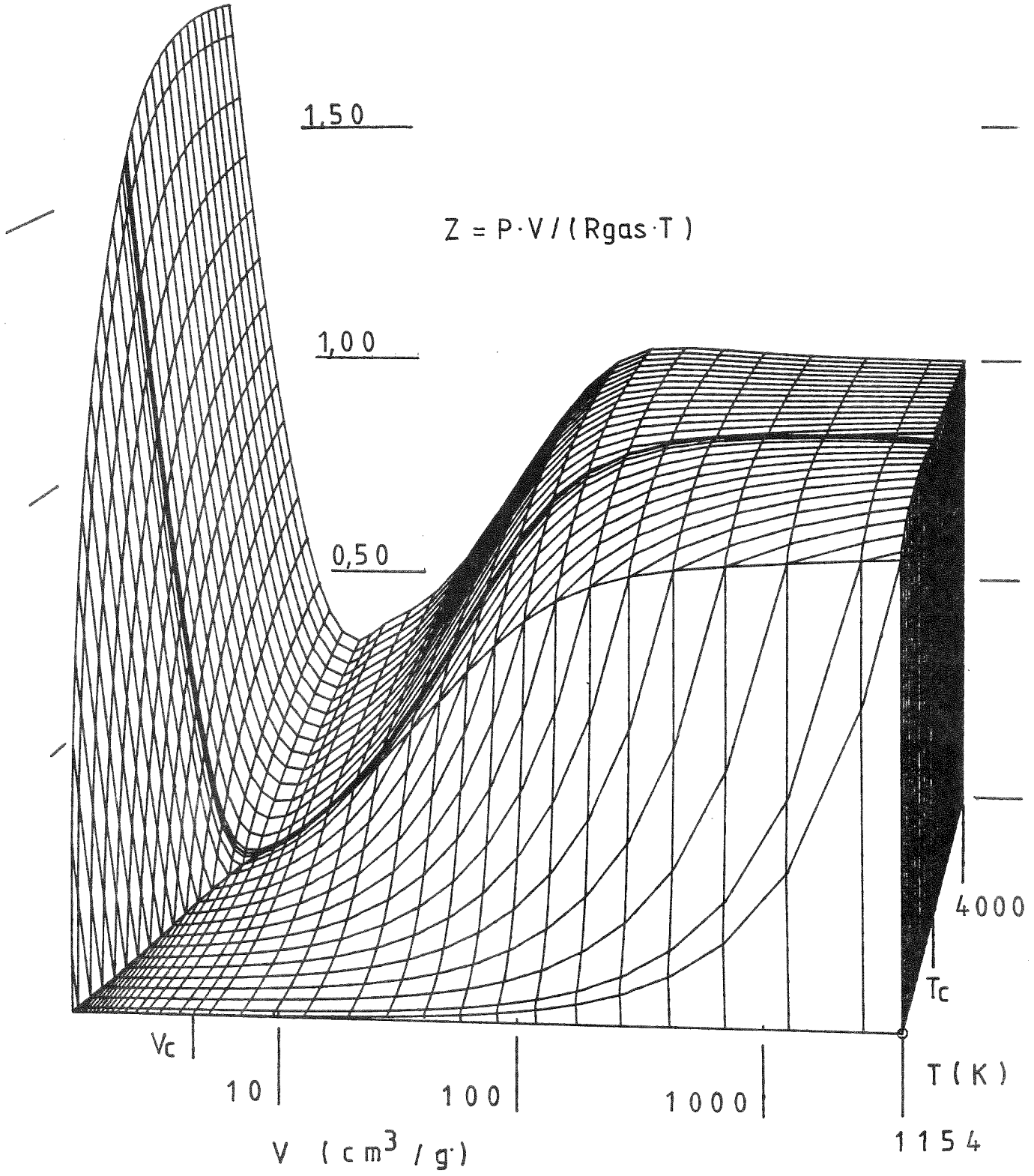


FIG. 29 SODIUM . THE V - T - SURFACE OF THE FACTOR OF REALITY

Z( V , T )

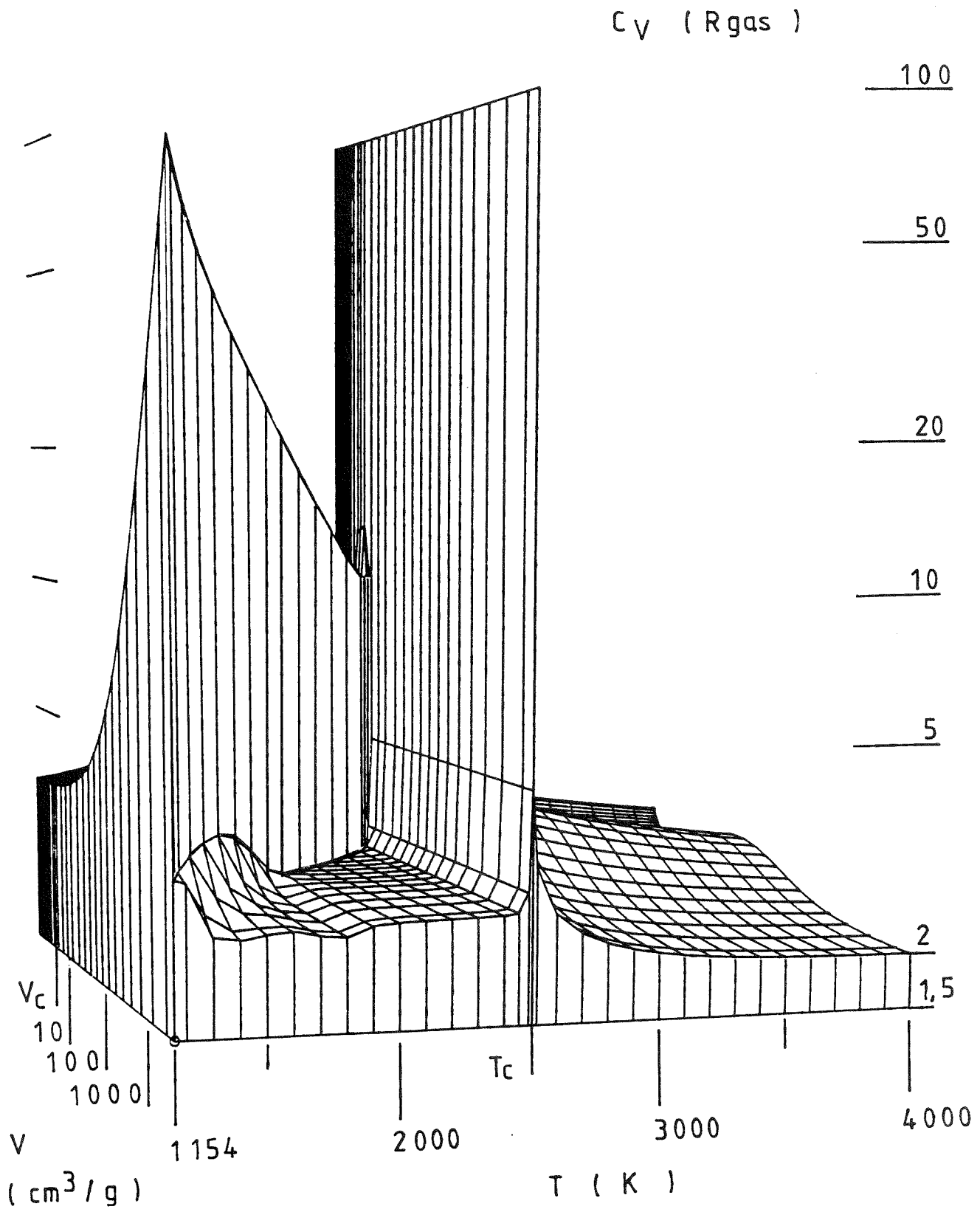


FIG. 31 SODIUM . THE CV - V - T - SURFACE , VAPOR SIDE

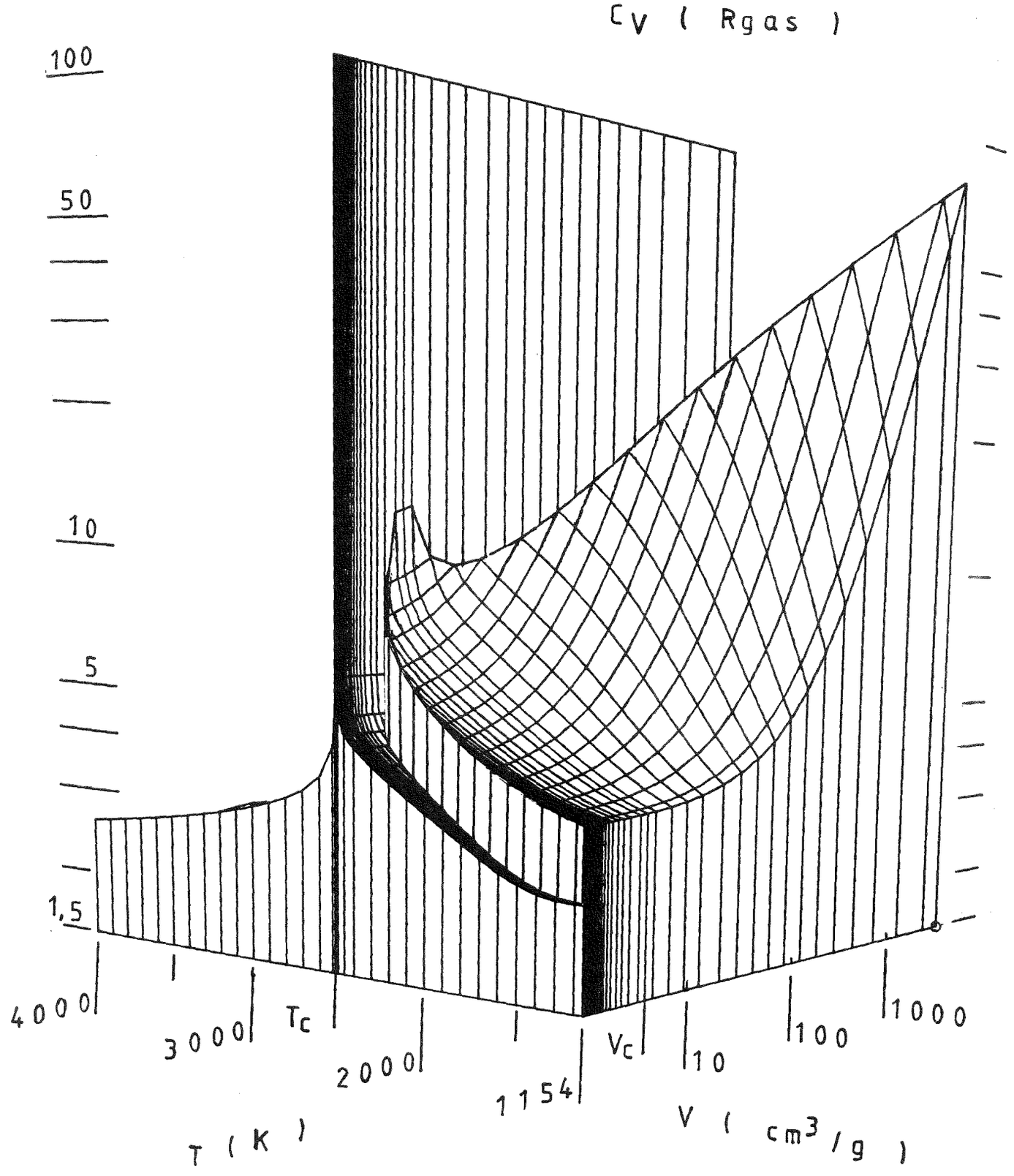


FIG. 30 SODIUM . THE CV - V - T - SURFACE , LIQUID SIDE

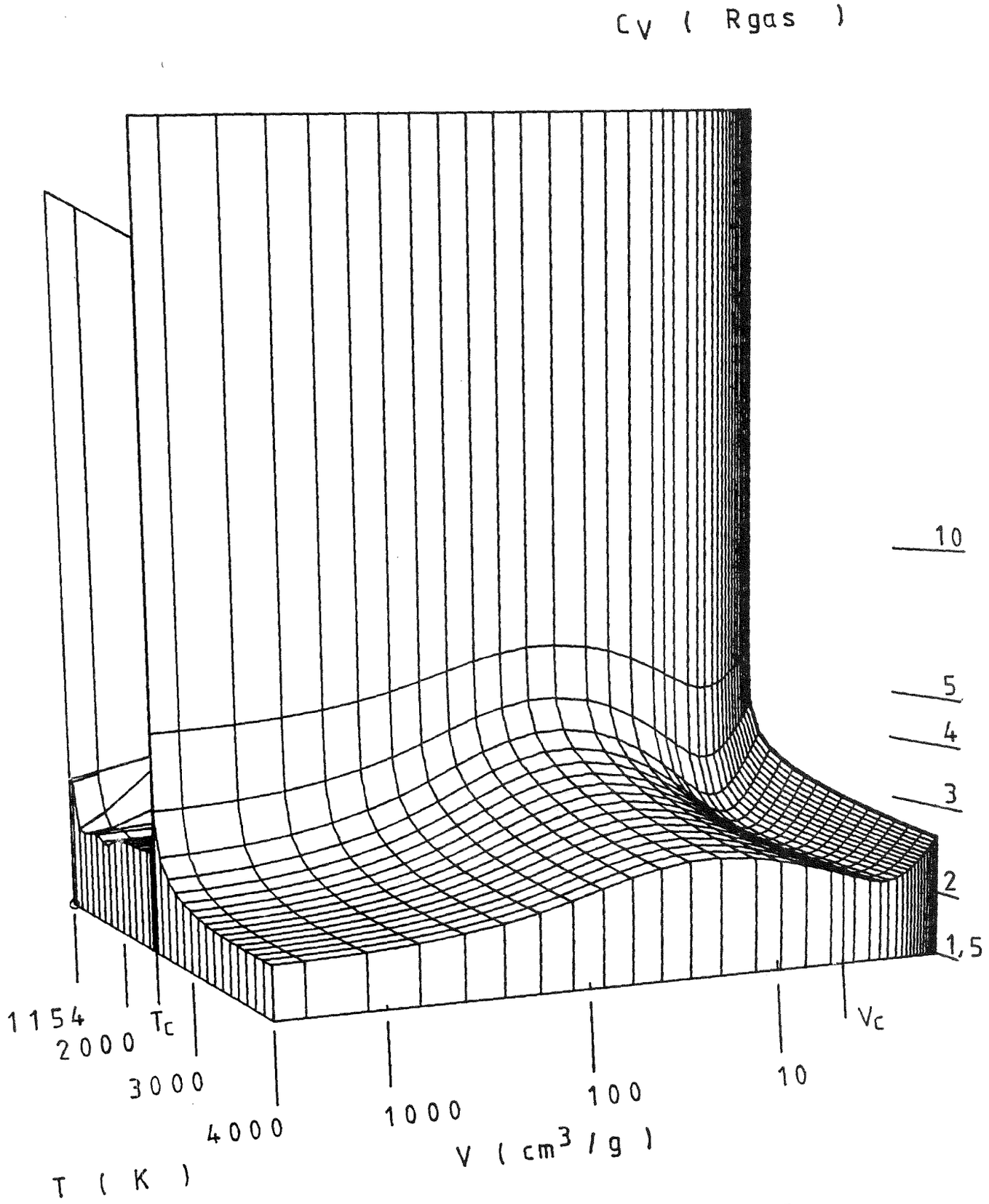


FIG. 32 SODIUM . THE CV - V - T - SURFACE , SUPERCRITICAL SIDE

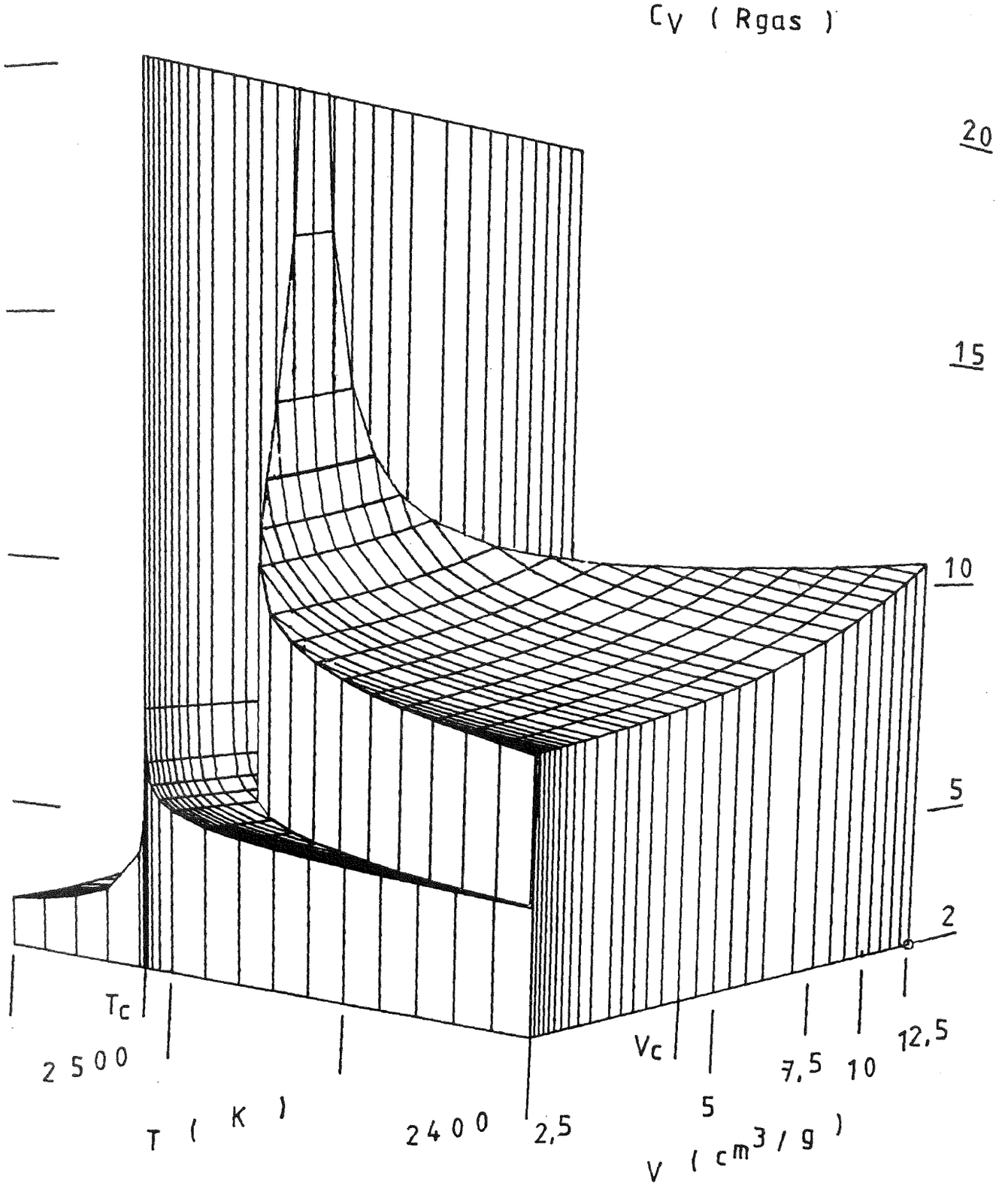


FIG. 33 SODIUM . THE NEAR-CRITICAL PART OF THE CV - SURFACE

LIQUID SIDE

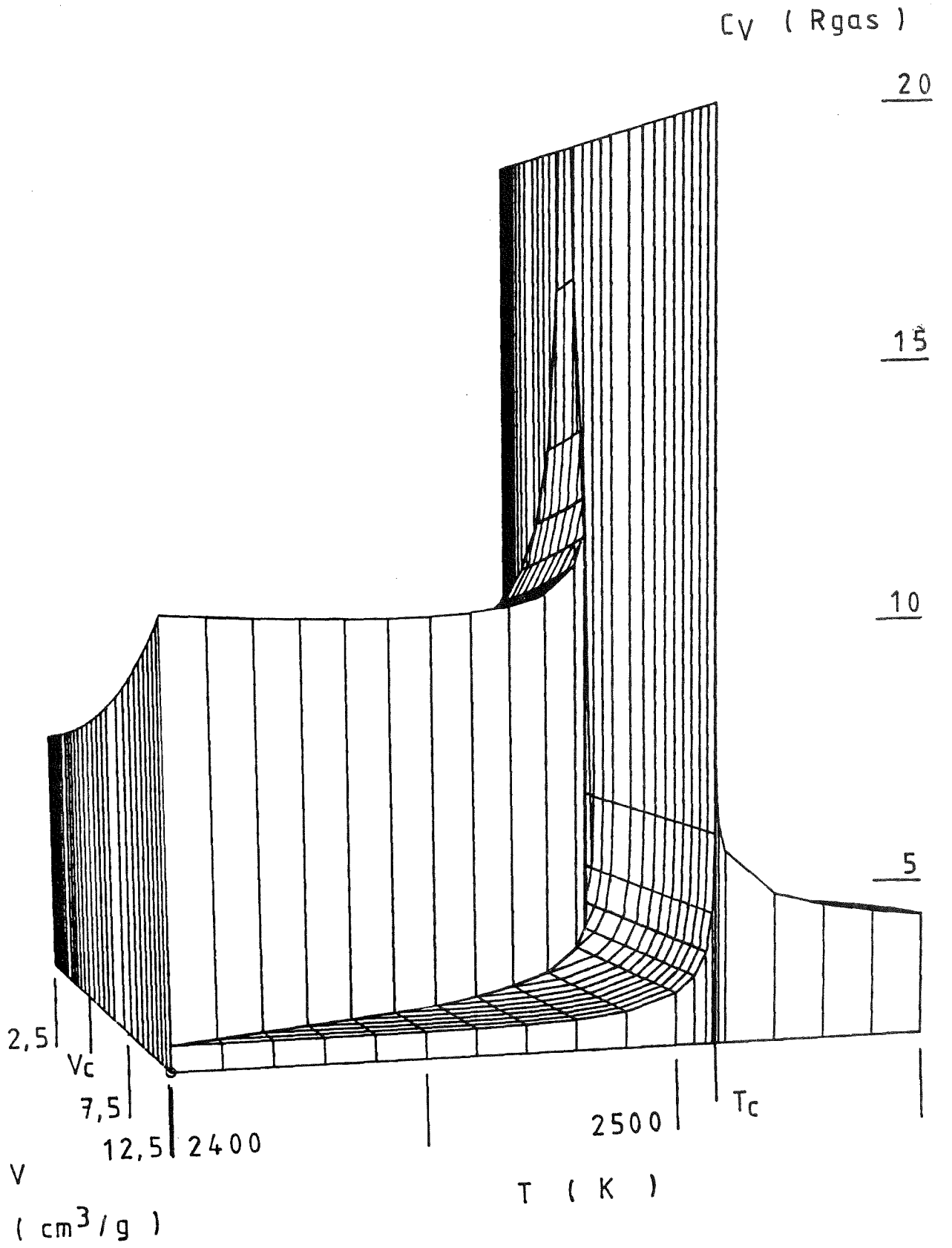


FIG. 34 SODIUM . THE NEAR-CRITICAL PART OF THE CV - SURFACE

VAPOR SIDE

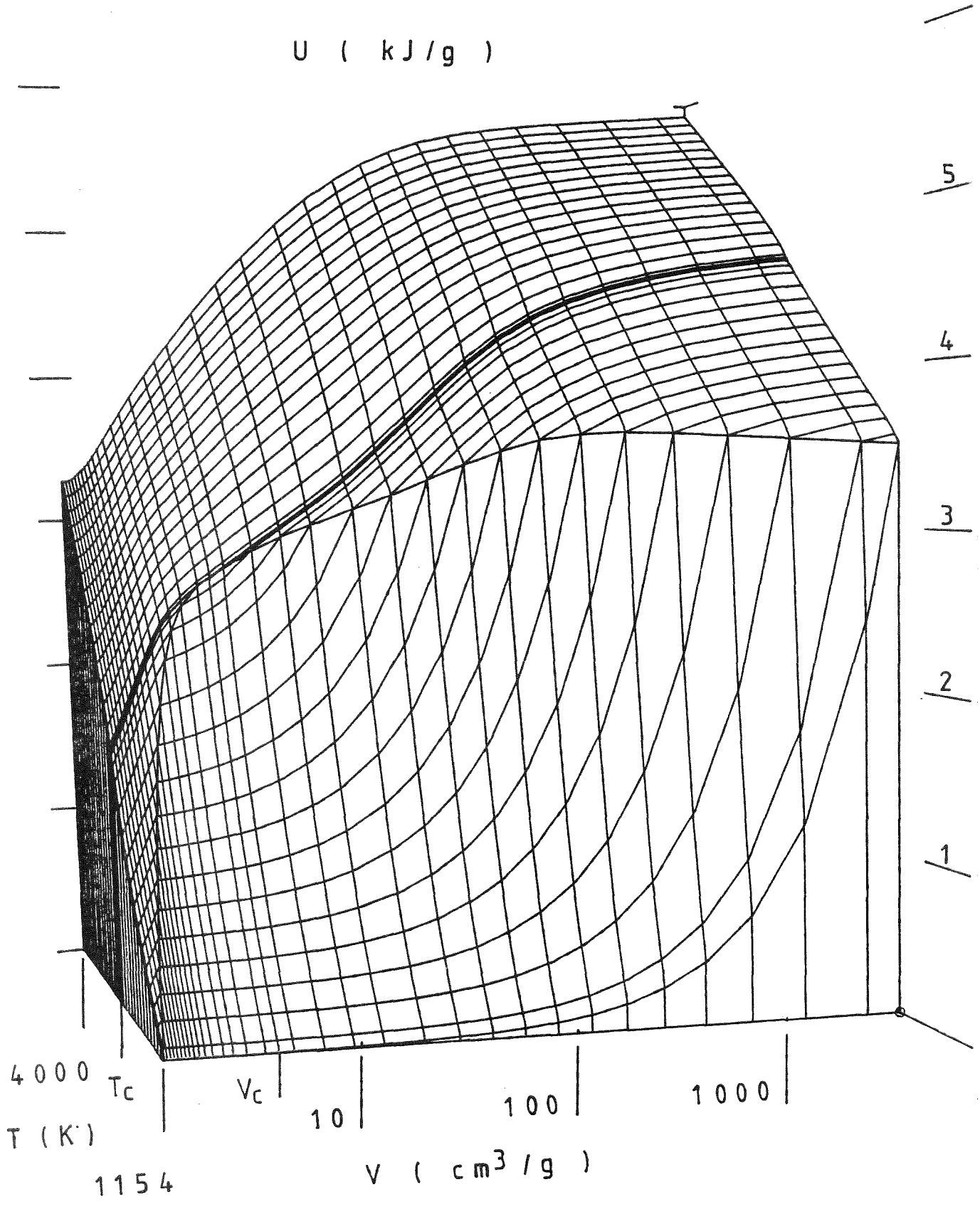


FIG. 35 SODIUM . THE V - T - SURFACE OF THE INTERNAL ENERGY

U( V , T )

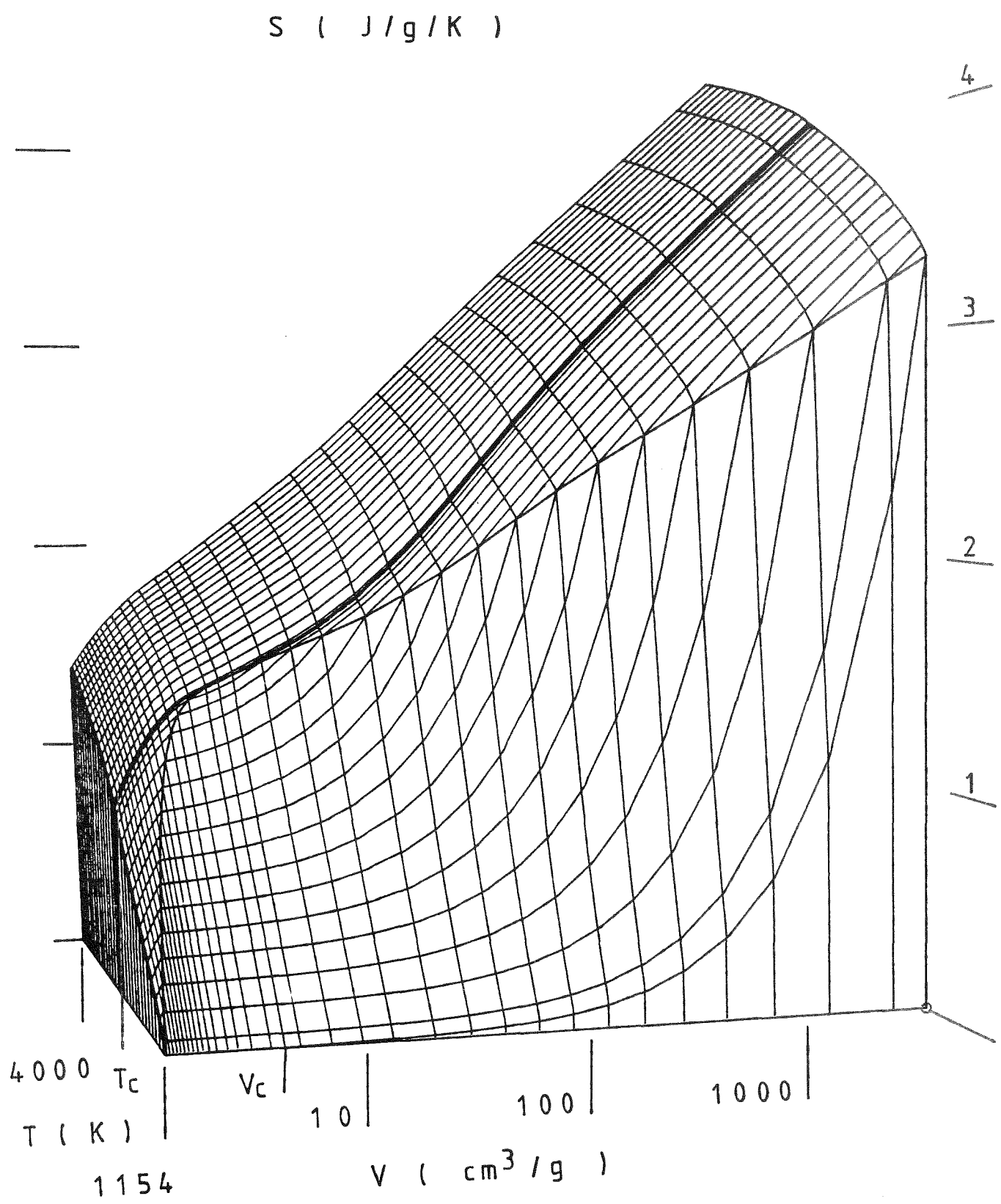


FIG. 36 SODIUM . THE V - T - SURFACE OF THE ENTROPY S( V , T )

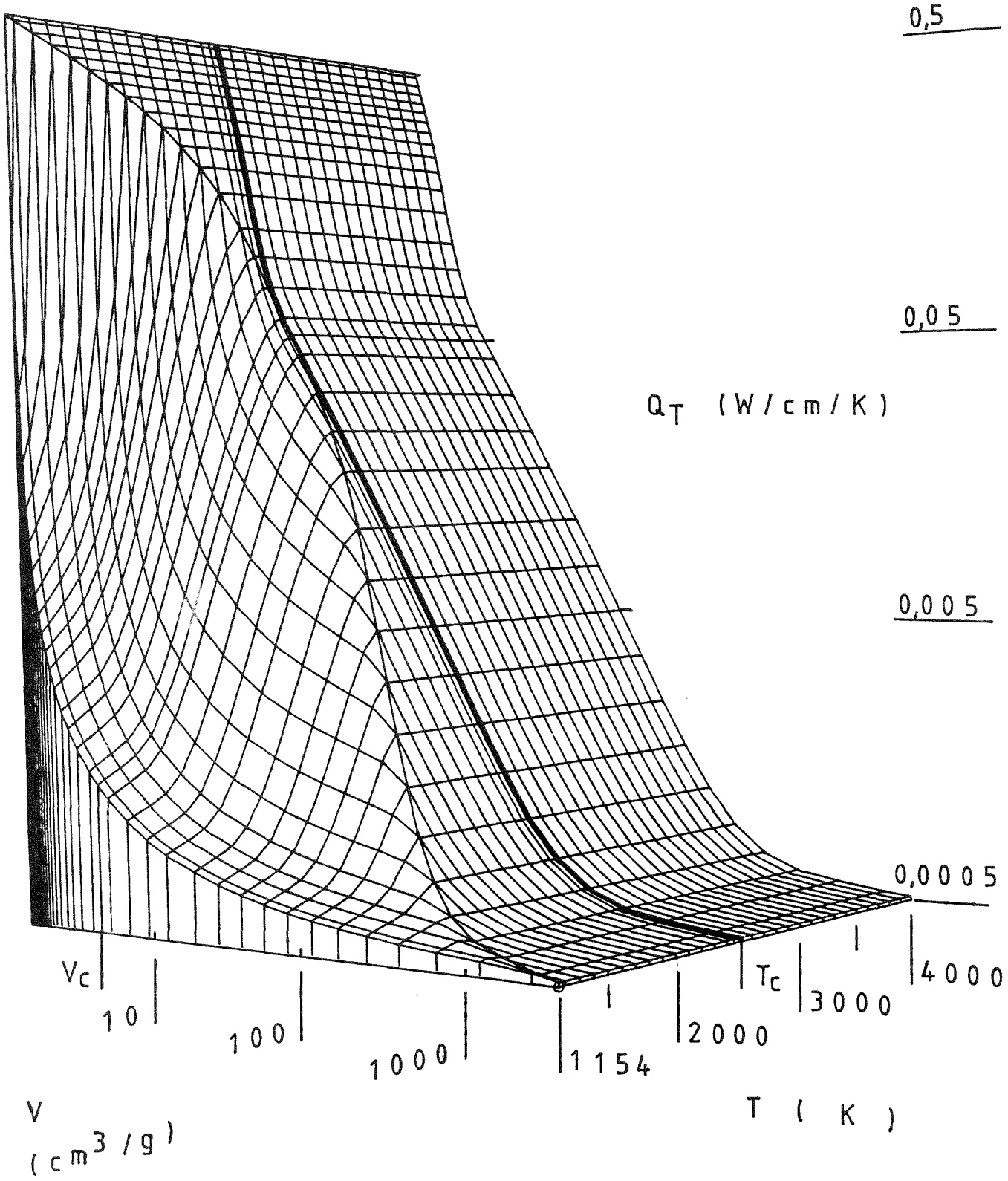


FIG. 37 SODIUM . THE V - T - SURFACE OF THE THERMAL CONDUCTOVITY

QT( V , T )

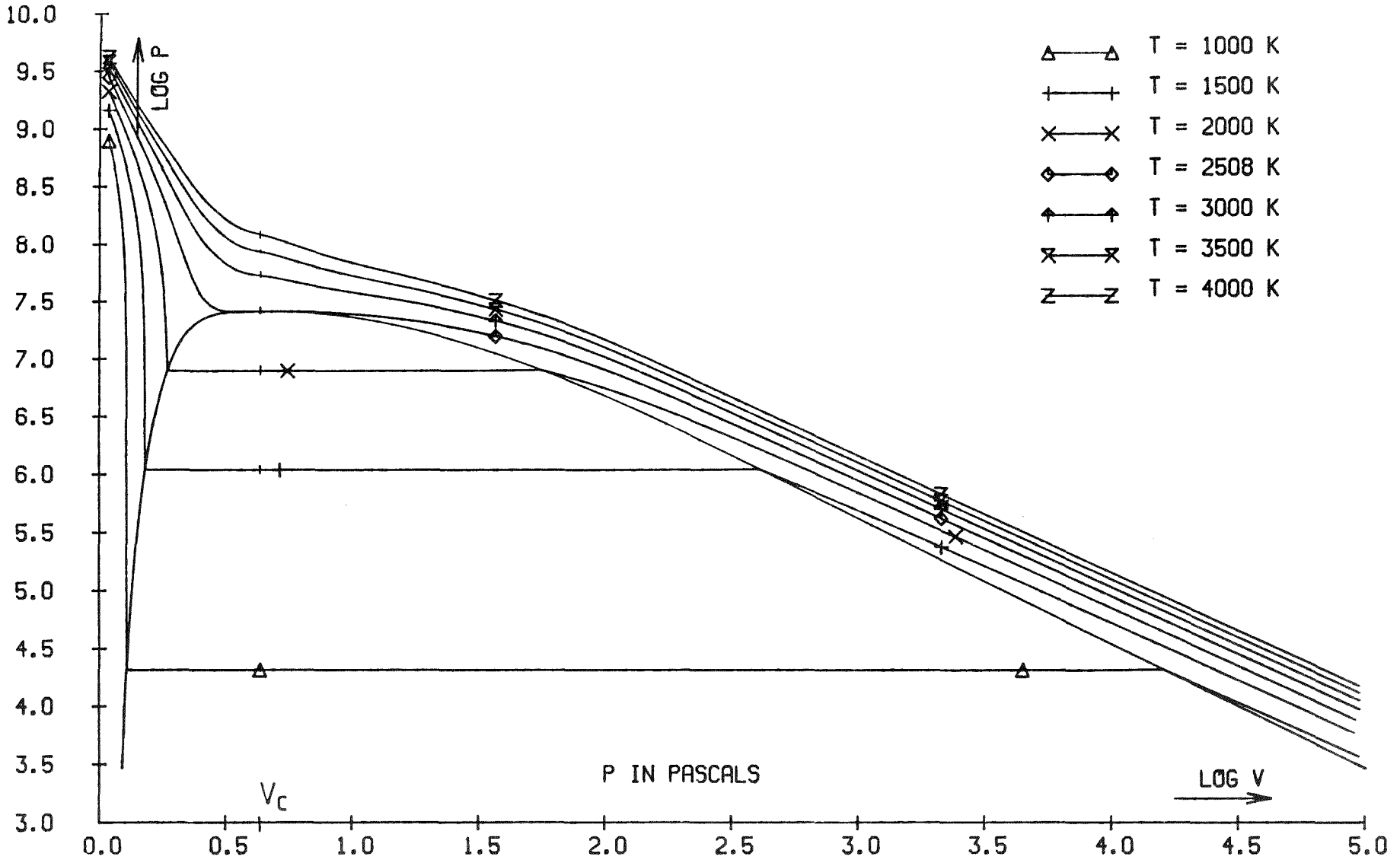


FIG. 38 SODIUM . THE PRESSURE - VOLUME CHART

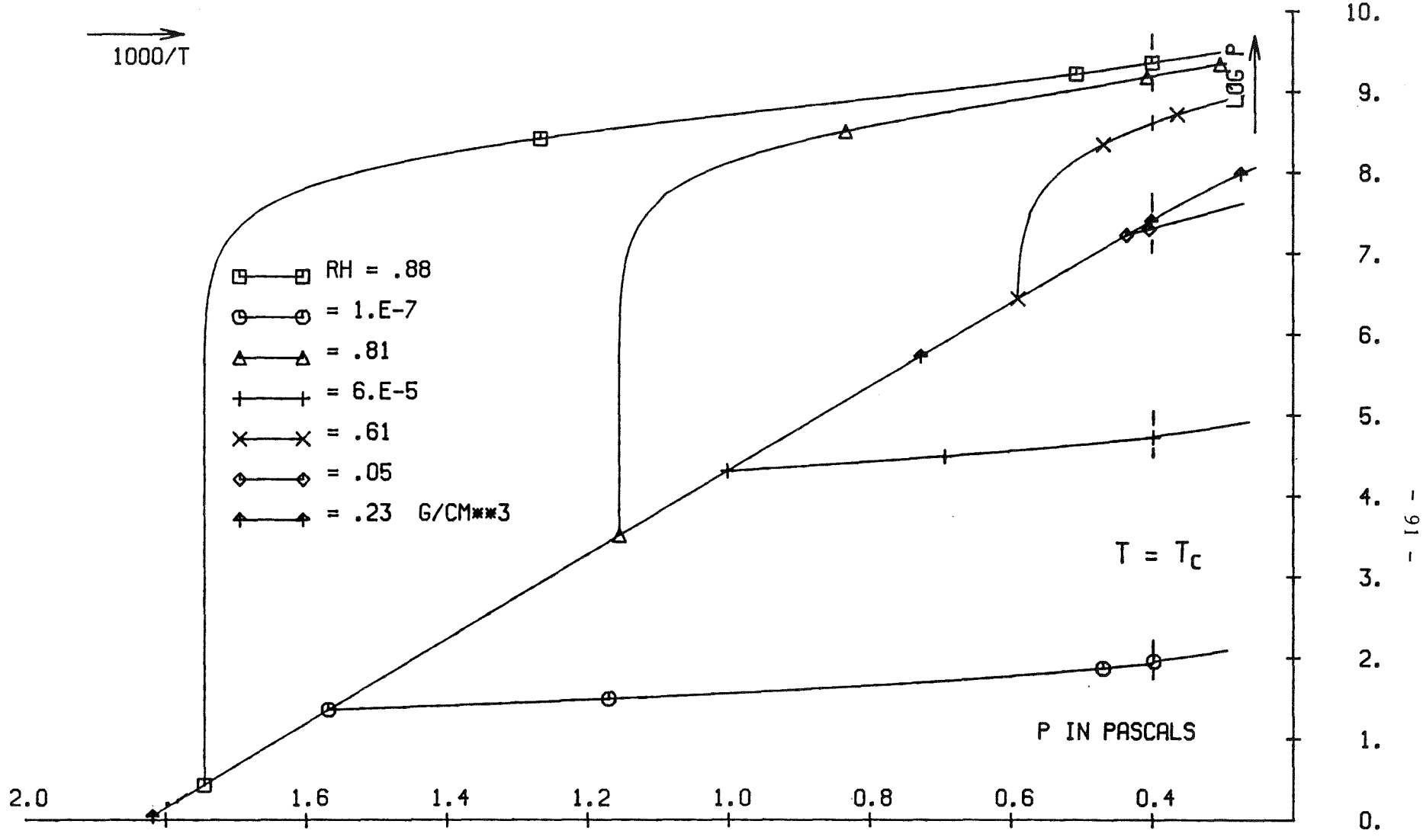




FIG. 39 SODIUM . THE PRESSURE - TEMPERATURE CHART

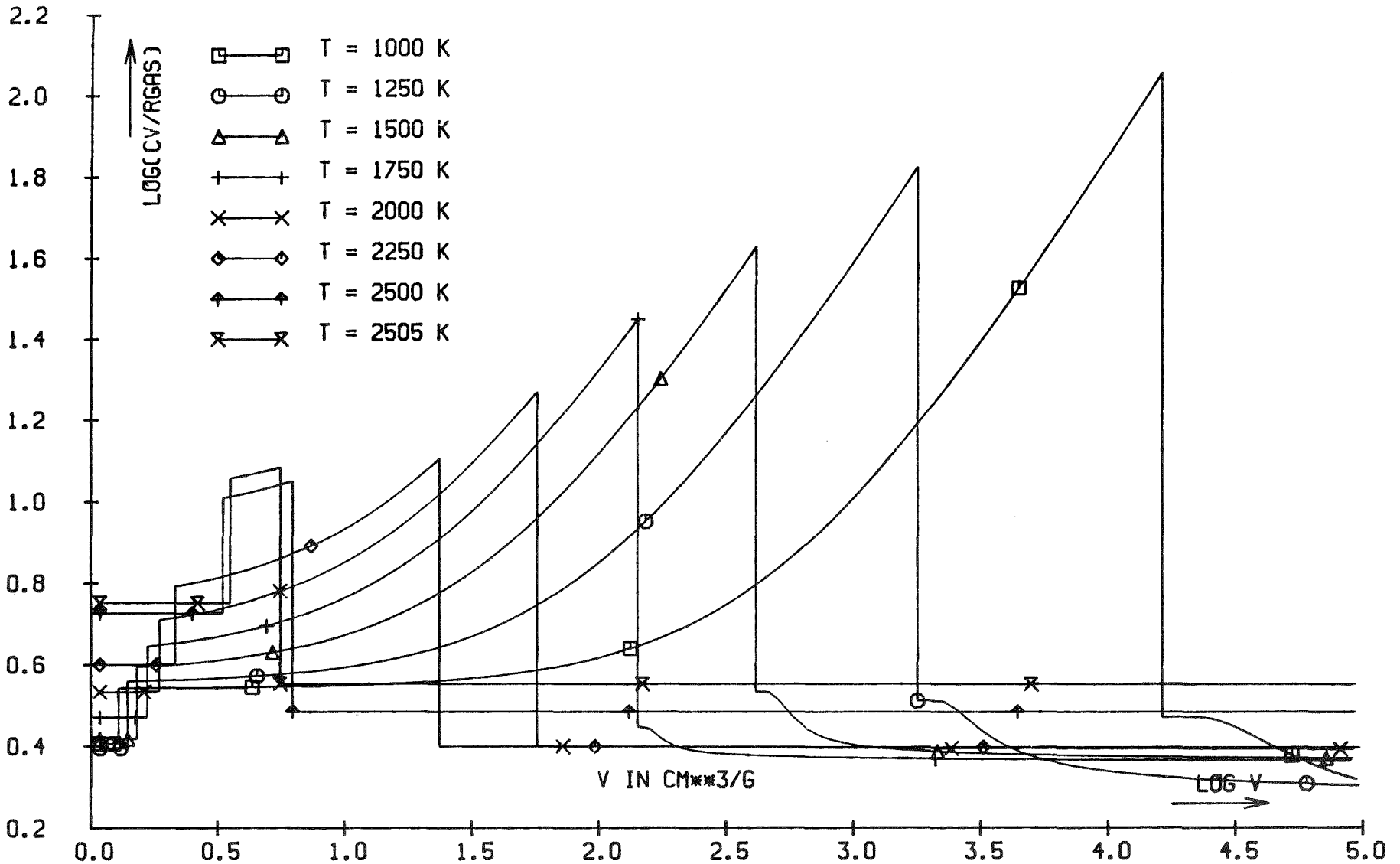


FIG. 40 SODIUM . THE SPECIFIC HEAT - VOLUME CHART

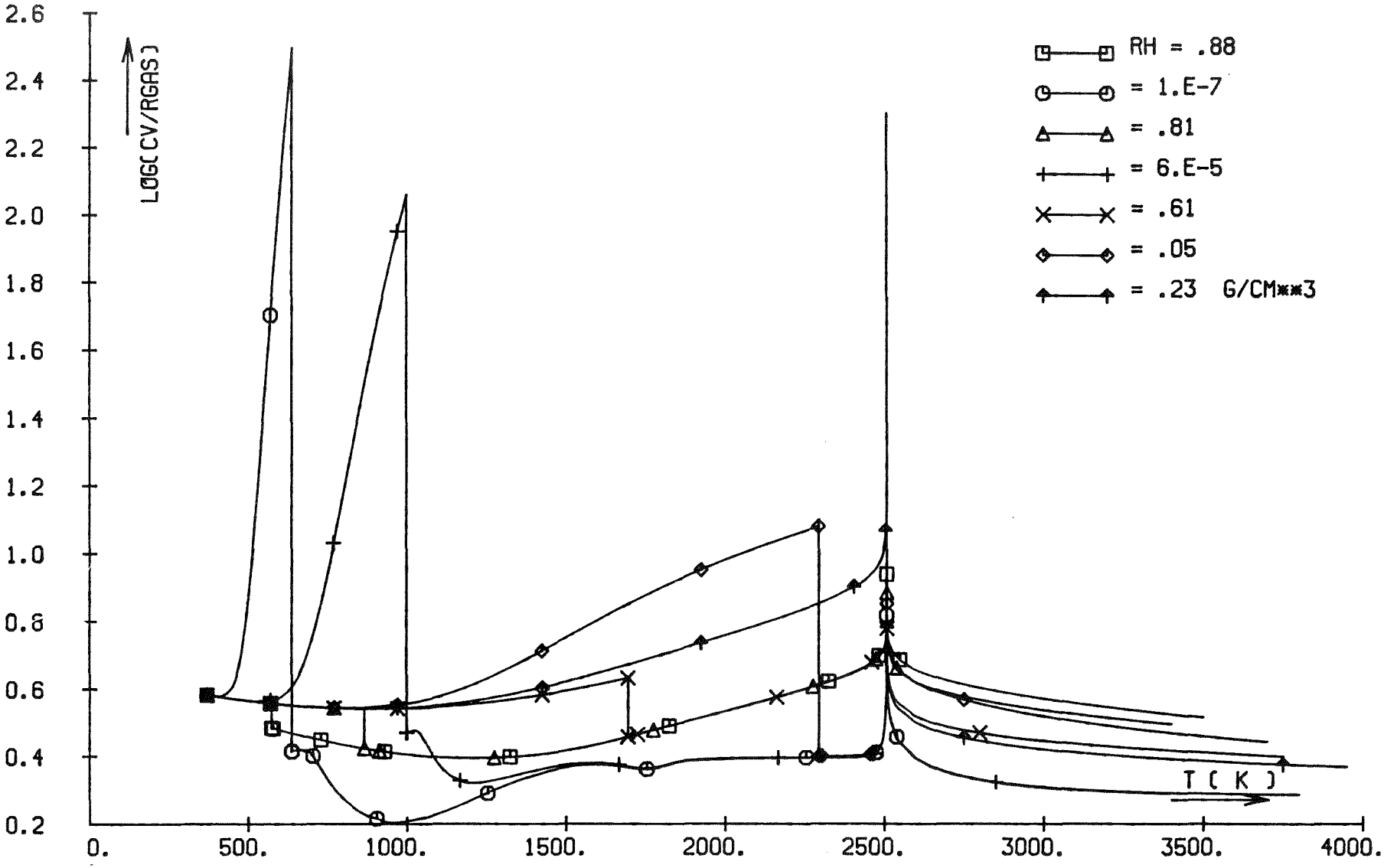


FIG. 41 SØDIUM . THE SPECIFIC HEAT - TEMPERATURE CHART

Appendix P

The sodium property subroutines KANAST and KANAPT.

For the benefit of potential users of the STPS-Karlsruhe the following property-codes have been developed and tested:

KANAST calculates for given T and $\varrho$ the properties P, $P_\varrho$, $P_T$, $C_v$, $Q_T$ and $\xi$ ,

KANAPT calculates for given T and P the properties $\varrho$ , $P_\varrho$, $P_T$, $C_p$, $Q_T$, $P^x$, $\varrho_L$, $\varrho_v$.

To accelerate the calculations KANAST uses not all the descriptions given in Appendix C directly; the saturated properties $C_v$, $P_T$, $Q_T$ and the saturated densities are stored in the code point for point, corresponding to the temperatures 370 - 402 - 434 - ... - 2386 - 2418 K. For a temperature between these values the properties are calculated by cubic interpolation. The use of the time consuming high-temperature property-formulas is restricted to the remaining part of the SL.

Also for the reason of time-saving the integral $\Delta C_v$ (eq. (94)) - needed for the heat capacity in the overheated vapor - is pre-calculated and stored in the code as a function of both variables T and $T^x/T$ (a typical running time for this code is a half msec on the IBM 3033).

KANAPT calculates the sodium properties by iteration: the first density, corresponding to a given T and P is estimated, then KANAPT calls KANAST to check this value. If the corresponding KANAST-pressure does not agree with P, the density is corrected using $\Delta P$ and $P_\varrho$. On average one KANAPT run gives rise to three KANAST calls.

All the property-surfaces and charts of the Figs. 26 - 41 have been calculated with KANAST.